

# Introduction to Biofluid Mechanics

*Portonovo S. Ayyaswamy*

## OUTLINE

16.1. Introduction	779	Exercises	849
16.2. The Circulatory System in the Human Body	780	Acknowledgment	850
16.3. Modeling of Flow in Blood Vessels	796	Literature Cited	851
16.4. Introduction to the Fluid Mechanics of Plants	844	Supplemental Reading	852

## CHAPTER OBJECTIVES

- To properly introduce the subject of biofluid mechanics including the necessary language
- To describe the components of the human circulation system and document their nominal characteristics
- To present analytical results of relevant models of steady and pulsatile blood flow
- To review the parametric impact of the properties of rigid, flexible, branched, and curved tubes on blood flow
- To provide an overview of fluid transport in plants.

## 16.1. INTRODUCTION

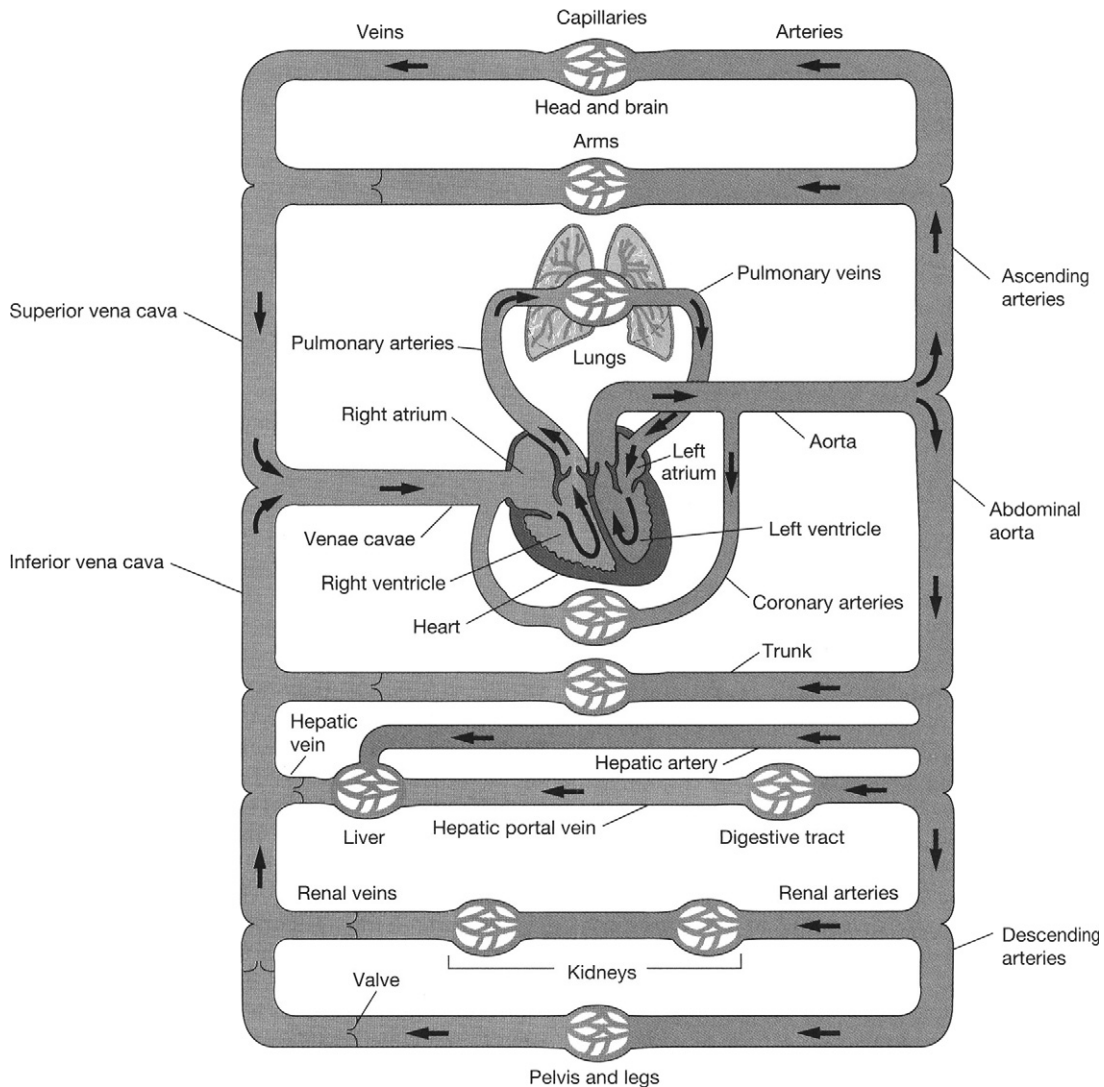
This chapter is intended to be of an introductory nature to the vast field of biofluid mechanics. Here, we shall consider the ideas and principles of the preceding chapters in the context of fluid motion in biological systems. Topical emphasis is placed on fluid motion in the human body, and some aspects of the fluid mechanics of plants.

The human body is a complex system that requires materials such as air, water, minerals, and nutrients for survival and function. Upon intake, these materials have to be transported and distributed around the body as required. The associated biotransport and distribution processes involve interactions with membranes, cells, tissues, and organs comprising the body. Subsequent to cellular metabolism in the tissues, waste byproducts have to be transported to the excretory organs for synthesis and removal. In addition to these functions, biotransport systems and processes are required for homeostasis (physiological regulation—for example, maintenance of pH and of body temperature), and for enabling the movement of immune substances to aid in the body's defense and recovery from infection and injury. Furthermore, in certain other specialized systems such as the cochlea in the ear, fluid transport enables hearing and motion sensing. Evidently, in the human body, there are multiple types of fluid dynamic systems that operate at macro-, micro-, nano-, and pico-scales. Systems at the micro and macro levels, for example, include cells (micro), tissue (micro–macro), and organs (macro). Transport at the micro, nano, and pico levels include ion channeling, binding, signaling, endocytosis, and so on. Tissues constitute organs, and organs as systems perform various functions. For example, the cardiovascular system consists of the heart, blood vessels (arteries, arterioles, venules, veins, capillaries), lymphatic vessels, and the lungs. Its function is to provide adequate blood flow and to regulate that flow as required by the various organs of the body. In this chapter, as related to the human body, we shall restrict attention to some aspects of the cardiovascular system for blood circulation.

## 16.2. THE CIRCULATORY SYSTEM IN THE HUMAN BODY

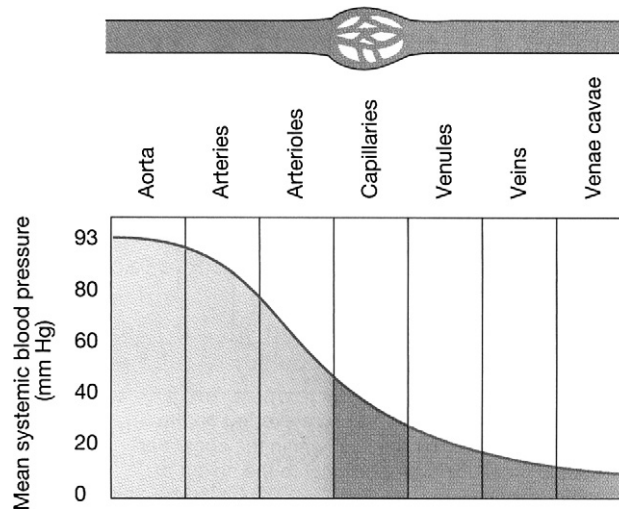
The primary functions of the cardiovascular system are: 1) to pick up oxygen and nutrients from the lungs and the intestine, respectively, and deliver them to tissues (cells) of the body, 2) to remove waste and carbon dioxide from the body for excretion through the kidneys and the lungs, respectively, and 3) to regulate body temperature by advecting the heat generated and transferring it to the environment outside the skin. The circulatory system in a normal human body (as in all vertebrates and some other select groups of species) can be considered as a closed system, meaning that the blood never leaves the system of blood vessels. The motive mechanism for blood flow is the prevailing pressure gradient.

The circulations associated with the cardiovascular system may be considered under three subsystems. These are the 1) systemic circulation, 2) pulmonary circulation, and 3) coronary circulation (see [Figure 16.1](#)). In the systemic circulation, blood flows to all of the tissues in the body except the lungs. Contraction of the left ventricle of the heart pumps oxygen-rich blood to a relatively high pressure and ejects it through the aortic valve into the aorta. Branches from the aorta supply blood to the various organs via systemic arteries and arterioles. These, in turn, carry blood to the capillaries in the tissues of various organs. Oxygen and nutrients are transported by diffusion across the walls of the capillaries to the tissues. Cellular metabolism in the tissues generates carbon dioxide and byproducts (waste). Carbon dioxide dissolves in the blood and waste is carried by the bloodstream. Blood drains into venules and veins. These vessels ultimately empty into two large veins called the *superior vena cava* (SVC) and



**FIGURE 16.1** Schematic of blood flow in systemic and pulmonary circulation showing the major branches. Reproduced with permission from Silverthorn, D. U. (2001), *Human Physiology: An Integrated Approach*, 2nd ed., Prentice Hall, Upper Saddle River, NJ.

*inferior vena cava* (IVC) that return carbon dioxide-rich blood to the right atrium. The mean blood pressure of the systemic circulation ranges from a high of 93 mm Hg in the arteries to a low of a few mm Hg in the venae cavae. Figure 16.2 shows that pressure falls continuously as blood moves farther from the heart. The highest pressure in the vessels of the circulatory system is in the aorta and in the systemic arteries while the lowest pressure is in the venae cavae.

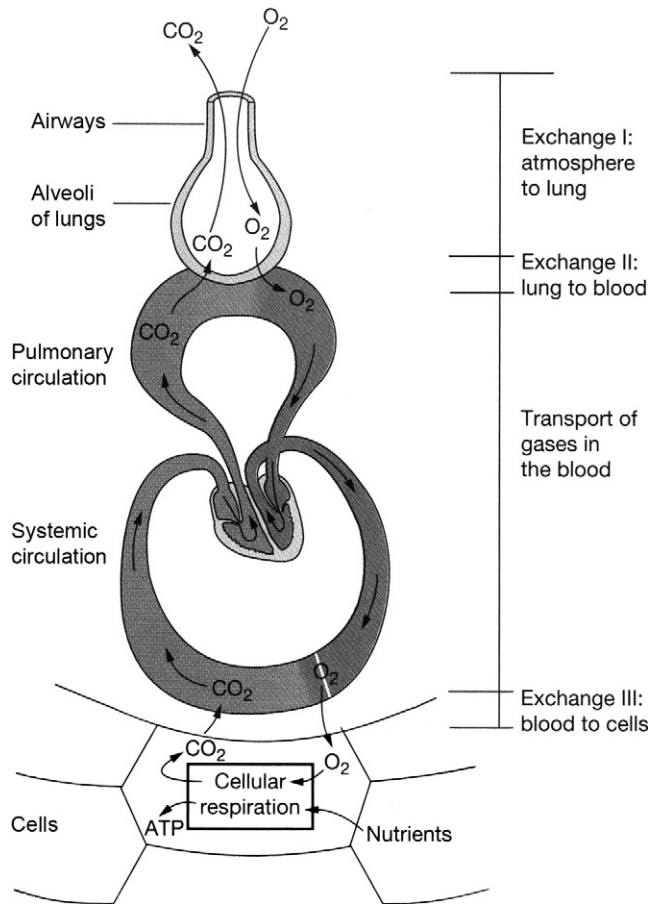


**FIGURE 16.2** Pressure gradient in the blood vessels. The highest pressures are found in the aorta which conveys oxygen-rich blood away from the heart. The lowest pressures are found in the largest veins which convey oxygen-poor blood toward the heart. *Reproduced with permission from Silverthorn, D. U. (2001), Human Physiology: An Integrated Approach, 2nd ed., Prentice Hall, Upper Saddle River, NJ.*

In pulmonary circulation, contraction of the right atrium ejects carbon dioxide-rich blood through the tricuspid valve into the right ventricle. Contraction of the right ventricle pumps the blood through the pulmonic valve (also called *semilunar valve*) into the pulmonary arteries. These arteries bifurcate and transport blood into the complex network of pulmonary capillaries in the lungs. These capillaries lie between and around the alveoli walls. During respiratory inhalation, the concentration of oxygen in the air is greater in the air sacs of the alveolar region than in the capillary blood. Oxygen diffuses across capillary walls into the blood. Simultaneously, the concentration of carbon dioxide in the blood is higher than in the air and carbon dioxide diffuses from the blood into the alveoli. Carbon dioxide exits through the mouth and nostrils. Oxygenated blood leaves the lungs through the pulmonary veins and enters the left atrium. When the left atrium contracts, it pumps blood through the bicuspid (mitral) valve into the left ventricle. [Figures 16.3 and 16.4](#) provide an overview of external and cellular respiration and the branching of the airways, respectively.


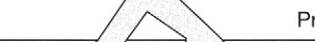

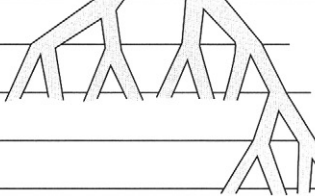






Blood is pumped through the systemic and pulmonary circulations at a rate of about 5.2 liters per minute under normal conditions. The systemic and pulmonary circulations described above constitute one cardiac cycle. The cardiac cycle denotes any one or all of such events related to the flow of blood that occur from the beginning of one heartbeat to the beginning of the next. Throughout the cardiac cycle, the blood pressure increases and decreases. The frequency of the cardiac cycle is the heart rate. The cardiac cycle is controlled by a portion of the autonomic nervous system (that part of the nervous system which does not require the brain's involvement in order to function).

In coronary circulation, blood is supplied to and from the heart muscle itself. The muscle tissue of the heart, or myocardium, is thick and it requires coronary blood vessels



**FIGURE 16.3** Overview of external and cellular respiration. Cells collect oxygen and nutrients from the stream blood and discard carbon dioxide and wastes into the bloodstream. *Reproduced with permission from Silverthorn, D. U. (2001), Human Physiology: An Integrated Approach, 2nd ed., Prentice Hall, Upper Saddle River, NJ.*

to deliver blood deep into the myocardium. The vessels that supply blood with a high concentration of oxygen to the myocardium are known as *coronary arteries*. The main coronary artery arises from the root of the aorta and branches into the left and right coronary arteries. Up to about seventy-five percent of the coronary blood supply goes to the left coronary artery, with the remainder going to the right coronary artery. Blood flows through the capillaries of the heart and returns through the cardiac veins which remove the deoxygenated blood from the heart muscle. The coronary arteries that run on the surface of the heart are relatively narrow vessels and are commonly affected by atherosclerosis and can become blocked, causing angina or a heart attack. The coronary arteries are classified as *end circulation*, since they represent the only source of blood supply to the myocardium.

	Name	Division	Diameter (mm)	How many?	Cross-sectional area (cm)
Conducting system	 Trachea	0	15-22	1	2.5
	 Primary bronchi	1	10-15	2	
	 Smaller bronchi 	2	1-10	4	
		3			
		4			
		5			
		6-11		$1 \times 10^4$	
Exchange surface	 Bronchioles	12-23	0.5-1	$2 \times 10^4$  $8 \times 10^7$	100  $5 \times 10^3$
	 Alveoli	24	0.3	$3-6 \times 10^8$	$>1 \times 10^6$

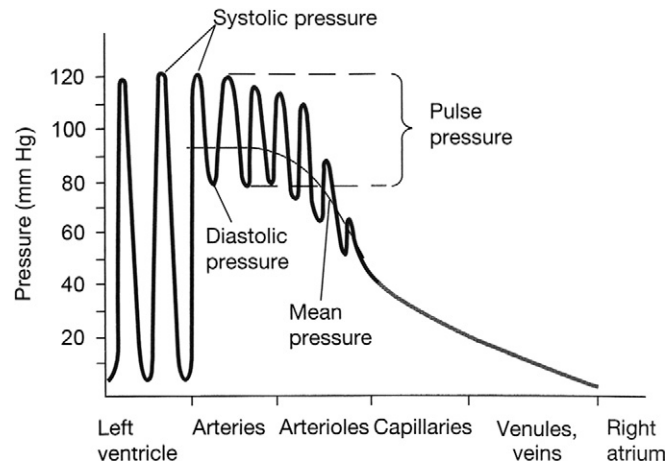
**FIGURE 16.4** Branching of the airways in the human lungs. Areas have units of cm<sup>2</sup>. *Reproduced with permission from Silverthorn, D. U. (2001), Human Physiology: An Integrated Approach, 2nd ed., Prentice Hall, Upper Saddle River, NJ.*

## The Heart as a Pump

The heart has four pumping chambers—two atria (upper) and two ventricles (lower). The left and right parts of the heart are separated by a muscle called the *septum* which keeps the blood volumes in each part separate. The upper chambers interact with the lower chambers via the heart valves. The heart has four valves which ensure that blood flows only in the desired direction. The atrio-ventricular valves (AV) consist of the tricuspid (three flaps) valve between the right atrium and the right ventricle, and the bicuspid (two flaps, also called the *mitral*) valve between the left atrium and the left ventricle. The pulmonary valve is between the right ventricle and the pulmonary artery, and the aortic valve is between the left ventricle and the aorta. Both the pulmonary and aortic valves have three symmetrical half-moon-shaped valve flaps (cusps), and are called the *semilunar valves*. The function of the four chambers in the heart is to pump blood through pulmonary and systemic circulations. The atria receive blood from the veins—the right atrium receives carbon dioxide-rich blood from the SVC and IVC, and the left atrium receives oxygen-rich blood from the pulmonary veins. The heart is controlled by a single electrical impulse and both sides of the heart act synchronously. Electrical activity stimulates the heart muscle (myocardium) of the chambers of the heart to make them contract. This is immediately followed by mechanical contraction of the heart. Both atria contract at the same time. The contraction of the atria moves the blood from the upper chambers through the valves into the ventricles. The atrial muscles are electrically separated from the ventricular muscles except for one pathway through which an electrical impulse is conducted from the atria to the ventricles. The impulse reaching the ventricles is delayed by about 110 ms while the conduction occurs through the pathway. This delay allows the ventricles to be filled before they contract. The left ventricle is a high-pressure pump and its contraction supplies systemic circulation while the right ventricle is a low-pressure pump supplying pulmonary circulation (lungs offer much less resistance to flow than systemic organs).

From the above discussions, we see that the pumping action of the heart can be regarded as a two-step process—a contraction step (systole) and a filling (relaxation) step (diastole). Systole describes that portion of the heartbeat during which contraction of the heart muscle and hence ejection of blood takes place. A single *beat* of the heart involves three operations: atrial systole, ventricular systole, and complete cardiac diastole. Atrial systole is the contraction of the heart muscle of the left and right atria, and occurs over a period of 0.1 s. As the atria contract, the blood pressure in each atrium increases, which forces the mitral and tricuspid valves to open, forcing blood into the ventricles. The AV valves remain open during atrial systole. Following atrial systole, ventricular systole, which is the contraction of the muscles of the left and right ventricles, occurs over a period of 0.3 s. The ventricular systole generates enough pressure to force the AV valves to close, and the aortic and pulmonic valves open. (The aortic and pulmonic valves are always closed except for the short period of ventricular systole when the pressure in the ventricle rises above the pressure in the aorta for the left ventricle and above the pressure in the pulmonary artery for the right ventricle.) During systole, the typical pressures in the aorta and the pulmonary artery rise to 120 mm Hg and 24 mm Hg, respectively (1 mm Hg = 133 Pa). In normal adults, blood flow through the aortic valve begins at the start of ventricular systole and rapidly

accelerates to a peak value of approximately 1.35 m/s during the first one-third of systole. Thereafter, the blood flow begins to decelerate. Pulmonic valve peak velocities are lower, and in normal adults they are about 0.75 m/s. Contraction of the ventricles in systole ejects about two-thirds of the blood from these chambers. As the left ventricle empties, its pressure falls below the pressure in the aorta, and the aortic valve closes. Similarly, as the pressure in the right ventricle falls below the pressure in the pulmonary artery, the pulmonic valve closes. Thus, at the end of the ventricular systole, the aortic and pulmonic valves close, with the aortic valve closing a little earlier than the pulmonic valve. Diastole describes that portion of the heartbeat during which the chamber refilling takes place. The cardiac diastole is the period of time when the heart relaxes after contraction in preparation for refilling with circulating blood. The ventricles refill or ventricular diastole occurs during atrial systole. When the ventricle is filled and ventricular systole begins, then the AV valves are closed and the atria begin refilling with blood, or atrial diastole occurs. About a period of 0.4 s following ventricular systole, both the atria and the ventricles begin refilling and both chambers are in diastole. During this period, both AV valves are open and aortic and pulmonic valves are closed. The typical diastolic pressure in the aorta is 80 mm Hg, and in the pulmonary artery it is 8 mm Hg. Thus, the typical systolic and diastolic pressure ratios are 120/80 mm Hg for the aorta and 24/8 mm Hg for the pulmonary artery. The systolic pressure minus the diastolic pressure is called the *pressure pulse*, and for the aorta (left ventricle) it is 40 mm Hg. The pulse pressure is a measure of the strength of the pressure wave. It increases with increased stroke volume (say, due to activity or exercise). Pressure waves created by the ventricular contraction diminish in amplitude with the distance from the heart and are not perceptible in the capillaries. Figure 16.5 shows the pressure throughout the systemic circulation.

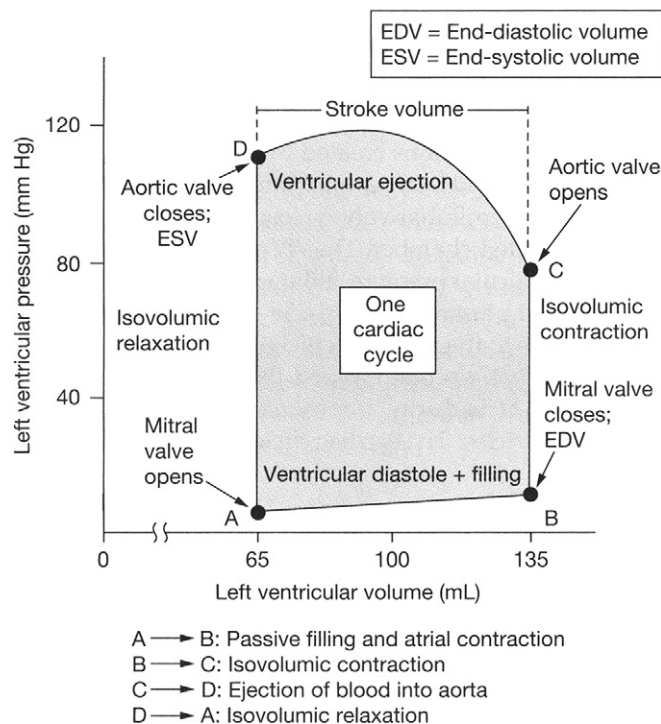


**FIGURE 16.5** Pressure variations throughout the systemic circulation. The largest pressure fluctuations occur in the left ventricle. These are gradually damped out by the flexibility of the arteries, blood viscosity, and the branched nature of the system. Reproduced with permission from Silverthorn, D. U. (2001), *Human Physiology: An Integrated Approach*, 2nd ed., Prentice Hall, Upper Saddle River, NJ.



### Net Work Done by the Ventricle on the Blood During One Cardiac Cycle

The work done by the ventricle on blood may be calculated from the area enclosed by the pressure–volume curve for the ventricle. Consider, for example, the left ventricle (LV). Figure 16.6 shows the pressure–volume curve for the LV. Blood pressure is measured in mm of Hg, and the volume in mL. At A, the ventricular pressure and volume are at their lowest values. With the increase of atrial pressure, the bicuspid valve will open and let blood flow into the ventricle. AB represents diastolic ventricular filling. During AB work is being done by the blood in the LV to increase the volume. At B, the ventricular volume is filled to its maximum and this volume is called the *end diastolic volume* (EDV). The ventricular muscles begin to contract, pressure increases, and the bicuspid valve closes. BC is the constant-volume contraction of the ventricle. No work is done during BC but energy is stored as elastic energy in the muscles. At C, ventricular pressure is greater than that in the aorta, the aortic valve opens, and blood is ejected into the aorta. Ventricular volume decreases, but the ventricle continues to contract and the pressure increases. However, at D, pressure in the aorta exceeds that of the ventricular pressure and the aortic valve closes. During CD, work is done by the heart muscles on blood. The volume in the LV at D is at its lowest value,



**FIGURE 16.6** Left ventricular pressure–volume curve for one cardiac cycle. The work done by the left ventricle is the shaded area. The cardiac cycle follows the edge of the shaded area in the counterclockwise direction. Reproduced with permission from Silverthorn, D. U. (2001), *Human Physiology: An Integrated Approach*, 2nd ed., Prentice Hall, Upper Saddle River, NJ.

and this is called the *end systolic volume* (*ESV*). *DA* is the constant-volume pressure decrease in the ventricle due to muscle relaxation and no work is done during this process. Ventricular pressure falls below that in the aorta causing the aortic valve to close. *ABCD* constitutes one cardiac cycle, and the area within the pressure-volume diagram represents the net work done by the *LV* on blood. The energy required to perform this work is derived from the oxygen in the blood. A similar development applies for the right ventricle.

Typically, the work done by the heart is only about 10–15% of the total input energy. The remainder is dissipated as heat.

The volume of blood pumped by the *LV* into the systemic circulation in a cardiac cycle is called the *stroke volume* (*SV*), and it is expressed in mL/beat. The normal stroke volume is 70 mL/beat.

$$SV = EDV - ESV \quad (16.1)$$

A parameter that is related to stroke volume is ejection fraction (*EF*). *EF* is the fraction of blood ejected by the *LV* during systole. At the start of systole, the *LV* is filled with blood to the *EDV*. During systole, the *LV* contracts and ejects blood until it reaches *ESV*. *EF* is given by

$$EF = (SV/EDV) \times 100\%. \quad (16.2)$$

Cardiac output (*CO*) is the volume of blood being pumped by the heart (in particular, by a ventricle) in a minute. It is the time-averaged flow rate. It is equal to the heart rate multiplied by the stroke volume. Thus,

$$CO = SV \times HR, \quad (16.3)$$

where *HR* is the heart rate in beats/min. For a normal adult, the typical *HR* is between 70 and 75 beats per minute. With 70 beats per minute, and 70 mL blood ejection with each beat of the heart, the *CO* is 4900 mL/m. This value is typical for a normal adult at rest, although *CO* may reach up to 30 L/m during extreme activity (say, exercise). Heart rate can vary by a factor of approximately 3, between 60 and 180 beats per minute, while the stroke volume can vary between 70 and 120 mL, a factor of only 1.7. The cardiac index (*CI*) relates *CO* with the body surface area, *BSA*, as given by:

$$CI = CO/BSA = SV \times HR/BSA, \quad (16.4)$$

where *BSA* is in square meters.

## Nature of Blood

Blood is about 7% of the human body weight. Its density is approximately 1054 kg/m<sup>3</sup>. The pH of normal blood is in the range 7.35 < pH < 7.45. The normal adult has a blood volume of about 5 liters. At any given time, about 13% of the total blood volume resides in the arteries and about 7% resides in the capillaries. Blood is a complex circulating liquid tissue consisting of several types of formed elements (corpuscles or cells; about 45% by volume) suspended in a fluid medium known as *plasma* (about 55% by volume; 2.7–3.0 liters in a normal human). The plasma is a dilute electrolyte solution (almost 92% water) containing, about 8% by weight, three major types of blood proteins—fibrinogen (5%), globulin (45%), and albumin (50%) in water. Beta lipoprotein and lipalbumin are also present in trace

amounts. Plasma proteins are large molecules with high molecular weight and do not pass through the capillary wall. The formed elements (cells) consist of red blood cells (erythrocytes; about 45% of blood volume), white blood cells (leukocytes; about 1% of blood volume), and platelets (thrombocytes; <1% of blood volume). Thus, the formed elements in blood consist of 95% red blood cells, 0.13% white blood cells, and about 4.9% platelets. The specific gravity of red blood cells is about 1.06. The white blood cells further consist of monocytes, lymphocytes, neutrophils, eosinophils, and basophils.

In humans, mature red blood cells lack a nucleus and organelles. They are produced in the bone marrow, and the cell life span is about 125 days. The red blood cell is biconcave in shape. It consists of a concentrated solution of hemoglobin, an oxygen-carrying protein, surrounded by a flexible membrane. The hemoglobin transports oxygen (and some carbon dioxide) from the lungs to capillaries in various tissues. The cell is about  $8.5\ \mu\text{m}$  in diameter with transverse dimensions of  $2.5\ \mu\text{m}$  at the thickest portion and about  $1\ \mu\text{m}$  at the thinnest portion. However, its flexibility is such that it can bend and pass through capillaries as small as  $5\ \mu\text{m}$  in diameter. The surface area of the cell is about  $163\ (\mu\text{m})^2$ , and the intracellular fluid volume is about  $87\ (\mu\text{m})^3$ . There are approximately  $5 \times 10^6$  red blood cells in each  $\text{mm}^3$  of blood. The biconcave shape of the cell provides it with a very large ratio of surface area to volume. This enables efficient gas exchange in the capillaries. The percentage of blood volume made up by red blood cells is referred to as the *hematocrit*. Hematocrit ranges from 42 to 45 in normal blood, and plays a major role in determining the rheological properties of blood. White blood cells, or leukocytes, are cells of the immune system which defend the body against infectious disease and foreign materials. Several different and diverse types of leukocytes exist and they are all produced in the bone marrow. There are normally about  $10^4$  white blood cells in each  $\text{mm}^3$  of blood. Platelets or thrombocytes are cell fragments circulating in blood that are involved in the cellular mechanisms of hemostasis leading to the formation of blood clots. They are smaller in size than red or white blood cells. Low levels of platelets predisposes to a person bleeding, while high levels increase the risk of thrombosis (coagulation of blood in the heart or a blood vessel).

Blood is a non-Newtonian fluid. Its viscosity depends on the viscosity of the plasma, its protein content, the hematocrit, the temperature, the shear rate (also called the *rate of shearing strain*), and the narrowness of the vessel in which it is flowing (for example, a narrow diameter capillary). The dependence on the narrowness of the vessel diameter is called the *Fahraeus-Lindqvist effect*. The presence of white cells and platelets does not significantly affect the viscosity since they are such a small fraction of the formed elements. We will briefly discuss the various dependencies of blood viscosity.

The viscosity of plasma and blood are often given in terms of relative viscosity as compared to that of water (viscosity of water is about 0.8 centipoise at  $30^\circ\text{C}$ ; 1 centipoise (1 cP) =  $0.01\ \text{Poise} = 1\ \text{dyne s/cm}^2 = 0.1\ \text{N s/m}^2$ ). The viscosity of plasma depends on its protein content and ranges between 1.1 and 1.6 centipoise. The viscosity of whole blood at a physiological hematocrit of 45% is about 3.2 cP. Higher hematocrit results in higher viscosity. At a hematocrit of 60%, the relative viscosity of blood is about 8. Blood viscosity increases with decreasing temperature, and the increase is approximately 2% for each  $^\circ\text{C}$ . The dependence of viscosity on flow rate in vessels is complicated. As noted in earlier chapters, flow rates through tubes are significantly influenced by the shear stress,  $\tau$ , and the associated rate of shearing strain (or shear rate),  $\dot{\gamma}$ . For Newtonian fluids,  $\tau$  is linearly related to  $\dot{\gamma}$ .

For example,  $\tau = \mu\dot{\gamma}$  and the slope of this characteristic is the viscosity,  $\mu$ . For whole blood, this relationship between  $\tau$  and  $\dot{\gamma}$  is complicated for the following reasons. In a blood volume at rest, above a minimum hematocrit of about 5–8%, blood cells form a continuous structure. A finite stress (called the *yield stress*),  $\tau_y$ , is required to break this continuous structure into a suspension of aggregates in the plasma. This yield stress also depends on the concentration of plasma proteins, in particular, fibrinogen. An empirical correlation for the yield stress is given by the expression:

$$\sqrt{\tau_y} = (H - 0.1)(C_F + 0.5), \quad (16.5)$$

where  $H$  is the hematocrit expressed as a fraction and it is  $> 0.1$ , and  $C_F$  is the fibrinogen content in grams per 100 mL and  $0.21 < C_F < 0.46$ . For 45% hematocrit blood, the yield stress is in the range  $0.01 < \tau_y < 0.06$  dyne/cm<sup>2</sup> (1 dyne/cm<sup>2</sup> = 0.1 N/m<sup>2</sup>). Beyond the yield stress, when sheared in the bulk, up to about  $\dot{\gamma} < 50$  sec<sup>-1</sup>, the aggregates in blood break into smaller units called *rouleaux formations*. For shear rates up to about 200 sec<sup>-1</sup>, the rouleaux progressively break into individual cells. Beyond this, no further reduction in structure is noted to occur with an increase in the shearing rate.

For whole blood, at low shear rates,  $\dot{\gamma} < 200$  sec<sup>-1</sup>, the variation of  $\tau$  with  $\dot{\gamma}$  is noted to be nonlinear. This behavior at low  $\dot{\gamma}$  is non-Newtonian. Low  $\dot{\gamma}$  values are associated with flows in small arteries and capillaries (microcirculation). At higher shear rates,  $\dot{\gamma} > 200$  sec<sup>-1</sup>, the relationship between  $\tau$  and  $\dot{\gamma}$  is linear, and the viscosity approaches an asymptotic value of about 3.5 cP. Blood flows in large arteries have such high shear rates, and the viscosity in such cases may be assumed as constant and equal to 3.5 cP. Since whole blood behaves like a non-Newtonian yield stress fluid, the slope of the shear stress—rate of strain characteristic at any given point on the curve—is defined as the apparent viscosity of blood at that point,  $\mu_{app}$ . Clearly,  $\mu_{app}$  is not a constant but depends on the prevailing  $\dot{\gamma}$  at that point (see Figure 16.7). There are a number of constitutive equations available in the literature that attempt to model the relationship between shear stress and shear rate of flowing blood. A commonly used one is called the *Casson model* and it is expressed as follows:

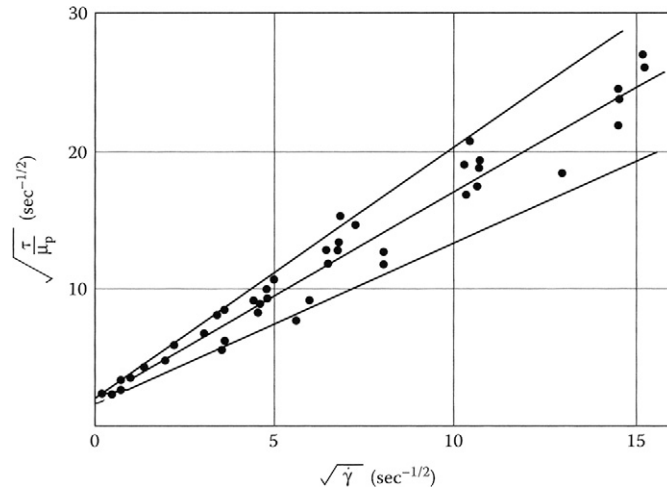
$$\sqrt{\frac{\tau}{\mu_p}} = k_c \sqrt{\dot{\gamma}} + \sqrt{\frac{\tau_y}{\mu_p}}, \quad (16.6)$$

where  $\mu_p$  is plasma viscosity and  $k_c$  is the Casson viscosity coefficient (a dimensionless number). An expression based on a least squares fit of the experimental data and expressed in Casson form is that of Whitmore (1968):

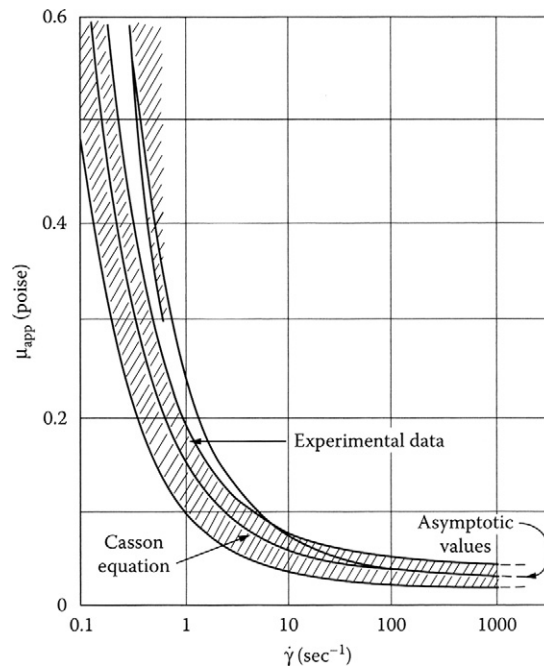
$$\sqrt{\frac{\tau}{\mu_p}} = 1.53\sqrt{\dot{\gamma}} + 2.0. \quad (16.7)$$

This expression is plotted in Figure 16.8. Apparent viscosity significantly increases at low rates of shear. It must be noted that although the Casson model is suitable at low shear rates, it still assumes that blood can be modelled as a homogeneous fluid.

In blood vessels of less than about 500  $\mu\text{m}$  in diameter, the inhomogeneous nature of blood starts to have an effect on the apparent viscosity. This feature will be discussed next.



**FIGURE 16.7** Shear stress versus shear rate for blood flow. Note that the shear stress is finite at small (approximately zero) shear rates. Blood is a non-Newtonian fluid. *Reproduced with permission from Whitmore, R. L. (1968), Rheology of Circulation, Pergamon Press, New York.*



**FIGURE 16.8** A least square fit of apparent viscosity as a function of shear rate in Casson form. The apparent viscosity of blood falls with increasing shear rate making it a shear-thinning fluid. *Reproduced with permission from Whitmore, R. L. (1968), Rheology of Circulation, Pergamon Press, New York.*

### Fahraeus-Lindqvist Effect

When blood flows through narrow tubes of decreasing radii, approximately in the range  $15\ \mu\text{m} < d < 500\ \mu\text{m}$ , the apparent viscosity,  $\mu_{app}$ , decreases with decreasing radius of the vessel. This is a second non-Newtonian characteristic of blood and is called the *Fahraeus-Lindqvist (FL) effect*. The reduced viscosity in narrow tubes is beneficial to the pumping action of the heart.

The basis for the FL effect is the Fahraeus effect. When blood of constant hematocrit (feed hematocrit or bulk hematocrit,  $H_F$ ) flows from a large vessel into a small vessel (vessel sizes in the ranges cited earlier), the hematocrit in the small vessel (dynamic or tube hematocrit,  $H_T$ ) decreases as the tube diameter decreases (see Figure 16.9). This phenomenon is called the *Fahraeus effect* and must not be confused with a diminution of particle concentration in the smaller vessel because of an entrance effect whereby particle entry into the smaller vessel is hindered (see Goldsmith et al., 1989, for detailed discussions). To separate such an entry-screening effect and confirm the Fahraeus effect,  $H_T$  may be compared with the hematocrit in the blood flowing out (discharge hematocrit,  $H_D$ ) from the smaller tube into a discharge vessel of comparable size to the feed vessel. In the steady state,  $H_F = H_D$ . In vivo and in vitro experiments show that  $H_T < H_D$  in tubes up to about  $15\ \mu\text{m}$  in diameter. The  $H_T/H_D$  ratio decreases from about 1 to about 0.46 as the capillary diameter decreases from about  $600\ \mu\text{m}$  to about  $15\ \mu\text{m}$ . While the discharge hematocrit value may be 45%, the corresponding dynamic hematocrit in a narrow-sized vessel such as an arteriole may be just 20%. As a consequence, the apparent viscosity decreases in the diameter range  $15\ \mu\text{m} < d < 500\ \mu\text{m}$ . However, for tubes less than about  $15\ \mu\text{m}$  in diameter, the ratio  $H_T/H_D$  starts to increase.

Why does the hematocrit decrease in small blood vessels? The reason for this effect is not fully understood at this time. In blood vessel flow, there seems to be a tendency for the red cells to move toward the axis of the tube, leaving a layer of plasma, whose width, usually designated by  $\delta$ , increases with increasing shear rate. This tendency to move away from the wall is not observed with rigid particles; thus, the deformability of the red cell appears to be the reason for lateral migration. Deformable particles are noted to experience a net radial hydrodynamic force even at low Reynolds numbers and tend to migrate toward the tube axis (see Fung, 1993, for detailed discussions). Chandran et al. (2007) state that as the blood flows through a tube, the blood cells (with their deformable biconcave shape) rotate (spin) in the shear field. Due to this spinning, they tend to move away from the wall and toward the center of the tube. The cell-free plasma layer reduces the tube hematocrit. As the size of the vessel gets smaller, the fraction of the volume occupied by the cell-free layer increases, and the tube

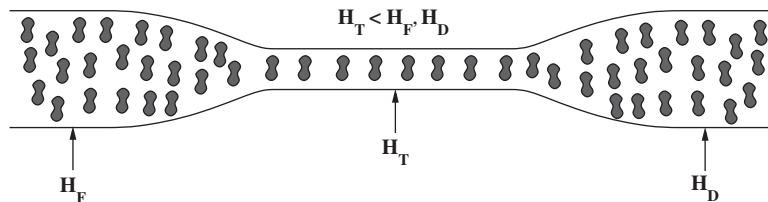


FIGURE 16.9 The Fahraeus effect. Here the hematocrit falls as blood moves from larger to smaller vessels because of non-Newtonian effects, the particulate nature of blood cells, and other factors.

hematocrit is further lowered. A numerical validation of this reasoning is available in a paper by Liu and Liu (2006). There is yet another reason. Blood vessels have many smaller-sized branches. If a branching daughter vessel is so located that it draws blood from the larger parent vessel, mainly from the cell-free layer, then the hematocrit in the branch will end up being lower. This is called *plasma skimming*. In all these circumstances, the tube hematocrit is lowered. The viscosity of blood at the core may be higher due to a higher core hematocrit,  $H_c$ , there, but the overall apparent viscosity in the tube flow is lower.

As the tube diameter becomes less than about  $6\text{ }\mu\text{m}$ , the apparent viscosity increases dramatically. The erythrocyte is about  $8\text{ }\mu\text{m}$  in diameter and can enter tubes somewhat smaller in size, and a tube of about  $2.7\text{ }\mu\text{m}$  is about the smallest size that an RBC can enter (Fournier, 2007; Fung, 1993). When the tube diameter becomes very small, the pressure drop associated with the flow increases greatly and there is increase in apparent viscosity.

If we consider laminar blood flow in straight, horizontal, circular, feed, and capillary tubes, a number of straightforward relationships among  $Q_F$ ,  $Q_c$ ,  $Q_p$ ,  $H_F$ ,  $H_T$ ,  $H_c$ ,  $\delta$ , and  $a$  may be established based on the law of conservation of blood cells. Here,  $Q$  denotes flow rate, subscripts  $c$  and  $p$  denote core and plasma regions, respectively, and  $a$  is the radius of the capillary tube. Thus,

$$Q_F H_F = Q_c H_c, \quad Q_c + Q_p = Q_F, \quad \text{and} \quad H_T a^2 = H_c (a - \delta)^2, \quad (16.8)$$

where  $a$  is the radius of the capillary tube. Equation (16.8) will be useful in modeling the FL phenomenon. A simple mathematical model for the FL effect is included in a subsequent section.

## Nature of Blood Vessels

All blood vessels other than capillaries are usually composed of three layers: the tunica intima, tunica media, and tunica adventitia. The tunica intima consists of a layer of endothelial cells lining the lumen of the vessel (the hollow internal cavity in which the blood flows), as well as a subendothelial layer made up of mostly loose connective tissue. The endothelial cells are in direct contact with the blood flow. An internal elastic lamina often separates the tunica intima from the tunica media. The tunica media is composed chiefly of circumferentially arranged smooth muscle cells. Again, an external elastic lamina often separates the tunica media from the tunica adventitia. The tunica adventitia is primarily composed of loose connective tissue made up of fibroblasts and associated collagen fibers. In the largest arteries, such as the aorta, the amount of elastic tissue is considerable. Veins have the same three layers as arteries, but boundaries are indistinct, walls are thinner, and elastic components are not as well developed.

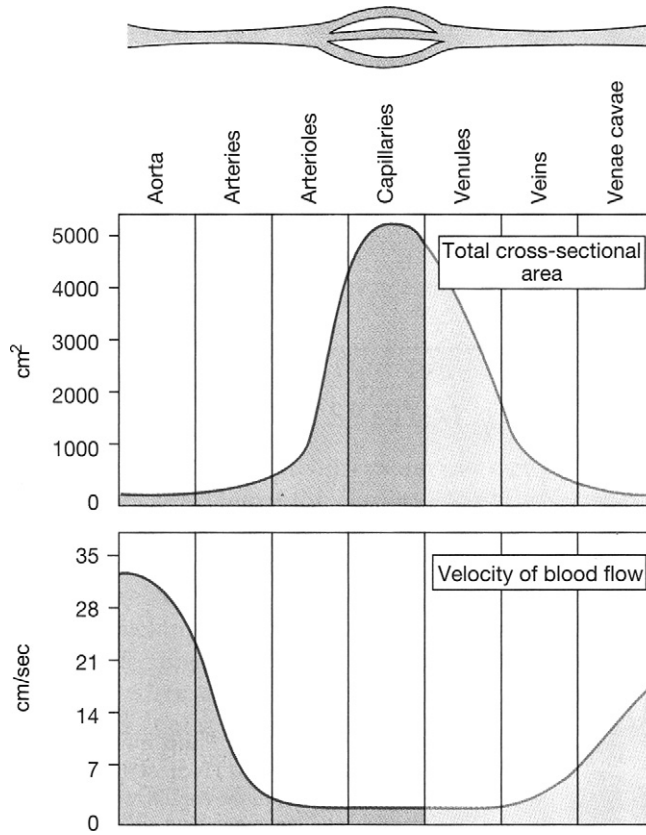
Blood flows under high pressure in the aorta (about 120 mm Hg systolic, 80 mm Hg diastolic, pressure pulse of 40 mm Hg at the root) and the major arteries. These vessels have strong walls. The aorta is an elastic artery, about 25 mm in diameter with a wall thickness of about 2 mm, and is quite distensible. During left ventricular systole (about one-third of the cardiac cycle), the aorta expands. This stretching provides the potential energy that will help maintain blood pressure during diastole. During the diastole (about two-thirds of the cardiac cycle), the pressure pulse decays exponentially and the aorta contracts

passively. Medium arteries are about 4 mm in diameter with a wall thickness of about 1 mm. Arterioles are about 50  $\mu\text{m}$  in diameter and have thin muscular walls (usually only one to two layers of smooth muscle) of about 20  $\mu\text{m}$  thickness. Their vascular tone is controlled by regulatory mechanisms, and they constrict or relax as needed to maintain blood pressure. Arterioles are the primary site of vascular resistance and blood-flow distribution to various regions is controlled by changes in resistance offered by various arterioles. True capillaries average from 9 to 12  $\mu\text{m}$  in diameter, just large enough to permit passage of cellular components of blood. The thin wall consists of extremely attenuated endothelial cells. In cross section, the lumen of small capillaries may be encircled by a single endothelial cell, while larger capillaries may be made up of portions of 2 or 3 cells. No smooth muscle is present. Venules are about 20  $\mu\text{m}$  in diameter and allow deoxygenated blood to return from the capillary beds to the larger veins. They have three layers: an inner endothelium layer which acts as a membrane, a middle layer of muscle and elastic tissue, and an outer layer of fibrous connective tissue. The middle layer is poorly developed. The walls of venules are about 2  $\mu\text{m}$  in thickness, and thus are very much thinner than those of arterioles. Veins are thin-walled, distensible, and collapsible tubes. Some of them may be collapsed in normal function. They transport blood at a lower pressure than the arteries. They are about 5 mm in diameter and the wall thickness is about 500  $\mu\text{m}$ . They are surrounded by helical bands of smooth muscles which help maintain blood flow to the right atrium. Most veins have one-way flaps called *venous valves*. These valves prevent gravity from causing blood to flow back and collect in the lower extremities. Veins more distal to the heart have more valves. Pulmonary veins and the smallest venules have no valves. Veins also have a thick collagen outer layer, which helps maintain blood pressure. In the venous system, a large increase in the blood volume results in a relatively small increase in pressure compared to the arterial system (see [Chandran et al., 2007](#)). The veins act as the main reservoir for blood in the circulatory system and the total capacity of the veins is more than sufficient to hold the entire blood volume of the body. This capacity is reduced through the constriction of smooth muscles, minimizing the cross-sectional area (and hence volume) of the individual veins and therefore the total venous system. The superior vena cava is a large, yet short vein that carries deoxygenated blood from the upper half of the body to the heart's right atrium. The inferior vena cava is the large vein that carries deoxygenated blood from the lower half of the body into the heart. The vena cava is about 30 mm in diameter with a wall thickness of about 1.5 mm. The venae cavae have no valves. [Figure 16.10](#) shows the cross-sectional areas of different parts of the systemic circulation with velocity of blood flow in each part. The fastest flow is in the arterial system. The slowest flow is in the capillaries and venules.

As stated earlier, arterioles are the primary site of vascular flow resistance, and blood-flow distribution to various regions is controlled by changes in resistance offered by various arterioles. To quantify the resistance of the arterioles in an averaged sense, the concept of *total peripheral resistance* is introduced. Total peripheral resistance essentially refers to the cumulative resistance of the thousands of arterioles involved in the systemic or pulmonary circulation, respectively. For systemic circulation, with time averaging of quantities over a cardiac cycle:

$$\text{Total Peripheral Resistance} = R = \frac{\Delta \bar{p}}{Q}, \quad (16.9)$$





**FIGURE 16.10** Vessel diameter, total cross-sectional area, and velocity of flow. The total cross-sectional area available for flow is largest at the capillary size because there are so many. The highest blood-flow speeds are found in the largest arteries and veins. *Reproduced with permission from Silverthorn, D. U. (2001), Human Physiology: An Integrated Approach, 2nd ed., Prentice Hall, Upper Saddle River, NJ.*

where  $R$  denotes resistance,  $\Delta\bar{p}$  is the difference between the time-averaged pressure at the aortic valve and the time-averaged venous pressure at the right atrium, and  $Q$  is the time-averaged flow rate (cardiac output). The units of peripheral resistance would therefore be in mm Hg per  $\text{cm}^3/\text{s}$ . This unit of measuring resistance is called the *peripheral resistance unit (PRU)*. Letting  $\bar{p}_A$  and  $\bar{p}_V$  denote the time-averaged pressures at the aortic valve and at the right atrium, respectively:

$$\Delta\bar{p} = \bar{p}_A - \bar{p}_V, \quad (16.10)$$

and, with  $\bar{p}_V = 0$ ,  $\Delta\bar{p} = \bar{p}_A$ , the time-averaged arterial pressure. Then,  $\bar{p}_A = QR$ . The average pressure,  $\bar{p}_A$ , may be estimated as:

$$\bar{p}_A = \frac{1}{3}p_S + \frac{2}{3}p_D = p_D + \frac{1}{3}(p_S - p_D), \quad (16.11)$$

where  $p_s$  is the systolic pressure,  $p_D$  is the diastolic pressure, and  $(p_s - p_D)$  is the pressure pulse (see Kleinstreuer, 2006). For a normal person at rest, with  $\bar{p}_A = 100$  mmHg and  $Q = 86.6$  cm<sup>3</sup>/s, then  $R = 1.2$  PRU. An expression similar to that in (16.9) would apply for pulmonary circulation and would involve the difference between time-averaged pressures at the pulmonary artery and at the left atrium, and the flow rate in pulmonary circulation (same as that in systemic circulation). Since the difference between time-averaged pressures in pulmonary circulation is about an order of magnitude smaller than in the systemic circulation, the corresponding PRU would be an order of magnitude smaller.

### 16.3. MODELING OF FLOW IN BLOOD VESSELS

There are approximately 100,000 km of blood vessels in the adult human body (Brown et al., 1999). In this section, we examine several models for describing blood flow in some important vessels.

Blood flow in the circulatory system is in general unsteady. In most regions it is pulsatile due to the systolic and diastolic pumping. In pulsatile flow, the flow has a periodic behavior and a net directional motion over the cycle. Pressure and velocity profiles vary periodically with time, over the duration of a cardiac cycle. A dimensionless parameter called the *Womersley number*,  $\alpha$ , is used to characterize the pulsatile nature of blood flow, and it is defined by:

$$\alpha = a\sqrt{\frac{\omega}{\nu}}, \quad (16.12)$$

where  $a$  is the radius of the tube,  $\omega$  is the frequency of the pulse wave (heart rate expressed in radians/sec), and  $\nu$  is the kinematic viscosity. This definition shows that the Womersley number is a composite parameter of the Reynolds number,  $Re = 2au/\nu$ , and the Strouhal number,  $St = 2a\omega/u$ . The square of the Womersley number is called the *Stokes number*. The Womersley number denotes the ratio of unsteady inertial forces to viscous forces in the flow. It ranges from as large as about 20 in the aorta, to significantly greater than 1 in all large arteries, to as small as about  $10^{-3}$  in the capillaries.

Let us estimate the Womersley number for an illustration. With a normal heart rate of 72 beats per minute,  $\omega = (2\pi \cdot 72/60) \approx 8$  rad/s. Take  $\rho = 1.05$  g cm<sup>-3</sup>,  $\mu = 0.04$  g cm<sup>-1</sup> s<sup>-1</sup>, and an artery of radius  $a = 0.5$  cm. Then  $\alpha \approx 7$ . Decreasing  $\alpha$  values correspond to increasing role of viscous forces and, for  $\alpha < 1$ , viscous effects are dominant. In that highly viscous regime, the flow may be regarded as quasi-steady. With increasing  $\alpha$ , inertial forces become important. In pulsatile flows, flow separation may occur both by a geometric adverse pressure gradient, and/or by time-varying changes in the driving pressure. Geometric adverse-pressure gradients may arise due to varying cross-sectional areas through which the flow passes. On the other hand, time-varying changes in a cardiac cycle result in acceleration and deceleration during the cycle. An adverse-pressure gradient during the deceleration phase may result in flow separation.

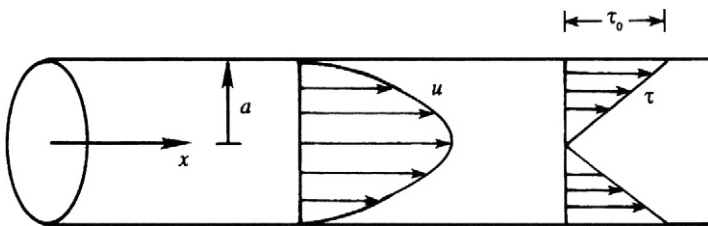
Blood vessel walls are viscoelastic in their behavior. The ability of a blood vessel wall to expand and contract passively with changes in pressure is an important function of large

arteries and veins. This ability of a vessel to distend and increase volume with increasing transmural pressure difference (inside minus outside pressure) is quantified as vessel compliance. During systole, pressure from the left ventricle is transmitted as a wave due to the elasticity of the arteries. Due to the compliant nature of the arteries and their finite thickness, the pressure travels like a wave at a speed much faster than the flow velocity. Since blood vessels may have many branches, the reflection and transmission of waves in such branching vessels significantly complicate the understanding of such flows. In this chapter, a reasonably simplified picture of these various complex features will be presented. Further reading in advanced treatments such as the book by Fung (1997) will be necessary to obtain a comprehensive understanding.

## Steady Blood Flow Theory

First we start with the study of laminar, steady flow of blood in circular tubes, and in subsequent sections, we shall consider more realistic models. In the simplest model, blood flow in a vessel is modeled as a laminar, steady, incompressible, fully developed flow of a Newtonian fluid through a straight, rigid, cylindrical, horizontal tube of constant circular cross section (see Figure 16.11). Such a flow is called *circular Poiseuille flow* or more commonly *Hagen-Poiseuille flow*, and is covered in Section 8.2. The primary question here is: How valid is a Hagen-Poiseuille model for blood flow? Issues related to the assumptions inherent in Hagen-Poiseuille flow are summarized in the following paragraphs.

In the normal body, blood flow in vessels is generally laminar. However, at high flow rates, particularly in the ascending aorta, the flow may become turbulent at or near peak systole. Disturbed flow may occur during the deceleration phase of the cardiac cycle (Chandran et al., 2007). Turbulent flow may also occur in large arteries at branch points. However, under normal conditions, the critical Reynolds number,  $Re_c$ , for transition of blood flow in long, straight, smooth blood vessels is relatively high, and the blood flow remains laminar. Let us consider some estimates. The aorta is about 40 cm long and the average velocity  $u$  of flow in it is about 40 cm/s. The lumen diameter at the root of the aorta is  $d = 25$  mm, and the corresponding  $Re = \rho u d / \mu$  is  $\sim 3000$ . The maximum Reynolds number may be as high as 9000. The average value for  $Re$  in the vena cava is also about 3000. Arteries have varying sizes and the maximum  $Re$  is about 1000. For Newtonian fluid flow in a straight cylindrical rigid tube,  $Re_c$  is about  $\sim 3000$ . However, aorta and arteries are distensible tubes, and this  $Re_c$  criterion does not apply. In the case of blood flow, laminar flow conditions generally prevail even at Reynolds numbers as high as 10,000 (Mazumdar, 2004). In summary, the laminar flow assumption is reasonable in many cases.



**FIGURE 16.11** Poiseuille flow. Here the  $x$ -axis is coincident with the tube axis, and the radial coordinate is  $r$ . The fluid velocity has a parabolic profile and is entirely in the  $x$ -direction. The shear within the flow is zero at  $r = 0$  and increases linearly with  $r$ , reaching a maximum at  $r = a$ , the tube radius.

Blood flow in the circulatory system is generally unsteady and pulsatile. The large arteries have elastic walls and are subject to substantially pulsatile flow. The steady-flow assumption is inapplicable until the flow has reached smaller muscular arteries and arterioles in the circulatory system. Blood flow in arteries has been described by several authors (see McDonald, 1974; Pedley, 1980; Ku, 1997).

In the heart chambers and blood vessels, blood may be considered incompressible. In the walls of the heart and in the blood vessel walls, it may not be considered as incompressible (Fung, 1997).

The fully developed flow assumption is very restrictive in describing blood flow in vessels. Since blood flow remains laminar at very high Reynolds numbers, the entry length is very large in many cases, and branches and curved vessels hinder flow development.

Flow in large blood vessels may be generally regarded as Newtonian. The Newtonian fluid assumption is inapplicable at low shear rates such as those that would occur in arterioles and capillaries.

Many blood vessels are not straight but are curved and have branches. However, flow may be regarded to occur in straight sections in many cases of interest.

Arterial walls are not rigid but are viscoelastic and distensible. The pressure pulse generated during left ventricular contraction travels through the arterial wall. The speed of wave propagation depends upon the elastic properties of the wall and the fluid-structure interaction. Arterial branches and curves may cause reflections of the wave.

Gravitational and hydrostatic effects become very important for orientations of the body other than the supine position.

Systemic arteries are generally circular tubes but may have tapering cross sections, while the veins and pulmonary arteries tend to be elliptical.

However, there remain many situations where the Hagen-Poiseuille model is reasonably applicable. Thus, a recapitulation of the results from Chapter 8 is provided here using cylindrical coordinates  $(r, \theta, x)$  where  $x$  is the axial coordinate,  $r$  is the radial distance from the  $x$ -axis, and  $\theta$  is the circumferential (azimuthal) angle. The axial flow velocity,  $u = u(r)$ , in a pipe of radius,  $a$  (see (8.6)) is:

$$u(r) = \frac{r^2 - a^2}{4\mu} \left( \frac{dp}{dx} \right). \quad (16.13)$$

In a fully developed flow, the pressure gradient,  $(dp/dx)$ , is a constant, and it may be expressed in terms of the overall pressure difference:

$$\left( \frac{dp}{dx} \right) = -\frac{\Delta p}{L} = -\frac{(p_1 - p_2)}{L}, \quad (16.14)$$

where  $\Delta p$  is the imposed pressure difference, subscripts 1 and 2 denote inlet and exit ends, respectively, and  $L$  is the length of the entire tube. With (16.14), (16.13) becomes

$$u(r) = \left( \frac{a^2 \Delta p}{4\mu L} \right) \left( 1 - \frac{r^2}{a^2} \right). \quad (16.15)$$

The maximum velocity occurs at the center of the tube,  $r = 0$ , and is given by

$$u_{\max} = \left[ \frac{\Delta p}{4\mu L} a^2 \right]. \quad (16.16)$$

The volume flow rate is:

$$Q = \int_0^a u 2\pi r dr = -\frac{\pi a^4}{8\mu} \left( \frac{dp}{dx} \right) = \frac{\pi a^4}{8\mu} \frac{(p_1 - p_2)}{L} = \frac{\pi a^4}{8\mu} \frac{\Delta p}{L} = \frac{u_{\max}}{2} \pi a^2. \quad (16.17)$$

Equation (16.17) is called the *Poiseuille formula*. The average velocity over the cross section is:

$$V = \frac{Q}{A} = \frac{Q}{\pi a^2} = \frac{u_{\max}}{2}, \quad (16.18)$$

where  $A$  is the cross section of the tube. The shear stress at the tube wall is:

$$\tau_{xr}|_{r=a} = \tau = -\mu \left( \frac{du}{dr} \right) \Big|_{r=a} = -\frac{a}{2} \left( \frac{dp}{dx} \right) = -\frac{a}{2} \frac{\Delta p}{L}, \quad (16.19)$$

where the negative sign has been included to give  $\tau > 0$  with  $(du/dr) < 0$  (the velocity decreases from the tube centerline to the tube wall). The maximum shear stress occurs at the walls, and the stress decreases toward the center of the vessel.

The Hagen-Poiseuille equation and its derivatives are most applicable to flow in the muscular arteries. Modifications are likely to be required outside this range (see Brown et al., 1999). For an application of Poiseuille flow relationships in the context of perfused tissue heat transfer and thermally significant blood vessels, see Baish et al. (1986a, 1986b).

With the results for the Hagen-Poiseuille flow, we have from (16.9):

$$\text{Total Peripheral Resistance} = R = \frac{\Delta \bar{p}}{Q} = \frac{8\mu L}{\pi a^4} \quad (16.20)$$

Equation (16.20) shows that peripheral resistance to the flow of blood is inversely proportional to the fourth power of vessel diameter.

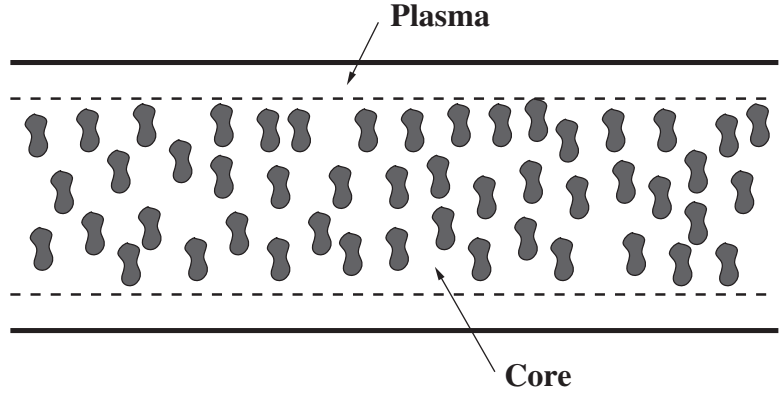
### **Hagen-Poiseuille Flow and the Fahraeus-Lindqvist Effect**

Consider laminar, steady flow of blood through a straight, rigid, cylindrical, horizontal tube of constant circular cross section and radius  $a$ , as shown in Figure 16.12, and let the flow be divided into two regions: a central core containing RBCs with axial velocity  $u_c$  and a cell-free plasma layer of thickness  $\delta$  surrounding the core with axial velocity  $u_p$ . In addition, let the viscosities of the core and the plasma layer be  $\mu_c$  and  $\mu_p$ , respectively. Let the shear rates be such that each region can be considered Newtonian, and that we could employ Hagen-Poiseuille theory.

The shear stress distribution in the core region is governed by:

$$\tau_{xr} = -\mu_c \frac{du^c}{dr} = -\frac{r}{2} \frac{\Delta p}{L}, \quad (16.21)$$

**FIGURE 16.12** Fahraeus-Lindqvist effect. When the core and the plasma flows have different viscosities and occupy different regions of the tube, the relationship between the volume flow rate and the pressure drop in a round tube can be found in terms of the geometry and the viscosities.



subject to conditions:

$$\frac{du^c}{dr} = 0, \quad \text{at } r = 0, \quad (16.22)$$

$$\tau_{xr}|_c = \tau_{xr}|_p, \quad \text{at } r = (a - \delta). \quad (16.23)$$

The shear stress distribution in the plasma region is governed by:

$$\tau_{xr} = -\mu_p \frac{du^p}{dr} = -\frac{r}{2} \frac{\Delta p}{L}, \quad (16.24)$$

subject to conditions:

$$u^c = u^p, \quad \text{at } r = (a - \delta), \quad (16.25)$$

$$u^p = 0, \quad \text{at } r = a. \quad (16.26)$$

Integration of (16.21) and (16.24) subject to the indicated conditions yields the following expressions for the axial velocities in the plasma and core regions:

$$u^p = \frac{a^2}{4\mu_p} \frac{\Delta p}{L} \left[ 1 - \left( \frac{r}{a} \right)^2 \right], \quad \text{for } a - \delta \leq r \leq a, \quad (16.27)$$

and

$$u^c = \frac{a^2}{4\mu_p} \frac{\Delta p}{L} \left[ 1 - \left( \frac{a - \delta}{a} \right)^2 - \frac{\mu_p}{\mu_c} \left( \frac{r}{a} \right)^2 + \frac{\mu_p}{\mu_c} \left( \frac{a - \delta}{a} \right)^2 \right], \quad \text{for } 0 \leq r \leq a - \delta. \quad (16.28)$$

The volume flow rates in the plasma,  $Q_p$ , and core region,  $Q_c$ , are:

$$Q_p = 2\pi \int_{a-\delta}^a u^p r dr = \frac{\pi \Delta p}{8\mu_p L} [a^2 - (a - \delta)^2]^2, \quad (16.29)$$

and

$$Q_c = 2\pi \int_0^{a-\delta} u^c r dr = \frac{\pi a^2 \Delta p}{4\mu_p L} \left[ a^2 - \left( 1 - \frac{\mu_p}{2\mu_c} \right) \frac{(a-\delta)^4}{a^2} \right]. \quad (16.30)$$

The total flow rate of blood within the tube,  $Q$ , is the sum of the flow rates in the plasma and core regions. Therefore:

$$Q = Q_p + Q_c = \frac{\pi a^4 \Delta p}{8\mu_p L} \left[ 1 - \left( 1 - \frac{\delta}{a} \right)^4 \left( 1 - \frac{\mu_p}{\mu_c} \right) \right]. \quad (16.31)$$

From (16.31), we could calculate the apparent viscosity of the two-region fluid by measuring  $Q$  and  $\Delta p/L$ . Define  $\mu_{app}$ , by analogy with Hagen-Poiseuille flow, as given by:

$$Q = \frac{\pi a^4 \Delta p}{8\mu_{app} L}. \quad (16.32)$$

From (16.31) and (16.32), the apparent viscosity,  $\mu_{app}$ , may be expressed in terms of  $\mu_p$  as:

$$\mu_{app} = \mu_p \left[ 1 - \left( 1 - \frac{\delta}{a} \right)^4 \left( 1 - \frac{\mu_p}{\mu_c} \right) \right]^{-1}. \quad (16.33)$$

In the limit  $(\delta/a) \ll 1$ ,  $\left( 1 - \frac{\delta}{a} \right)^4 \approx (1 - 4\delta/a)$ . Then, (16.33) reduces to:

$$\mu_{app} = \mu_c \left[ 1 + 4 \frac{\delta}{a} \left( \frac{\mu_c}{\mu_p} - 1 \right) \right]^{-1} \rightarrow \mu_c \rightarrow \mu. \quad (16.34)$$

In (16.31) and (16.33),  $\delta$  and  $\mu_c$  are unknown. From (16.8), we have  $H_c/H = 1 + (Q_p/Q_c)$ . We still need input from experimental data to set up a modeling procedure for the Fahraeus-Lindqvist effect. Fournier (2007) recommends the use of Charm and Kurland's (1974) equation for this purpose (see reference for details):

$$\mu_c = \mu_p \frac{1}{1 - \alpha_c H_c'}, \quad (16.35)$$

where,

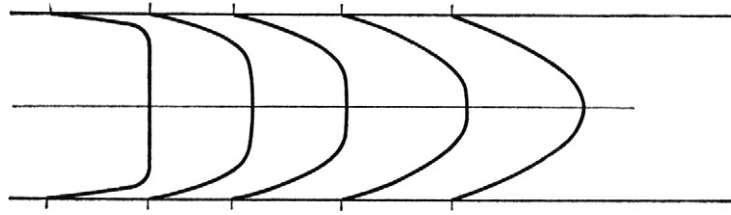
$$\alpha_c = 0.070 \exp \left[ 2.49 H_c + \frac{1107}{T} \exp(-1.69 H_c) \right], \quad (16.36)$$

and  $T$  is temperature in K. Equation (16.36) may be used to a hematocrit of 0.60. With this input, a modeling procedure can be developed for various flow and tube parameters.

### Effect of Developing Flow

When we discussed Poiseuille flow, we noted that the fully developed flow assumption that is often invoked in the study of blood flow in vessels is very restrictive. We will now learn about some of the limitations of this assumption.

When a fluid under the action of a pressure gradient enters a cylindrical tube, it takes a certain distance called the *inlet* or *entrance length*,  $l$ , before the flow in the tube becomes



**FIGURE 16.13** Developing velocity profile in a tube flow. The first profile on the left corresponds to the beginning of flow development: The wall shear stress is high and a large fraction of the flow is still at a uniform speed. As the fluid moves down the tube, the influence of the wall shear stress spreads toward the tube centerline and eventually the flow reaches a smooth, unchanging profile that is parabolic for Newtonian fluids.

steady and fully developed. When the flow is fully developed and laminar, the velocity profile is parabolic. Within the inlet length, the velocity profile changes in the direction of the flow and the fluid accelerates or decelerates as it flows. There is a balance among pressure, viscous, and inertia (acceleration) forces. Compared to fully developed flow, the entrance region is subject to large velocity gradients near the wall and these result in high wall-shear stresses. The entry of blood from the ventricular reservoir into the aortic tube or from a large artery into a smaller branch will involve an entrance length. It must be understood, however, that the inlet length with pulsating flow (say, in the proximal aorta) is different from that for a steady flow.

If we assume that the fluid enters the tube from a reservoir, the profile at the inlet is virtually flat. The transition from a flat velocity distribution, at the entrance of a tube, to the fully developed parabolic velocity profile is illustrated in [Figure 16.13](#). Once inside the tube, the layer of fluid immediately in contact with the wall will become stationary (no-slip condition) and the laminae adjacent to it slide on it subject to viscous forces and a boundary layer is formed. The presence of the endothelial lining on the inside of a blood vessel wall does not negate the no-slip condition. The motion of the bulk of the fluid in the central region of the tube will not be affected by the viscous forces and will have a flat velocity profile. As flow progresses down the tube, the boundary layer will grow in thickness as the viscous shear stress slows more and more of the fluid.

Eventually, the boundary layer fills the whole of the tube and steady viscous flow is established or the flow is fully developed. In the literature (see, for example, [Mohanty & Asthana, 1979](#)), there are discussions which divide the entrance region into two parts, the inlet region and the filled region. At the end of the inlet region, the boundary layers meet at the tube axis but the velocity profiles are not yet similar. In the filled region, adjustment of the completely viscous profile takes place until the Poiseuille similar profile is attained at the end of it. In our discussion here, we will treat the entrance region as a region with a potential core and a developing boundary layer at the wall. The shape of the velocity profile in the tube depends on whether the flow is laminar or turbulent, as does the length of the entrance region,  $l$ . This is a direct consequence of the differences in the nature of the shear stress in laminar and turbulent flows. The magnitude of the pressure gradient,  $\partial p / \partial x$ , is larger in the entrance region than in the fully developed region. There is also an expenditure of kinetic energy involved in transition from a flat to a parabolic profile. For steady flow of a Newtonian fluid in a rigid-walled horizontal circular tube, the entrance length may be estimated from:



$$\begin{aligned}\frac{\ell}{d} &= 0.06 Re \quad \text{for laminar flow and } Re > 50, \\ \frac{\ell}{d} &= 0.693 Re^{1/4} \quad \text{for turbulent flow.}\end{aligned}\tag{16.37}$$

For steady flow at low Reynolds number, the entrance region is approximately one tube radius long (for  $Re \leq 0.001$ , say in capillaries,  $\ell/d = 0.65$ ). In large arteries, the entrance length is relatively long and over a significant length of the artery the velocity gradients are high near the wall. This affects the mass exchange of gas and nutrient molecules between the blood and artery wall.

Unsteady flow through the entrance region with a pulsating flow depends on the Womersley and Reynolds numbers. For a medium-sized artery, the Reynolds number is typically on the order of 100 to 1000, and the Womersley number ranges from 1 to 10. [Pedley \(1980\)](#) has estimated the wall shear stress in the entrance region for pulsatile flow using asymptotic boundary-layer theory while [He and Ku \(1994\)](#) have employed a spectral element simulation to investigate unsteady entrance flow in a straight tube. For a mean  $Re$  of 200 and  $\alpha$  varying from 1.8–12.5 and an inlet waveform  $1 + \sin \omega t$ , He and Ku have computed variations in entrance length during the pulsatile cycle. The amplitude of the entrance-length variation decreases with an increase in  $\alpha$ . The phase lag between the entrance length and the inlet flow waveform increases for  $\alpha$  up to 5.0 and decreases for larger values of  $\alpha$ . For low  $\alpha$ , the maximum entrance length during pulsatile flow is approximately the same as the steady entrance length for the peak flow and is primarily dependent on the Reynolds number. For high  $\alpha$ , the Stokes boundary-layer growth is faster and the entrance length is more uniform during the cycle. For  $\alpha \geq 12.5$ , the pulsatile entrance length is approximately the same length as the entrance length of the mean flow. At all  $\alpha$ , the wall-shear rate converges to its fully developed value at about half the length at which the centerline velocity converges to its fully developed value. This leads to the conclusion that the upstream flow conditions leading to a specific artery may or may not be fully developed and can be predicted only by the magnitudes of the Reynolds number and Womersley number.

### ***Effect of Tube Wall Elasticity on Poiseuille Flow***

Here, we will include the elastic behavior of the vessel wall and examine the effect on the Hagen-Poiseuille model. Consider a pressure-gradient-driven, laminar, steady flow of a Newtonian fluid in a long, circular, cylindrical, thin-walled, elastic tube. Let the initial radius of the tube be  $a_0$ , and  $h$  be the wall thickness, and it is small compared to  $a_0$ . Because the tube is elastic, it will distend more at the high pressure end (inlet) than at the outlet end. The tube radius,  $a$ , will now be a function of  $x$ .

The variation in tube radius due to wall elasticity has to be ascertained. The difference between the exterior pressure on the outside of the tube,  $p_e$ , and the pressure inside the tube,  $p(x)$ , at any cross section of the tube (the negative of transmural pressure difference), is  $(p_e - p(x))$ . This pressure difference acts across  $h$  at every cross section, and will induce a circumferential stress. There will be a corresponding circumferential strain. This strain is the ratio of the change in radius to the original radius of the tube. In this way, we can ascertain the cross section at  $x$ .

Consider the static force equilibrium on a cylindrical segment of the blood vessel consisting of the top half cross section and of unit length. Let  $\sigma_{\theta\theta}$  denote the average circumferential (hoop) stress in the tube wall. The net downward force due to the pressure difference will be balanced by the net upward force; this balance is:

$$2\sigma_{\theta\theta}h = \int_0^\pi (p(x) - p_e) a(x) \sin \theta d\theta, \quad (16.38)$$

which results in:

$$\sigma_{\theta\theta} = \frac{(p(x) - p_e)a(x)}{h}. \quad (16.39)$$

From Hooke's law, the circumferential strain  $\sigma_{\theta\theta}$  is given by:

$$e_{\theta\theta} = \frac{\sigma_{\theta\theta}}{E} = \frac{(a(x) - a_0)}{a_0} = \left( \frac{a(x)}{a_0} \right) - 1, \quad (16.40)$$

where  $E$  is the Young's modulus of the tube wall material, and we have neglected the radial stress  $\sigma_{rr}$  as compared to  $\sigma_{\theta\theta}$  in the thin-walled tube. The wall is considered thin if  $(h/a) \ll 1$ . From (16.39) and (16.40), we get the pressure-radius relationship:

$$a(x) = a_0 \left[ 1 - \frac{a_0}{Eh} (p(x) - p_e) \right]^{-1}. \quad (16.41)$$

Since the flow is laminar and steady, we can still apply the Hagen-Poiseuille formula, (16.17), to the flow. Thus,

$$Q = -\frac{\pi}{8\mu} \left( \frac{dp}{dx} \right) (a(x))^4. \quad (16.42)$$

Therefore,

$$\frac{dp}{dx} = -\frac{8\mu Q}{\pi(a(x))^4}. \quad (16.43)$$

With (16.41):

$$\left[ 1 - \frac{a_0}{Eh} (p(x) - p_e) \right]^{-4} dp = -\frac{8\mu}{\pi a_0} Q dx. \quad (16.44)$$

This is subject to the conditions,  $P = P_1$  at  $x = 0$ , and  $P = P_2$  at  $x = L$ . By integration of (16.44) and from the boundary conditions:

$$\frac{Eh}{3a_0} \left\{ \left[ 1 - \frac{a_0}{Eh} (p_2 - p_e) \right]^{-3} - \left[ 1 - \frac{a_0}{Eh} (p_1 - p_e) \right]^{-3} \right\} = -\frac{8\mu}{\pi a_0} L Q. \quad (16.45)$$

Solving for  $Q$ ,

$$Q = \frac{\pi a_0^3 Eh}{24\mu L} \left\{ \left[ 1 - \frac{a_0}{Eh} (p_1 - p_e) \right]^{-3} - \left[ 1 - \frac{a_0}{Eh} (p_2 - p_e) \right]^{-3} \right\}. \quad (16.46)$$

From (16.46), we see that the flow is a nonlinear function of pressure drop if wall elasticity is taken into account. In the above development, we have assumed Hookean behavior for the stress-strain relationship. However, blood vessels do not necessarily obey Hooke's law, their zero-stress states are open sectors, and their constitutive equations may be nonlinear (see [Zhou & Fung, 1997](#)).

## Pulsatile Blood Flow Theory

As stated earlier, blood flow in the arteries is pulsatile in nature. One of the earliest attempts to model pulsatile flow was carried out by Otto Frank in 1899 (see [Fung, 1997](#)).

### *Elasticity of the Aorta and the Windkessel Theory*

Recall that when the left ventricle contracts during systole, pressure within the chamber increases until it is greater than the pressure in the aorta, leading to the opening of the aortic valve. The ventricular muscles continue to contract, increasing the chamber pressure while ejecting blood into the aorta. As a result, the ventricular volume decreases. The pressure in the aorta starts to build up and the aorta begins to distend due to wall elasticity. At the end of the systole, ventricular muscles start to relax, the ventricular pressure rapidly falls below that of the aorta, and the aortic valve closes. Not all of the blood pumped into the aorta, however, immediately goes into systemic circulation. A part of the blood is used to distend the aorta and a part of the blood is sent to peripheral vessels. The distended aorta acts as an elastic reservoir or a Windkessel (the name in German for an elastic reservoir), the rate of outflow from which is determined by the total peripheral resistance of the system. As the distended aorta contracts, the pressure diminishes in the aorta. The rate of pressure decrease in the aorta is much slower compared to that in the heart chamber. In other words, during the systole part of the heart pumping cycle, the large fluctuation of blood pressure in the left ventricle is converted to a pressure wave with a high mean value and a smaller fluctuation in the distended aorta ([Fung, 1997](#)). This behavior of the distended aorta was thought to be analogous to the high-pressure air chamber (Windkessel) of nineteenth-century fire engines in Germany, and hence the name Windkessel theory was used by Otto Frank to describe this phenomenon.

In the Windkessel theory, blood flow at a rate  $Q(t)$  from the left ventricle enters an elastic chamber (the aorta) and a part of this flows out into a single rigid tube representative of all of the peripheral vessels. The rigid tube offers constant resistance,  $R$ , equal to the total peripheral resistance that was evaluated in the Hagen-Poiseuille model, (16.9). From the law of conservation of mass, assuming blood is incompressible:

$$\begin{aligned} \text{Rate of Inflow into Aorta} &= \text{Rate of change of volume of elastic chamber} \\ &+ \text{Rate of outflow into rigid tube.} \end{aligned} \quad (16.47)$$

Let the instantaneous blood pressure in the elastic chamber be  $p(t)$ , and its volume be  $v(t)$ . The pressure on the outside of the aorta is taken to be zero. The rate of change of volume of an elastic chamber is given by:

$$\frac{dv}{dt} = \left( \frac{dv}{dp} \right) \left( \frac{dp}{dt} \right). \quad (16.48)$$

In (16.48), the quantity  $(dv/dp)$  is the compliance,  $K$ , of the vessel and is a measure of the distensibility. Compliance at a given pressure is the change in volume for a change in pressure. Here pressures are always understood to be transmural pressure differences. Compliance essentially represents the distensibility of the vascular walls in response to a certain pressure. Also, from (16.9), the rate of flow into peripherals is given by  $(p(t)/R)$ , where we have assumed  $\bar{p}_V = 0$ . Therefore, (16.47) becomes

$$Q(t) = K \left( \frac{dp}{dt} \right) + \left( \frac{p(t)}{R} \right). \quad (16.49)$$

Equation (16.49) is a linear equation of the form:

$$Q = \frac{dy}{dx} + Py, \quad (16.50)$$

whose solution is

$$ye^{\int P dx} = A + \int Qe^{\int P dx} dx. \quad (16.51)$$

From (16.49) and (16.51), with  $p_0$  denoting  $p$  at  $t = 0$ , the instantaneous pressure  $p$  in the aorta as a function of the left ventricular ejection rate  $Q(t)$  is given by

$$p(t) = \frac{1}{K} e^{-t/RK} \int_0^t Q(\tau) e^{\tau/RK} d\tau + p_0 e^{-t/RK}. \quad (16.52)$$

In (16.52),  $p_0$  would be the aortic pressure at the end of diastolic phase.

A fundamental assumption in the Windkessel theory is that the pressure pulse wave generated by the heart is transmitted instantaneously throughout the arterial system and disappears before the next cardiac cycle. In reality, pressure waves require finite but small transmission times, and are modified by reflection at bifurcations, bends, tapers, and at the end of short tubes of finite length, and so on. We will now account for some of these features.

### ***Pulse Wave Propagation in an Elastic Tube: Inviscid Theory***

Consider a homogeneous, incompressible, and inviscid fluid in an infinitely long, horizontal, cylindrical, thin-walled, elastic tube. Let the fluid be initially at rest. The propagation of a disturbance wave of small amplitude and long wavelength compared to the tube radius is of interest to us. In particular, we wish to calculate the wave speed. Since the disturbance wavelength is much greater than the tube diameter, the time-dependent internal pressure can be taken to be a function only of  $(x, t)$ .

Before we embark on developing the solution, we need to understand the inviscid approximation. For flow in large arteries, the Reynolds and Womersley numbers are large; the wall boundary layers are very thin compared to the radius of the vessel. The inviscid approximation may be useful in giving us insights in understanding such flows. Clearly, this will not be the case with arterioles, venules, and capillaries. However, the inviscid analysis is strictly of limited use since it is the viscous stress that is dominant in determining flow stability in large arteries.

Under the various conditions prescribed, the resulting flow may be treated as one dimensional.

Let  $A(x,t)$  and  $u(x,t)$  denote the cross-sectional area of the tube and the longitudinal velocity component, respectively. The continuity equation is:

$$\frac{\partial A}{\partial t} + \frac{\partial(Au)}{\partial x} = 0, \quad (16.53)$$

and the equation for the conservation of momentum is:

$$\rho A \left( \frac{\partial u}{\partial t} + u \frac{\partial u}{\partial x} \right) = - \frac{\partial((p - p_e)A)}{\partial x}, \quad (16.54)$$

where  $(p - p_e)$  is the transmural pressure difference. Since the tube wall is assumed to be elastic (not viscoelastic), under the further assumption that  $A$  depends on the transmural pressure difference  $(p - p_e)$  alone, and the material obeys Hooke's law, we have from (16.41) the pressure-radius relationship (referred to as the *tube law*):

$$p - p_e = \frac{Eh}{a_0} \left( 1 - \frac{a_0}{a} \right) = \frac{Eh}{a_0} \left[ 1 - \left( \frac{A_0}{A} \right)^{\frac{1}{2}} \right], \quad (16.55)$$

where  $A = \pi a^2$ , and  $A_0 = \pi a_0^2$ . The equations (16.53), (16.54), and (16.55) govern the wave propagation. We may simplify this equation system further by linearizing it. This is possible if the pressure amplitude  $(p - p_e)$  compared to  $p_0$ , the induced fluid speed  $u$ , and  $(A - A_0)$  compared to  $A_0$ , and their derivatives are all small. If the pulse is moving slowly relative to the speed of sound in the fluid, the wave amplitude is much smaller than the wavelength, and the distension at one cross section has no effect on the distension elsewhere, the assumptions are reasonable. As discussed by Pedley (2000), in normal human beings, the mean blood pressure, relative to atmospheric, at the level of the heart is about 100 mm Hg, and there is a cyclical variation between 80 and 120 mm Hg, so the amplitude-to-mean ratio is 0.2, which is reasonably small. Also, in the ascending aorta, the pulse wave speed,  $C$ , is about 5 m/s, and the maximum value of  $u$  is about 1 m/s, and  $(u/c)$  is also around 0.2. In that case, the system of equations reduce to

$$\frac{\partial A}{\partial t} + A_0 \frac{\partial u}{\partial x} = 0, \quad (16.56)$$

and

$$\rho \frac{\partial u}{\partial t} = - \frac{\partial p}{\partial x}, \quad (16.57)$$

and

$$p - p_e = \frac{Eh}{2a_0 A_0} (A - A_0), \quad \text{and} \quad \frac{\partial p}{\partial A} = \frac{Eh}{2a_0 A_0}. \quad (16.58)$$

Differentiating (16.56) with respect to  $t$  and (16.57) with respect to  $x$ , and subtracting the resulting equations, we get

$$\frac{\partial^2 A}{\partial t^2} = \frac{A_0}{\rho} \frac{\partial^2 p}{\partial x^2}, \quad (16.59)$$

and with (16.58), we obtain:

$$\frac{\partial^2 p}{\partial t^2} = \frac{Eh}{2a_0 A_0} \frac{\partial^2 A}{\partial t^2} = \frac{\partial p}{\partial A} \frac{A_0}{\rho} \frac{\partial^2 p}{\partial x^2}. \quad (16.60)$$

Combining (16.59) and (16.60), we produce:

$$\frac{\partial^2 p}{\partial x^2} = \frac{1}{c^2} \frac{\partial^2 p}{\partial t^2}, \quad \text{or,} \quad \frac{\partial^2 p}{\partial t^2} = c^2 (A_0) \frac{\partial^2 p}{\partial x^2}, \quad (16.61)$$

where  $c^2 = \frac{Eh}{2\rho a_0} = \frac{A}{\rho} \frac{dp}{dA}$ . Equation (16.61) is the wave equation, and the quantity,

$$c = \sqrt{\frac{Eh}{2\rho a_0}} = \sqrt{\frac{A}{\rho} \frac{dp}{dA}} \quad (16.62)$$

is the speed of propagation of the pressure pulse. This is known as the *Moens-Korteweg wave speed*. If the thin wall assumption is not made, following Fung (1997), by evaluating the strain on the midwall of the tube:

$$c = \sqrt{\frac{Eh}{2\rho(a_0 + h/2)}}. \quad (16.63)$$

Next, similar to (16.61), we can develop:

$$\frac{\partial^2 u}{\partial x^2} = \frac{1}{c^2} \frac{\partial^2 u}{\partial t^2}, \quad (16.64)$$

for the velocity component  $u$ . The wave equation (16.61) has the general solution:

$$p = f_1\left(t - \frac{x}{c}\right) + f_2\left(t + \frac{x}{c}\right), \quad (16.65)$$

where  $f_1$  and  $f_2$  are arbitrary functions;  $f_2$  is zero if the wave propagates only in the  $+x$  direction. This result states that the small-amplitude disturbance can propagate along the tube, in either direction, without change of shape of the waveform, at speed  $c(a_0)$ . Also, the velocity waveform is predicted to be of the same shape as the pressure waveform.

In principle, the Moens-Korteweg wave speed given in (16.63) must enable the determination of the arterial modulus  $E$  as a function of  $a$  by noninvasive measurement of the values of arterial dimensions ( $a$ ,  $h$ ), the waveforms of the arterial inner radius at two sites, the transit time (as the time interval between the waveform peaks), and hence the pulse-wave velocity. More details in this regard are available in the book by Mazumdar (1999).

Next, consider the solutions of wave equations (16.61) and (16.64):

$$p = \hat{p}_1 f(x - ct) + \hat{p}_2 g(x + ct), \quad (16.66)$$

and

$$u = \hat{u}_1 f(x - ct) + \hat{u}_2 g(x + ct), \quad (16.67)$$

where  $\hat{p}_1$ ,  $\hat{u}_1$ ,  $\hat{p}_2$ , and  $\hat{u}_2$  are the pressure and velocity amplitudes for waves traveling in the positive  $x$ -direction and negative  $x$ -direction, respectively. From (16.57):

$$\hat{p}_1 = \rho c \hat{u}_1, \quad \text{and} \quad \hat{p}_2 = -\rho c \hat{u}_2. \quad (16.68)$$

This equation (16.68) relates the amplitudes of the pressure and velocity waves.

The above analysis would equally apply if the inviscid fluid in the tube was initially in steady motion, say from left to right. In that case,  $u$  would have to be regarded as a small perturbation superposed on the steady flow, and  $c$  would be the speed of the perturbation wave relative to the undisturbed flow.

Let us now examine the limitations of this model. For typical flow in the aorta, the speed of propagation of the pulse is about 4 m/s (Brown et al., 1999), about 5 m/s in the ascending aorta, rising to about 8 m/s in more peripheral arteries. These predictions are very close to measured values in normal subjects, either dogs or humans (Pedley, 2000). The peak flow speed is about 1 m/s. The speed of propagation in a collapsible vein might be as low as 1 m/s, and this may lead to phenomena analogous to sonic flow (Brown et al., 1999). From (16.62), for given  $E$ ,  $h$ ,  $\rho$ , and size of vessel, the wave speed is a constant. Experimental studies indicate, however, that the wave speed is a function of frequency. The shape of the waveform does not remain the same. The theory must be modified to account for peaking of the pressure pulse due to wave reflection from arterial junctions, wave-front steepening due to nonlinear dispersion effects (Lighthill, 1978), and observed velocity waveform by including dissipative effects due to viscosity (Lighthill, 1978; Pedley, 2000). The neglect of the inertial terms and the effects of viscosity have therefore to be examined to address these concerns and to develop a systematic understanding. These issues will be addressed in later sections in the following order. First, we will learn about pulsatile viscous flow in a single rigid-walled, straight tube. This implies the assumption of an infinite wave speed. Subsequent to that, we will examine the effects of wall elasticity on pulsatile viscous flow in a single tube to gain a more realistic understanding. This allows us to understand wave transmission at finite speed. Following this, we will study blood vessel bifurcation. This will be extended to understand the effects of wave reflection from arterial junctions under the inviscid flow approximation.

### ***Pulsatile Flow in a Rigid Cylindrical Tube: Viscous Effects Included, Infinite Wave Speed Assumption***

Consider the axisymmetric flow of a Newtonian incompressible fluid in a long, thin, circular, cylindrical, horizontal, rigid-walled tube. Clearly, the assumption of a rigid wall implies that the speed of wave propagation is infinite and unrealistic. However, the development presented here will provide us with useful insights and these will be helpful in formulating a much improved theory in the next section.

We again employ the cylindrical coordinates  $(r, \theta, x)$  with velocity components  $(u_r, u_\theta, \text{ and } u_x)$ , respectively. Let  $\lambda$  be the wavelength of the pulse. This is long, and  $a \ll \lambda$ . Since the wave speed is infinite, all the velocity components are very much smaller than the wave speed. These assumptions enable us to drop the inertial terms in the momentum equations. With

the additional assumptions of axisymmetry ( $u_\theta = 0$ , and  $\partial/\partial\theta = 0$ ), and rigid tube wall ( $u_r = 0$ ), and omitting the subscript  $x$  in  $u_x$  for convenience, the continuity equation may be written:

$$\frac{\partial u}{\partial x} = 0, \quad (16.69)$$

and the  $r$ -momentum equation is:

$$0 = -\frac{\partial p}{\partial r}; \quad (16.70)$$

the  $x$ -momentum equation is:

$$\rho \frac{\partial u}{\partial t} = -\frac{\partial p}{\partial x} + \mu \left[ \frac{\partial^2 u}{\partial r^2} + \frac{1}{r} \frac{\partial u}{\partial r} \right]. \quad (16.71)$$

We see that  $u = u(r, t)$  and  $p = p(x, t)$ . Therefore, we are left with just one equation:

$$\mu \left[ \frac{\partial^2 u}{\partial r^2} + \frac{1}{r} \frac{\partial u}{\partial r} \right] - \rho \frac{\partial u}{\partial t} = \frac{\partial p}{\partial x}. \quad (16.72)$$

In (16.72), since  $p = p(x, t)$ ,  $\partial p/\partial x$  will be a function only of  $t$ . Since the pressure waveform is periodic, it is convenient to express the partial derivative of pressure using a Fourier series. Such a periodic function depends on the fundamental frequency of the signal,  $\omega$ , heart rate (unit, rad/s), and the time  $t$ . Recall that  $\omega$  is also called the *circular frequency*,  $\omega/2\pi$  is the frequency (unit, Hz), and  $\lambda$  is the wavelength (unit,  $m$ ). Also,  $\lambda = c/(\omega/2\pi)$ , where  $c$  is wave speed. The wavelength is the wave speed divided by frequency, or the distance traveled per cycle.

We set

$$\frac{\partial p}{\partial x} = -Ge^{i\omega t}, \quad (16.73)$$

where  $G$  is a constant denoting the amplitude of the pressure gradient pulse and  $e^{i\omega t} = \cos \omega t + i \sin \omega t$ . With this representation for  $P(t)$ , (16.72) becomes:

$$\mu \left[ \frac{\partial^2 u}{\partial r^2} + \frac{1}{r} \frac{\partial u}{\partial r} \right] - \rho \left[ \frac{\partial u}{\partial t} \right] = \frac{\partial p}{\partial x} = -Ge^{i\omega t}. \quad (16.74)$$

This is a linear, second-order, partial differential equation with a forcing function. For  $\omega = 0$ , the flow is described by the Hagen-Poiseuille model. [Womersley \(1955a, 1955b\)](#), has solved this problem, and we will provide essential details.

For  $\omega \neq 0$ , we may try solutions of the form:

$$u(r, t) = U(r)e^{i\omega t}, \quad (16.75)$$

where  $U(r)$  is the velocity profile in any cross section of the tube. The real part in (16.75) gives the velocity for the pressure gradient  $G \cos \omega t$  and the imaginary part gives the velocity



for the pressure gradient  $G \sin \omega t$ . Assume that the flow is identical at each cross section along the tube. From (16.74) and (16.75), we get:

$$\frac{d^2 U}{dr^2} + \frac{1}{r} \frac{dU}{dr} - \frac{i\omega\rho}{\mu} U = \frac{G}{\mu}. \quad (16.76)$$

This is a Bessel's differential equation, and the solution involves Bessel functions of zeroth order and complex arguments. Thus,

$$U(r) = C_1 J_0\left(i\sqrt{i\omega\rho/\mu} \ r\right) + C_2 Y_0\left(i\sqrt{i\omega\rho/\mu} \ r\right) + \frac{G}{\omega\rho i}, \quad (16.77)$$

where  $C_1$  and  $C_2$  are constants. In (16.77), from the requirement that  $U$  is finite at  $r = 0$ ,  $C_2 = 0$ . For a rigid-walled tube,  $U = 0$  at  $r = a$ . Therefore,

$$C_1 J_0\left(i^{3/2}\sqrt{\omega\rho/\mu} \ a\right) + \frac{G}{\omega\rho i} = 0. \quad (16.78)$$

From (16.12), the Womersley number is defined by  $\alpha = a\sqrt{\omega/\nu}$ . Therefore, from (16.78), we may write,

$$C_1 = \frac{iG}{\omega\rho} \frac{1}{J_0(i^{3/2}\alpha)}. \quad (16.79)$$

Therefore, from (16.77),

$$U(r) = -\frac{iG}{\omega\rho} \left(1 - \frac{J_0(i^{3/2}\alpha \ r/a)}{J_0(i^{3/2}\alpha)}\right). \quad (16.80)$$

Introduce, for convenience:

$$F_1(\alpha) = \frac{J_0(i^{3/2}\alpha \ r/a)}{J_0(i^{3/2}\alpha)}. \quad (16.81)$$

Now, from (16.75):

$$u(r, t) = U(r)e^{i\omega t} = -\frac{iG}{\omega\rho}(1 - F_1(\alpha))e^{i\omega t} = \frac{Ga^2}{i\mu\alpha^2}(1 - F_1(\alpha))e^{i\omega t}. \quad (16.82)$$

In the above development, we have found the velocity as a function of radius  $r$  and time  $t$  for the entire driving-pressure gradient. Since we have represented both  $\partial p/\partial x$  and  $u(r, t)$  in terms of Fourier modes, we could also express the solution for both these quantities in terms of individual Fourier modes or harmonics explicitly as:

$$\frac{\partial p}{\partial x} = -\sum_{n=0}^N G_n e^{in\omega t}, \quad (16.83)$$

where  $N$  is the number of modes (harmonics), and the  $n = 0$  term represents the mean pressure gradient. Similarly, for velocity,

$$u(r, t) = u_0(r) + \sum_1^N u_n(r) e^{i n \omega t}. \quad (16.84)$$

In (16.84),

$$u_0(r) = \frac{G_0 a^2}{4\mu} \left(1 - \frac{r^2}{a^2}\right) \quad (16.85)$$

is the mean flow and is recognized as the steady Hagen-Poiseuille flow with  $G_0$  as the mean pressure gradient, and for each harmonic:

$$u_n(r) = \frac{G_n a^2}{i\mu\alpha_n^2} (1 - F_1(\alpha_n)). \quad (16.86)$$

We can now write down the expressions for  $u_n(r)$  in the limits of  $\alpha_n$  small and large. These are, for  $\alpha_n$  small:

$$u_n(r) \approx \frac{G_n a^2}{4\mu} \left(1 - \frac{r^2}{a^2}\right), \quad (16.87)$$

which represents a quasi-steady flow, and for  $\alpha_n$  large:

$$u_n(r) \approx \frac{G_n a^2}{i\mu\alpha_n^2} \left\{ 1 - \exp \left[ -\sqrt{\frac{\omega}{2\nu}} (1+i) (a-r) \right] \right\}, \quad (16.88)$$

which is the velocity boundary layer on a plane wall in an oscillating flow. This flow was discussed in Chapter 8 (Stokes' second problem).

The volume flow rate,  $Q(t)$ , may be obtained by integrating the velocity profile across the cross section. Thus, from (16.85) and (16.86):

$$Q(t) = \int_0^a u 2\pi r dr = \pi a^2 \left\{ \frac{G_0 a^2}{8\mu} + \frac{a^2}{i\mu} \sum_1^\infty \frac{G_n}{\alpha_n^2} [1 - F_2(\alpha_n)] e^{i n \omega t} \right\}, \quad (16.89)$$

or equivalently, with (16.82),

$$Q(t) = \int_0^a 2\pi e^{i\omega t} \frac{Ga^2}{i\mu\alpha^2} (1 - F_1(\alpha)) r dr = \frac{\pi a^4}{i\mu\alpha^2} G(1 - F_2(\alpha)) e^{i\omega t}, \quad (16.90)$$

where

$$F_2(\alpha) = \frac{2J_1(i^{3/2}\alpha)}{i^{3/2}\alpha J_0(i^{3/2}\alpha)}. \quad (16.91)$$

The real part of (16.90) gives the volume flow rate when the pressure gradient is  $G \cos \omega t$  and the imaginary part gives the rate when the pressure gradient is  $G \sin \omega t$ .

Next, the wall shear rate  $\tau(t)|_{r=a}$  is given by:

$$\tau(t)|_{r=a} = \frac{\partial u}{\partial r} \Big|_{r=a} = \frac{G_0 a}{2} + \frac{a}{2} \sum_1^N G_n F(\alpha_n) e^{i n \omega t}. \quad (16.92)$$

We may now examine the flow rates in the limit cases of  $\alpha \rightarrow 0$  and  $\alpha \rightarrow \infty$ . As  $\alpha \rightarrow 0$ , by Taylor's expansion,

$$F_2(\alpha) \approx 1 - \frac{i\alpha^2}{8} - O(\alpha^4), \quad (16.93)$$

and from (16.90) in the limit as  $\alpha \rightarrow 0$ ,

$$Q = \frac{\pi G a^4}{8\mu} e^{i\omega t}, \quad (16.94)$$

and the magnitude of the volumetric flow rate  $Q_0$  in the limit as  $\alpha \rightarrow 0$  is

$$|Q_0| = \frac{\pi G a^4}{8\mu}, \quad (16.95)$$

as would be expected (the Hagen-Poiseuille result). As  $\alpha \rightarrow \infty$ :

$$F_2(\alpha) \approx \frac{2}{i^{1/2}\alpha} \left(1 + \frac{1}{2\alpha}\right). \quad (16.96)$$

Next, in Hagen-Poiseuille flow, the steady flow rate is the maximum attainable and there is no phase lag between the applied pressure gradient and the flow. To understand the phase difference between the applied pressure gradient pulse and the flow rate in the present flow model, we set

$$(1 - F_2(\alpha)) = Z(\alpha), \quad Z(\alpha) = X(\alpha) + iY(\alpha). \quad (16.97)$$

Then from (16.90):

$$Q = \frac{\pi G a^4}{\mu \alpha^2} \left\{ [Y \cos(\omega t) + X \sin(\omega t)] - i[X \cos(\omega t) - Y \sin(\omega t)] \right\}. \quad (16.98)$$

The magnitude of  $Q$  is

$$|Q| = \frac{\pi G a^4}{\mu \alpha^2} \sqrt{X^2 + Y^2}. \quad (16.99)$$

The phase angle between the applied pressure gradient  $Ge^{i\omega t}$  and the flow rate (16.90) is now noted to be

$$\tan \phi = \frac{X}{Y}. \quad (16.100)$$

With increasing  $\omega$ , the phase lag between the pressure gradient and the flow rate increases, and the flow rate decreases. Thus, the magnitude of the volumetric flow rate,  $|Q|$ , given by (16.99) will be considerably less than the magnitude  $|Q_0|$  given by (16.95) as would be expected. For an arterial flow, with  $\alpha = 8$ ,  $X \approx 0.85$ ,  $Y \approx 0.16$ , the pulsed volumetric flow rate,  $|Q|$ , would be about one-tenth of the steady value,  $|Q_0|$ . For more detailed discussions and comparisons with measured values of pressure gradients and flow rates in blood vessels, see [Nichols and O'Rourke \(1998\)](#).

The preceding analysis assumed an infinite wave speed of propagation. In order to accommodate the requirement of wave transmission at a finite wave speed, we need to account for vessel wall elasticity. This is discussed in the next section.

### ***Wave Propagation in a Viscous Liquid Contained in an Elastic Cylindrical Tube***

Blood vessel walls are viscoelastic. But in large arteries the effect of nonlinear viscoelasticity on wave propagation is not so severe (Fung, 1997). Even where viscoelastic effects are important, an understanding based on elastic walls will be useful. In this section, we will first study the effects of elastic walls. Then, we will briefly discuss the effects of wall viscoelasticity.

Consider a long, thin, circular, cylindrical, horizontal elastic tube containing a Newtonian, incompressible fluid. Let this system be set in motion solely due to a pressure wave, and the amplitude of the disturbance be small enough so that quadratic terms in the amplitude are negligible compared with linear ones.

In the formulation, we have to consider the fluid flow equations together with the equations of motion governing tube wall displacements. Assume that the tube wall material obeys Hooke's law. Since the tube is thin, membrane theory for modeling the wall displacements is adequately accurate, and we will neglect bending stresses.

The primary question is, how does viscosity attenuate velocity and pressure in this flow?

We shall employ the cylindrical coordinates  $(r, \theta, x)$  with velocity components  $(u_r, u_\theta, \text{ and } u_x)$ , respectively. With the assumption of axisymmetry,  $u_\theta = 0$  and  $\partial/\partial\theta = 0$ . For convenience, we write the  $u_r$  component as  $v$ , and we omit the subscript  $x$  in  $u_x$ .

Restricting the analysis to small disturbances, the governing equations for the fluid are:

$$\frac{\partial u}{\partial x} + \frac{1}{r} \frac{\partial (rv)}{\partial r} = 0, \quad (16.101)$$

$$\rho \frac{\partial u}{\partial t} = -\frac{\partial p}{\partial x} + \mu \left( \frac{\partial^2 u}{\partial r^2} + \frac{1}{r} \frac{\partial u}{\partial r} + \frac{\partial^2 u}{\partial x^2} \right), \quad (16.102)$$

$$\rho \frac{\partial v}{\partial t} = -\frac{\partial p}{\partial r} + \mu \left( \frac{\partial^2 v}{\partial r^2} + \frac{1}{r} \frac{\partial v}{\partial r} + \frac{\partial^2 v}{\partial x^2} - \frac{v}{r^2} \right), \quad (16.103)$$

where  $u$  and  $v$  are the velocity components in the axial and radial directions, respectively.

These have to be supplemented with the tube wall displacement equations. Let the tube wall displacements in the  $(r, \theta, x)$  directions be  $(\eta, \zeta, \text{ and } \xi)$ , respectively, and the tube material density be  $\rho_w$ . The initial radius of the tube is  $a_0$ , and the wall thickness is  $h$ .

For this thin elastic tube, the circumferential (hoop) tension and the tension in the axial direction are related by Hooke's law as follows:

$$T_\theta = \frac{Eh}{1 - \bar{\nu}^2} \left( \frac{\eta}{a_0} + \bar{\nu} \frac{\partial \xi}{\partial x} \right), \quad (16.104)$$

and

$$T_x = \frac{Eh}{1 - \hat{\nu}^2} \left( \frac{\partial \xi}{\partial x} + \hat{\nu} \frac{\eta}{a_0} \right), \quad (16.105)$$

where  $\hat{\nu}$  is Poisson's ratio.

By a force balance on a wall element of volume ( $h \, r \, d\theta \, dx$ ), the equations governing wall displacements may be written as:

- $r$ -direction

$$\rho_w h \frac{\partial^2 \eta}{\partial t^2} = \sigma_{rr}|_{r=a} - \frac{T_\theta}{a_0}, \quad (16.106)$$

and

- $x$ -direction

$$\rho_w h \frac{\partial^2 \xi}{\partial t^2} = + \frac{\partial T_x}{\partial x} - \sigma_{rx}|_{r=a}. \quad (16.107)$$

There is no displacement equation for the  $\theta$  direction. In (16.106) and (16.107),  $\sigma_{rr}|_{r=a}$  and  $\sigma_{rx}|_{r=a}$  refer to radial and shear stresses, respectively, which the fluid exerts on the tube wall. These equations are based on the assumptions that shear and bending stresses in the tube wall material are negligible and the slope of the disturbed tube wall ( $\partial a / \partial x$ ) is small. These also imply that the ratios  $(a/\lambda)$  and  $(h/\lambda)$ , where  $\lambda$  is the wavelength of disturbance, are small.

From (16.104) through (16.107), we obtain

$$\rho_w h \frac{\partial^2 \eta}{\partial t^2} = \sigma_{rr}|_{r=a} - \frac{Eh}{1 - \hat{\nu}} \left( \frac{\eta}{a_0^2} + \frac{\hat{\nu}}{a_0} \frac{\partial \xi}{\partial x} \right), \quad (16.108)$$

and

$$\rho_w h \frac{\partial^2 \xi}{\partial t^2} = -\mu \left( \frac{\partial u}{\partial r} + \frac{\partial v}{\partial x} \right) \Big|_{r=a} + \frac{Eh}{1 - \hat{\nu}^2} \left( \frac{\partial^2 \xi}{\partial x^2} + \frac{\hat{\nu}}{a_0} \frac{\partial \eta}{\partial x} \right). \quad (16.109)$$

In the above equations, from the theory of fluid flow, the normal compressive stress due to fluid flow on an area element perpendicular to the tube's radius is given by:

$$\sigma_{rr} = +p - 2\mu \frac{\partial v}{\partial r}, \quad (16.110)$$

and the shear stress due to fluid flow acting in a direction parallel to the axis of the tube on an element of area perpendicular to a radius is

$$\sigma_{rx} = \mu \left( \frac{\partial u}{\partial r} + \frac{\partial v}{\partial x} \right). \quad (16.111)$$

These are the radial and shear stresses exerted by the fluid on the wall of the vessel. With (16.110) and (16.111), (16.108) and (16.109) become

$$\rho_w h \frac{\partial^2 \eta}{\partial t^2} = +p|_{r=a} - 2\mu \frac{\partial v}{\partial r} \Big|_{r=a} - \frac{Eh}{1 - \hat{v}^2} \left( \frac{\eta}{a_0^2} + \frac{\hat{v}}{a_0} \frac{\partial \xi}{\partial x} \right), \quad (16.112)$$

and

$$\rho_w h \frac{\partial^2 \xi}{\partial t^2} = -\mu \left( \frac{\partial u}{\partial r} + \frac{\partial v}{\partial x} \right) \Big|_{r=a} + \frac{Eh}{1 - \hat{v}^2} \left( \frac{\partial^2 \xi}{\partial x^2} + \frac{\hat{v}}{a_0} \frac{\partial \eta}{\partial x} \right). \quad (16.113)$$

We have to solve (16.101) through (16.103), together with (16.112), and (16.113) subject to prescribed conditions. The boundary conditions at the wall are that the velocity components of the fluid be equal to those of the wall. Thus,

$$u|_{r=a_0} = \frac{\partial \xi}{\partial t} \Big|_{r=a_0}, \quad (16.114)$$

and

$$v|_{r=a_0} = \frac{\partial \eta}{\partial t} \Big|_{r=a_0}. \quad (16.115)$$

We note that the boundary conditions given in (16.114) and (16.115) are linearized conditions, since we are evaluating  $u$  and  $v$  at the undisturbed radius  $a_0$ .

We now represent the various quantities in terms of Fourier modes. Thus,

$$\begin{aligned} u(x, r, t) &= \hat{u}(r) e^{i(kx - \omega t)}, & v(x, r, t) &= \hat{v}(r) e^{i(kx - \omega t)}, \\ p(x, t) &= \hat{p} e^{i(kx - \omega t)}, & \xi(x, t) &= \hat{\xi} e^{i(kx - \omega t)}, \\ \eta(x, t) &= \hat{\eta} e^{i(kx - \omega t)}, \end{aligned} \quad (16.116)$$

where  $\hat{u}(r)$ ,  $\hat{v}(r)$ ,  $\hat{p}$ ,  $\hat{\xi}$ , and  $\hat{\eta}$  are the amplitudes,  $\omega = 2\pi/T$  is a real constant, the frequency of the forced disturbance,  $T$  is the period of the heart cycle,  $k = k_1 + ik_2$  is a complex constant, with  $k_1$  being the wave number and  $k_2$  a measure of the decay of the disturbance as it travels along the vessel (damping constant),  $|k| = \sqrt{k_1^2 + k_2^2} = 2\pi/\lambda$ , where  $\lambda$  is the wavelength of the disturbance, and  $c = \omega/k_1$  is the wave speed.

The above formulation has been solved by [Morgan and Kiely \(1954\)](#) and by [Womersley \(1957a, 1957b\)](#), and we will provide the essential details here. The analysis will be restricted to disturbances of long wavelength, that is,  $a/\lambda \ll 1$ , and large Womersley number,  $\alpha \gg 1$ .

From (16.101):

$$\left| \frac{v}{u} \right| = \left| \frac{\hat{v}(r)}{\hat{u}(r)} \right| = O(|ak|). \quad (16.117)$$

For small damping, we note that  $|k| \approx k_1 = 2\pi/\lambda$ , and  $c = \omega/k_1$  is the wave speed.

From (16.102) and (16.103), we may make the following observations. In (16.102),  $\partial^2 u / \partial x^2$  may be neglected in comparison with the other terms since  $a/\lambda \ll 1$  and  $\lambda\alpha \gg 1$ . In (16.103),  $\partial p / \partial r$  is of a higher order of magnitude in  $a/\lambda$  than is  $\partial p / \partial x$ . In fact, we may neglect all

terms that are of order  $a/\lambda$ . In effect, we are neglecting radial acceleration and damping terms and taking the pressure to be uniform over each cross section. The fluid equations become:

$$\frac{\partial u}{\partial x} + \frac{1}{r} \frac{\partial}{\partial r} (rv) = 0, \quad (16.118)$$

$$\rho \frac{\partial u}{\partial t} = -\frac{\partial p}{\partial x} + \mu \left( \frac{\partial^2 u}{\partial r^2} + \frac{1}{r} \frac{\partial u}{\partial r} \right), \quad (16.119)$$

$$\frac{\partial p}{\partial r} = 0, \quad (16.120)$$

$$p = \hat{p} e^{i(kx - \omega t)}. \quad (16.121)$$

Now substitute the assumed forms given in (16.116) into (16.118) and (16.119) to produce:

$$\frac{d(r\hat{v})}{dr} = -ikr\hat{u}, \quad (16.122)$$

$$\frac{d^2 \hat{u}}{dr^2} + \frac{1}{r} \frac{d\hat{u}}{dr} + \frac{i\omega\rho}{\mu} \hat{u} = \frac{ik\hat{p}}{\mu}. \quad (16.123)$$

The boundary conditions given by (16.114) and (16.115) become:

$$\hat{u}(a_0) e^{i(kx - \omega t)} = -i\omega \hat{\xi} e^{i(kx - \omega t)}, \quad (16.124)$$

$$\hat{v}(a_0) e^{i(kx - \omega t)} = -i\omega \hat{\eta} e^{i(kx - \omega t)}. \quad (16.125)$$

We may now note that the linearization of the boundary conditions will involve an error of the same order as that caused by neglecting the nonlinear terms in the equations. The error would be small if  $\hat{\xi}$  and  $\hat{\eta}$  are very small compared to  $a$ .

Next, introduce the assumed form given in (16.116), and use (16.120) in the displacement equations (16.112) and (16.113) to develop:

$$-\rho_w h \omega^2 \hat{\eta} = \hat{p} - 2\mu \left( \frac{d\hat{v}}{dr} \right) \Big|_{r=a_0} - \frac{Eh}{1 - \hat{v}^2} \left( \frac{\hat{\eta}}{a_0^2} + \frac{\hat{v}k}{a_0} \hat{\xi} \right), \quad (16.126)$$

$$-\rho_w h \omega^2 \hat{\xi} = -\mu \left( \frac{d\hat{u}}{dr} + ik\hat{v} \right) \Big|_{r=a_0} + \frac{Eh}{1 - \hat{v}^2} \left( -k^2 \hat{\xi} + \frac{\hat{v}k}{a_0} \hat{\eta} \right). \quad (16.127)$$

Now invoke the assumptions that  $h/a \ll 1$ ,  $\rho$  is of the same order of magnitude as  $\rho_w$  and  $a^2/\lambda^2 \ll 1$  in (16.126) and (16.127). This amounts to neglecting the terms which represent tube inertia, and approximating  $\sigma_{rx}$  in (16.111) by  $\mu(\partial v/\partial x)$  and  $\sigma_{rr}$  in (16.110) by  $p$ . After considerable algebra, (16.126) and (16.127) reduce to:

$$\hat{p} = \frac{Eh}{a_0^2} \hat{\eta} - \frac{i\hat{v}}{a_0 k} \mu \frac{d\hat{u}}{dr} \Big|_{r=a_0}, \quad (16.128)$$

$$\hat{\xi} = \frac{i\hat{v}}{ka_0} \hat{\eta} - \frac{1 - \hat{v}^2}{Ehk^2} \mu \frac{d\hat{u}}{dr} \Big|_{r=a_0}. \quad (16.129)$$

We are now left with (16.122), (16.123), (16.128), and (16.129), subject to boundary conditions given by (16.124) and (16.125) and the pseudo boundary condition that  $u(r)$  be nonsingular at  $r = 0$ .

Equations (16.123) and (16.128) can be combined to give:

$$\frac{d^2\hat{u}}{dr^2} + \frac{1}{r} \frac{d\hat{u}}{dr} + \frac{i\omega\rho}{\mu} \hat{u} = \frac{ik}{\mu} \frac{Eh}{a_0^2} \hat{\eta} + \frac{\hat{v}}{a_0} \frac{d\hat{u}}{dr} \Big|_{r=a_0}. \quad (16.130)$$

Satisfying the pseudo boundary condition, the solution to this Bessel's differential equation is given by:

$$\hat{u}(r) = AJ_0(\beta r) + \frac{k}{\omega} \frac{Eh}{\rho a_0^2} \hat{\eta} - \frac{\hat{v}}{\beta a_0} AJ_1(\beta a_0), \quad (16.131)$$

where  $\beta = \sqrt{i\omega/\nu}$ , and  $A$  is an arbitrary constant. Next, from (16.122):

$$\hat{v} = -\frac{ik}{r} \int_0^r r \hat{u}(r) dr. \quad (16.132)$$

From (16.131) and (16.132):

$$\hat{v}(r) = -\frac{ikA}{\beta} J_1(\beta r) - \frac{ik^2}{\omega} \frac{Eh\hat{\eta}}{\rho a_0^2} \frac{r}{2} + \frac{ik\hat{v}}{\beta a_0} A \frac{r}{2} J_1(\beta a_0). \quad (16.133)$$

Equations (16.131) and (16.133) give the expressions for  $\hat{u}(r)$  and  $\hat{v}(r)$ , respectively. Subjecting them to the boundary conditions given in (16.124) and (16.125), introducing  $\hat{\beta} = \beta a_0$ , and eliminating  $\hat{\xi}$  by the use of (16.129), the following two linear homogeneous equations for  $\hat{\eta}$  are developed:

$$\hat{\eta} \left[ \frac{\omega}{k} \frac{\hat{v}}{a_0} - \frac{kEh}{\omega \rho a_0^2} \right] = A \left[ J_0(\hat{\beta}) + J_1(\hat{\beta}) \left\{ \frac{i\beta\omega\mu(1 - \hat{v}^2)}{Ehk^2} - \frac{\hat{v}}{\hat{\beta}} \right\} \right], \quad (16.134)$$

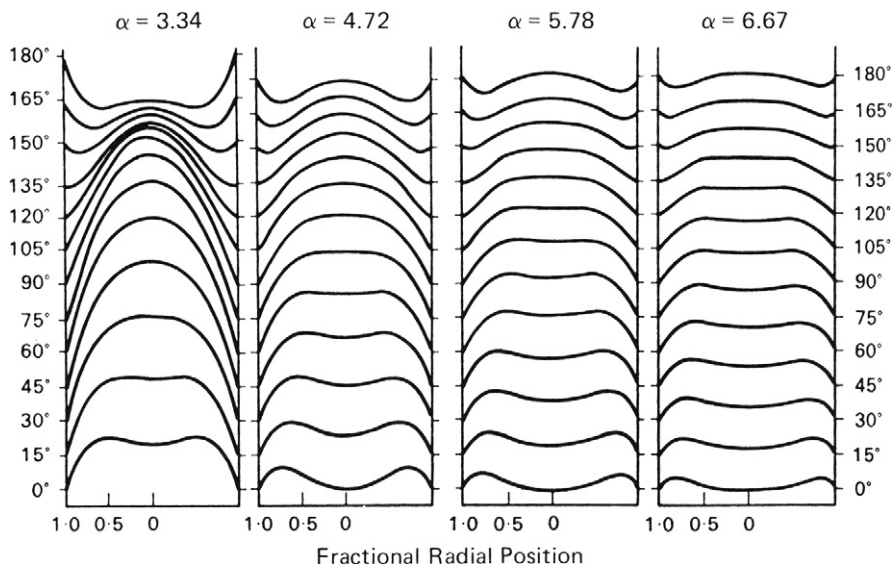
$$\hat{\eta} \left[ 1 - \frac{k^2 Eh}{\omega^2 2\rho a_0} \right] = AJ_1(\hat{\beta}) \left[ \frac{k}{\omega\hat{\beta}} - \frac{k\hat{v}}{2\omega\hat{\beta}} \right]. \quad (16.135)$$

For nonzero solutions, the determinant of the above set of linear algebraic equations in  $\hat{\eta}$  and  $A$  must be zero. As a result, the following characteristic equation is developed:

$$\left( \frac{k^2}{\omega^2} \frac{Eh}{2\rho a_0} \right)^2 \left[ 2\hat{\beta} \frac{J_0(\hat{\beta})}{J_1(\hat{\beta})} - 4 \right] + \left( \frac{k^2}{\omega^2} \frac{Eh}{2\rho a_0} \right) \left[ 4\hat{v} - 1 - 2\hat{\beta} \frac{J_0(\hat{\beta})}{J_1(\hat{\beta})} \right] + (1 - \hat{v}^2) = 0. \quad (16.136)$$

The solution to this quadratic equation will give  $k^2/\omega^2$  in terms of known quantities. Then we can find  $k/\omega = (k_1 + ik_2)/\omega$ . The wave speed,  $\omega/k_1$ , and the damping factor may be evaluated by determining the real and imaginary parts of  $k/\omega$ .





**FIGURE 16.14** Velocity profiles of a sinusoidally oscillating flow in a pipe. At the lowest value of  $\alpha$ , the Womersley number, the flow oscillations are slow enough so that the flow becomes fully developed, at least momentarily, during an oscillation. At higher values of  $\alpha$ , the flow is slower in the center of the tube but it moves like a solid object. Reproduced from McDonald, D. A. (1974), *Blood Flow in Arteries*, The Williams & Wilkins Company, Baltimore.

Morgan and Kiely (1954) have provided explicit results for the wave speed,  $c$ , and the damping constant,  $k_2$ , in the limits of small and large  $\alpha$ . Mazumdar (1999) has indicated that by an *in vivo* study, the wave speed,  $\omega/k_1$ , can be evaluated noninvasively by monitoring the transit time as the time interval between the peaks of ultrasonically measured waveforms of the arterial diameter at two arterial sites at a known distance apart. Then from (16.136),  $E$  can be calculated. From either (16.134) or (16.135),  $A$  can be expressed in terms of  $\hat{\eta}$ , and with that,  $\hat{u}(r)$  can be related to  $\hat{p}$ . Mazumdar gives details as to how the cardiac output may be calculated with the information developed in conjunction with pulsed Doppler flowmetry.

Figure 16.14 shows velocity profiles at intervals of  $\Delta\omega t = 15^\circ$  of the flow resulting from a pressure gradient varying as  $\cos(\omega t)$  in a tube. As this is harmonic motion, only half a cycle is illustrated, and for  $\omega t > 180^\circ$ , the velocity profiles are of the same form but opposite in sign. The Womersley number is  $\alpha$ . The reversal of flow starts in the laminae near the wall. As the Womersley number increases, the profiles become flatter in the central region, there is a reduction in the amplitudes of the flow, and the rate of reversal of flow increases close to the wall. At  $\alpha = 6.67$ , the central mass of the fluid is seen to reciprocate like a solid core.

### Effect of Viscoelasticity of Tube Material

In general, the wall of a blood vessel must be treated as viscoelastic. This means that the relations given in (16.104) and (16.105) must be replaced by corresponding relations for a tube of viscoelastic material. In this problem, all the stresses and strains in the

problem are assumed to vary as  $e^{i(kx - \omega t)}$ , and we will further assume that the effect of the strain rates on the stresses is small compared to the effect of the strains. For the purely elastic case, only two real elastic constants were needed. Morgan and Kiely (1954) have shown that by substituting suitable complex quantities for the elastic modulus and the Poisson's ratio, the viscoelastic behavior of the tube wall may be accommodated. They introduce:

$$E^* = E - i\omega E', \quad \text{and} \quad \hat{v}^* = \hat{v} - i\omega \hat{v}', \quad (16.137)$$

where,  $E'$  and  $\hat{v}'$  are new constants. In (16.104) and (16.105),  $E^*$  and  $\hat{v}^*$  replace  $E$  and  $\hat{v}$ , respectively. The formulation will otherwise remain the same. An equation for  $k/\omega$  will arise as before. The fact that  $E^*$  and  $\hat{v}^*$  are complex has to be taken into account while evaluating the wave velocity and the damping factor. Morgan and Kiely provide results appropriate for small and large  $\alpha$ .

Morgan and Ferrante (1955) extended the study by Morgan and Kiely (1954) to the situation for small  $\alpha$  values where there is Poiseuille-like flow in the thin, elastic-walled tube. The flow oscillations are small and they are superimposed on a large steady-stream velocity. The steady flow modifies the wave velocity. The wave velocity in the presence of a steady flow is the algebraic sum of the normal wave velocity and the steady-flow velocity. Morgan and Ferrante predict a decrease in the damping of a wave propagated in the direction of the stream and an increase in the damping when propagated upstream. However, the steady-flow component in arteries is so small in comparison with the pulse wave velocity that its role in damping is of little importance (see McDonald, 1974). Womersley (1957a) considered the situation where the flow oscillations are large in amplitude compared to the mean stream velocity (this is similar to the situation in an artery), predicting that the presence of a steady-stream velocity would produce a small increase in the damping.

### Blood Vessel Bifurcation: An Application of Poiseuille's Formula and Murray's Law

Blood vessels bifurcate into smaller daughter vessels which in turn bifurcate to even smaller ones. On the basis that the flow satisfies Poiseuille's formula in the parent and all the daughter vessels, and by invoking the principle of minimization of energy dissipation in the flow, we can determine the optimal size of the vessels and the geometry of bifurcation. We recall that Hagen-Poiseuille flow involves established (fully developed) flow in a long tube. Here, for simplicity, we will assume that established Poiseuille flow exists in all the vessels. This is obviously a drastic assumption but the analysis will provide us with some useful insights.

Let the parent and daughter vessels be straight, circular in cross section, and lie in a plane.

Consider a parent vessel AB of length  $L_0$  and radius  $a_0$  in which the flow rate is  $Q$ , which bifurcates into two daughter vessels BC and BD with lengths  $L_1$  and  $L_2$ , radii  $a_1$  and  $a_2$ , and flow rates  $Q_1$  and  $Q_2$ , respectively. The axes of vessels BC and BD are inclined at angles  $\theta$  and  $\phi$  with respect to the axis of AB, as shown in Figure 16.15. Points A, C, and D are fixed. The optimal sizes of the vessels and the optimal location of B have to be determined from the principle of minimization of energy dissipation.

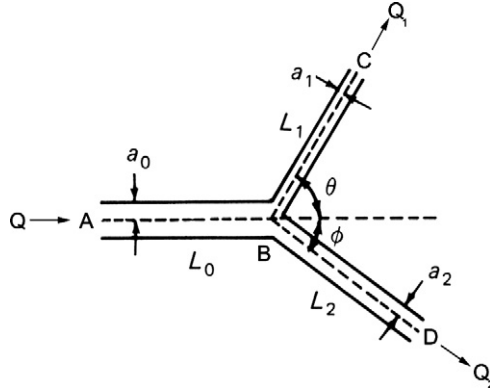


FIGURE 16.15 Schematic of an arterial bifurcation from one large vessel into two smaller ones. Here  $a_0$ ,  $a_1$ , and  $a_2$  are the vessel radii and the branching angles with respect to the incoming flow direction are  $\theta$  and  $\phi$ .

The total rate of energy dissipation by flow rate  $Q$  in a blood vessel of length  $L$  and radius  $a$  is equal to sum of the rate at which work is done on the blood,  $Q\Delta p$ , and the rate at which energy is used up by the blood vessel by metabolism,  $K\pi a^2 L$ , where  $K$  is a constant. For Hagen-Poiseuille flow, from (16.17):  $Q = \frac{\pi a^4}{8\mu} \frac{\Delta p}{L}$ . Therefore,

$$\text{Total energy dissipation} = \frac{8\mu L}{\pi a^4} Q^2 + K\pi a^2 L = \hat{E}_1 (\text{say}). \quad (16.138)$$

To obtain the optimal size of a vessel for transport, for a given length of vessel, we need to minimize this quantity with respect to radius of the vessel. Thus,

$$\frac{\partial \hat{E}_1}{\partial a} = -\frac{32\mu L}{\pi} Q^2 a^{-5} + 2K\pi La = 0. \quad (16.139)$$

Solving for  $a$ :

$$a = \left[ \frac{16\mu K}{\pi^2} \right]^{1/6} Q^{1/3}. \quad (16.140)$$

Equation (16.140) gives the optimal radius for the blood vessel indicating that minimum energy dissipation occurs under this condition. The optimal relationship,  $Q \sim a^3$ , is called *Murray's Law*.

With (16.140), the minimum value for energy dissipation is

$$\hat{E}_{1, \min} = \frac{3\pi}{2} KLa^2. \quad (16.141)$$

Next, consider the flow with the branches. The minimum value for energy dissipation with branches is

$$\hat{E}_{2, \min} = \frac{3\pi}{2} K(L_0 a_0^2 + L_1 a_1^2 + L_2 a_2^2). \quad (16.142)$$

Also,

$$a_0 = \left[ \frac{16\mu}{\pi^2} K \right]^{1/6} Q_0^{1/3}, \quad a_1 = \left[ \frac{16\mu}{\pi^2} K \right]^{1/6} Q_1^{1/3}, \quad \text{and} \quad a_2 = \left[ \frac{16\mu}{\pi^2} K \right]^{1/6} Q_2^{1/3}, \quad (16.143)$$

and from mass conservation:

$$Q = Q_1 + Q_2 \rightarrow a_0^3 = a_1^3 + a_2^3. \quad (16.144)$$

The lengths  $L_0$ ,  $L_1$ , and  $L_2$  depend on the location of point  $B$ . The optimum location of point  $B$  is determined by examining associated variational problems (see [Fung, 1997](#)).

Any small movement of  $B$  changes  $\hat{E}_{2, \min}$  by  $\delta \hat{E}_{2, \min}$  and

$$\delta \hat{E}_{2, \min} = \frac{3\pi}{2} K (\delta L_0 a_0^2 + \delta L_1 a_1^2 + \delta L_2 a_2^2). \quad (16.145)$$

The optimal location of  $B$  would make  $\delta \hat{E}_{2, \min} = 0$  for arbitrary small movement  $\delta L$  of point  $B$ . By making such displacements of  $B$ , one at a time, in the direction of  $AB$ , in the direction of  $BC$ , and finally in the direction of  $DB$ , and setting the value of the corresponding  $\delta \hat{E}_{2, \min}$  to zero, we develop a set of three conditions governing optimization. These are:

$$\cos \theta = \frac{a_0^4 + a_1^4 - a_2^4}{2a_0^2 a_1^2}, \quad \cos \phi = \frac{a_0^4 - a_1^4 + a_2^4}{2a_0^2 a_2^2}, \quad \cos(\theta + \phi) = \frac{a_0^4 - a_1^4 - a_2^4}{2a_1^2 a_2^2}. \quad (16.146)$$

Together with (16.144), the set (16.146) may be solved for the optimum angle  $\theta$  as

$$\cos \theta = \frac{a_0^4 + a_1^4 - (a_0^3 - a_1^3)^{4/3}}{2a_0^2 a_1^2}, \quad (16.147)$$

and a similar equation for  $\phi$ . Comparison of these optimization results with experimental data are noted to be excellent (see [Fung, 1997](#)).

### **Reflection of Waves at Arterial Junctions: Inviscid Flow and Long Wavelength Approximation**

Arteries have branches. When a pressure or a velocity wave reaches a junction where the parent artery 1 bifurcates into daughter tubes 2 and 3 as shown in [Figure 16.16](#), the incident wave is partially reflected at the junction into the parent tube and partially transmitted down the daughters. In the long wavelength approximation, we may neglect the flow at the junction. Let the longitudinal coordinate in each tube be  $x$ , with  $x = 0$  at the bifurcation. The incident wave in the parent tube comes from  $x = -\infty$ .

Let  $p_I$  be the oscillatory pressure associated with the incident wave, let  $p_R$  be associated with the reflected wave, and let  $p_{T1}$  and  $p_{T2}$  be associated with the transmitted waves. Let the pressure be a single valued and continuous function at the junction for all time  $t$ . The continuity requirement ensures that there are no local accelerations. Under these conditions, at the junction:

$$p_I + p_R = p_{T1} = p_{T2}. \quad (16.148)$$

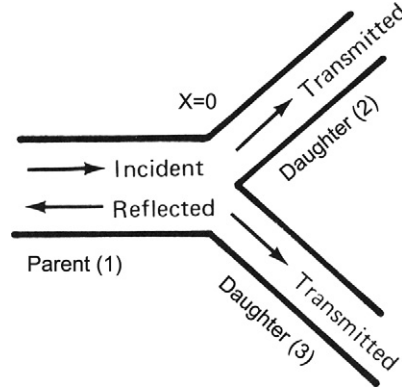


FIGURE 16.16 Schematic of an arterial bifurcation: reflection. Here the change in impedance at the junction can cause a reflected wave to travel backward along the parent artery.

Next, let  $Q_I$  be the flow rate associated with the incident wave, let  $Q_R$  be associated with the reflected wave, and let  $Q_{T1}$  and  $Q_{T2}$  be associated with the transmitted waves. The flow rate is also taken to be single valued and continuous at the junction for all time  $t$ . The continuity requirement ensures conservation of mass. At the junction,

$$Q_I - Q_R = Q_{T1} + Q_{T2}. \quad (16.149)$$

Let the undisturbed cross-sectional areas of the tubes be  $A_1$ ,  $A_2$ , and  $A_3$ , and the intrinsic wave speeds be  $c_1$ ,  $c_2$ ,  $c_3$ , respectively. In general, for a fluid of density  $\rho$  flowing under the influence of a wave with intrinsic wave speed  $c$ , through a tube of cross-sectional area  $A$ , the flow rate  $Q$  is related to the mean velocity  $u$  by

$$Q = Au = \pm \frac{A}{\rho c} p, \quad (16.150)$$

where we have employed the relationship given in (16.68). The plus or the minus sign applies depending on whether the wave is going in the positive  $x$ -direction or in the negative  $x$ -direction. The quantity  $A/\rho c$  is called the *characteristic admittance* of the tube and is denoted by  $Y$ , while  $\rho c/A$  is called the *characteristic impedance* of the tube and is denoted by  $Z$ . Admittance is seen to be the ratio of the oscillatory flow to the oscillatory pressure when the wave goes in the direction of the  $+x$  axis. With these definitions,

$$Q = Au = \pm Yp = \pm \frac{p}{Z}. \quad (16.151)$$

Equation (16.149) may be written in terms of admittances or impedances as:

$$Y_1(p_I - p_R) = \sum_{j=2}^3 Y_j p_{Tj}, \quad \text{or} \quad \frac{(p_I - p_R)}{Z_1} = \sum_{j=2}^3 \frac{p_{Tj}}{Z_j}. \quad (16.152)$$

We can simultaneously solve (16.148) and (16.152) to produce:

$$\frac{p_R}{p_I} = \frac{Y_1 - \sum Y_j}{Y_1 + \sum Y_j} = R, \quad \text{and} \quad \frac{p_{Tj}}{p_I} = \frac{2Y_1}{Y_1 + \sum Y_j} = T, \quad (16.153)$$

or,

$$\frac{p_R}{p_I} = \frac{Z_1^{-1} - \sum Z_j^{-1}}{Z_1^{-1} + \sum Z_j^{-1}}, \quad \text{and} \quad \frac{p_{Tj}}{p_I} = \frac{2Z_1^{-1}}{Z_1^{-1} + \sum Z_j^{-1}}. \quad (16.154)$$

In (16.153),  $R$  and  $T$  are called the *reflection* and *transmission coefficients*, respectively. From (16.153), the amplitudes of the reflected and transmitted pressure waves are  $R$  and  $T$  times the amplitude of the incident pressure wave. These relations can be written in more explicit manner as follows (see [Lighthill, 1978](#)).

The contribution of the incident wave to the pressure in the parent tube is given by

$$p_I = P_I f\left(t - \frac{x}{c_1}\right), \quad (16.155)$$

where  $P_I$  is an amplitude parameter and  $f$  is a continuous, periodic function whose maximum value is 1. The corresponding contribution to the flow rate is

$$Q_I = A_1 u = Y_1 P_I f\left(t - \frac{x}{c_1}\right). \quad (16.156)$$

The contributions to pressure from the reflected and transmitted waves to the parent and daughter tubes, respectively, are:

$$p_R = P_R g\left(t + \frac{x}{c_1}\right), \quad \text{and} \quad p_{Tj} = P_{Tj} h_j\left(t - \frac{x}{c_j}\right), \quad (j = 2, 3), \quad (16.157)$$

where  $P_R$  and  $P_T$  are amplitude parameters, and  $g$  and  $h$  are continuous, periodic functions. The corresponding contributions to the flow rates are:

$$Q_R = -Y_1 P_R g\left(t + \frac{x}{c_1}\right), \quad \text{and} \quad Q_{Tj} = Y_j P_{Tj} h_j\left(t - \frac{x}{c_j}\right), \quad (j = 2, 3). \quad (16.158)$$

Therefore, the pressure perturbation in the parent tube is given by (16.155) and (16.157) to be:

$$\frac{p}{P_I} = f\left(t - \frac{x}{c_1}\right) + \frac{P_R}{P_I} f\left(t + \frac{x}{c_1}\right), \quad (16.159)$$

and the flow rate, from (16.156) and (16.158), is:

$$Q = Y_1 P_I \left[ f\left(t - \frac{x}{c_1}\right) - \frac{P_R}{P_I} f\left(t + \frac{x}{c_1}\right) \right]. \quad (16.160)$$

The transmission of energy by the pressure waves is of interest. The rate of work done by the wave motion through the cross section of the tube or, equivalently, the rate of

transmission of energy by the wave is clearly  $pAu$  or  $pQ$ , which is the same as  $P^2/Z$  from (16.151). Now we can calculate the incident, reflected, and transmitted quantities at the junction. Thus,

$$\text{Rate of energy transmission by incident wave} = \frac{p_I^2}{Z_1}, \quad (16.161)$$

$$\text{Rate of energy transmission by reflected wave} = \frac{(Rp_I)^2}{Z_1} = R^2 \frac{p_I^2}{Z_1} \quad (16.162)$$

The quantity  $R^2$  is called the *energy reflection coefficient*. Similarly, the energy transmission coefficient, which is the rate of energy transfer in the two transmitted waves compared with that in the incident wave, may be defined by

$$\frac{\frac{p_{T2}^2}{Z_2} + \frac{p_{T3}^2}{Z_3}}{\frac{p_I^2}{Z_1}} = \frac{Z_2^{-1} + Z_3^{-1}}{Z_1^{-1}} \left( \frac{p_{T2}}{p_I} \right)^2 = \frac{Z_2^{-1} + Z_3^{-1}}{Z_1^{-1}} T^2, \quad (16.163)$$

where we have noted that in our case  $P_{T2} = P_{T3}$ .

A comparison of (16.159) and (16.160) shows that, if we include reflection at bifurcations, the pressure and flow waveforms are no longer of the same shape. [Pedley \(1980\)](#) has offered interesting discussions about the behavior of the waves at the junction. From (16.153), for real values of  $c_j$  and  $Y_j$ , if  $\sum Y_j < Y_1$ , then the reflected wave has the same sign as the incident wave, and the pressures in the two waves are in phase at  $x = 0$ . They combine additively to form a large-amplitude fluctuation at the junction, and the effect of the junction is similar to that of a closed-end ( $P_R = P_I$ ). If  $\sum Y_j > Y_1$ , there is a phase change at  $x = 0$ , the smallest-amplitude pressure fluctuation occurs there, and the junction resembles an open end ( $P_R = -P_I$ ). If  $\sum Y_j = Y_1$ , there is no reflected wave, and the junction is said to be perfectly matched. [Pedley \(2000\)](#) has noted that the increase in the pressure wave amplitude in the aorta with distance down the vessel may indicate that there is a closed-end type of reflection at (or beyond) the iliac bifurcation. Peaking of the pressure pulse is a consequence of the closed-end type of reflection in a blood vessel.

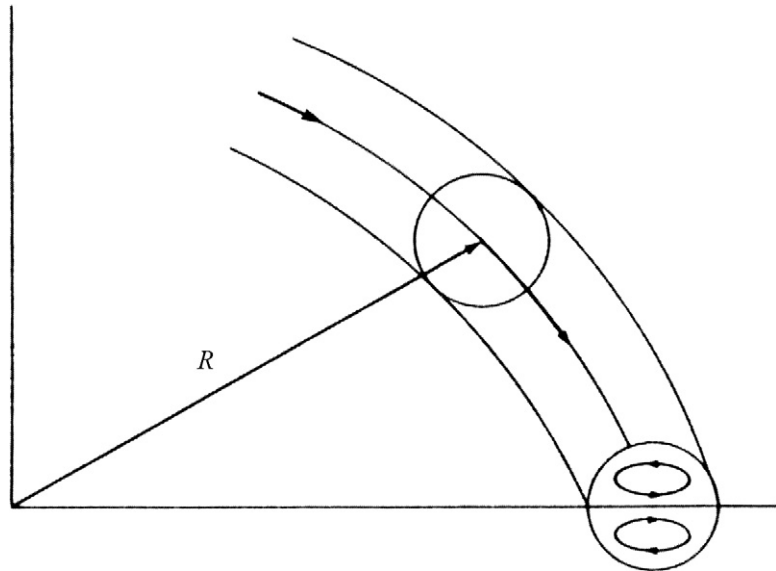
Waves in more complex systems consisting of many branches may be analyzed by repeated application of the results presented in this section.

Next, we will study blood flow in curved tubes. Almost all blood vessels have curvature and the curvature affects both the nature (stability) and volume flow rate.

## Flow in a Rigid-Walled Curved Tube

Blood vessels are typically curved and the curvature effects have to be accounted for in modeling in order to get a realistic understanding. The aortic arch is a 3D bend twisting through more than  $180^\circ$  ([Ku, 1997](#)). In a curved tube, fluid motion is not everywhere parallel to the curved axis of the tube (see [Figure 16.17](#)), secondary motions are generated, the velocity profile is distorted, and there is increased energy dissipation. However, curving of a tube increases the stability of flow, and the critical Reynolds number increases significantly,

**FIGURE 16.17** Schematic of flow in a curved tube. Here the radius of curvature is  $R$  and the curve of the tube causes a secondary flow within the tube.



and a critical Reynolds number of 5000 is easily obtained (see McDonald, 1974). Flows in curved tubes are discussed in detail by McConalogue and Srivastava (1968), Singh (1974), Pedley (1980), and Berger et al. (1983). In this section, we concentrate on some of the most important aspects of flow in a uniformly curved vessel of small curvature. The wall is considered to be rigid. Pulsatile flow through a curved tube can induce complicated secondary flows with flow reversals and is very difficult to analyze. It may be noted that steady viscous flow in a symmetrical bifurcation resembles that in two curved tubes stuck together. Thus, an understanding gained in studying curved flows will be beneficial in that regard as well.

Consider fully developed, steady, laminar, viscous flow in a curved tube of radius  $a$  and a uniform radius of curvature  $R$ . Let us employ the toroidal coordinate system  $(r', \alpha, \theta)$ , where  $r'$  denotes the distance from the center of the circular cross section of the pipe,  $\alpha$  is the angle between the radius vector and the plane of symmetry, and  $\theta$  is the angular distance of the cross section from the entry of the pipe (see Figure 16.18). Let the corresponding dimensional velocity components be  $(u', v', w')$ . As a fluid particle traverses a curved path of radius  $R$  (radius of curvature) with a (longitudinal) speed  $w'$  along the  $\theta$  direction, it will experience a lateral (centrifugal) acceleration of  $w'^2/R$ , and a lateral force equal to  $m_p w'^2/R$ , where  $m_p$  is the mass of the particle. The radii of curvature of the particle paths near the inner bend, the central axis, and the outer bend will be of increasing magnitude as we move away from the inner bend. Also, due to the no-slip condition, the velocities,  $w'$ , of particles near the inner and outer bends will be lower, while that of the particle at the central axis will be the highest. The particle at the central axis will experience the highest centrifugal force while that near the outer bend will experience the least. A lateral pressure gradient will cause the faster flowing fluid near the center to be swept toward the outside of the bend and to be replaced at the inside by the slower moving fluid near the wall. In effect, a secondary circulation will be set up resulting in two vortices,



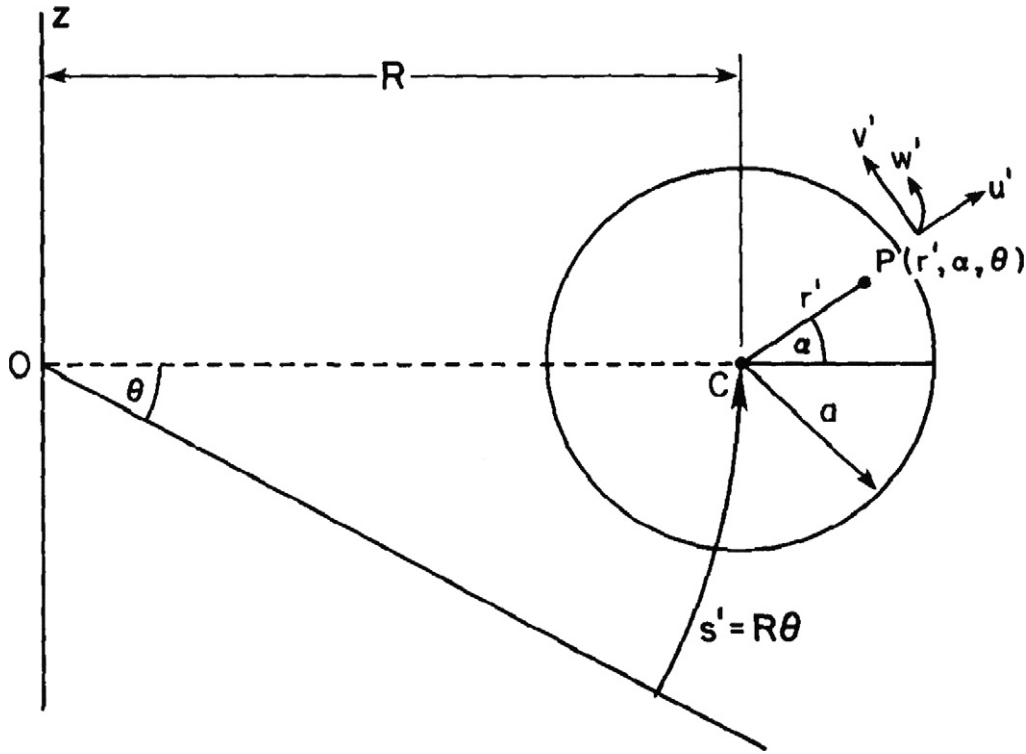


FIGURE 16.18 Toroidal coordinate system. This coordinate system is needed to analyze the flow in a round tube with radius  $a$  that has a constant radius of curvature  $R$ .

called *Dean vortices* because Dean (1928) was the first to systematically study these secondary motions in curved tubes (see Figure 16.17). Dean vortices significantly influence the axial flow. The wall shear near the outside of the bend is relatively higher than the (much reduced) wall shear on the inside of the bend. Fully developed flow upstream of or through curved tubes exhibits velocity that skews toward the outer wall of the bend. For most arterial flows, skewing will be toward the outer wall. If the flow into the entrance region of a curved tube is not developed, then the inviscid core of the fluid in the curve can act like a potential vortex with velocity skewing toward the inner wall.

Secondary flow in curved tubes is utilized in heart-lung machines to promote oxygenation of blood (Fung, 1997). In the machine, blood flows inside the curved tube and oxygen flows on the outside. The tube is permeable to oxygen. The secondary flow in the tube stirs up the blood and results in faster oxygenation.

Let us now analyze the flow in a curved tube to better understand the salient features. Introduce nondimensional variables,  $r = r'/a$ ,  $s = R\theta/a$ ,  $\mathbf{u} = \mathbf{u}'/\bar{W}_0$ , and  $p = p'/\rho\bar{W}_0^2$ , where  $\mathbf{u} = (u, v, w)$  is the velocity vector,  $P$  is the pressure,  $\rho$  is the density, and  $\bar{W}_0$  is the mean axial velocity in the pipe. Restrict consideration to the case where the flow is fully developed ( $\partial\mathbf{u}/\partial s = 0$ ). Introduce the dimensionless ratio,

$$\delta = \frac{\text{radius of tube cross section}}{\text{radius of curvature of the centerline}} = \frac{a}{R}. \quad (16.164)$$

We restrict consideration to a uniformly curved tube,  $\delta = \text{constant}$ , and with a slight curvature (weakly curved)  $\delta \ll 1$ . Since  $\delta$  is a constant, the velocity field is independent of  $s$ , the components are functions only of  $r$  and  $\alpha$ , and the pressure gradient  $\partial p / \partial s$  is independent of  $s$ . With  $\delta$  constant, the only way that the transverse velocities are affected by the axial velocity is through the centrifugal force, and it is the centrifugal force that drives the secondary motion. This means that the centrifugal force terms must be of the same order of magnitude as the viscous and inertial terms in the momentum equation, and this requires rescaling the velocities. The transformation that accomplishes this is  $(u, v, w) \rightarrow (\sqrt{\delta} \hat{u}, \sqrt{\delta} \hat{v}, \hat{w})$ . We will also let  $s = R\theta/a = \sqrt{1/\delta} \tilde{s}$  for convenience.

In the following, we shall omit writing the “ $\wedge$ ” on  $u, v, w$ , and the “ $\sim$ ” on  $s$  for convenience. When  $\delta \ll 1$ , the major contribution to the axial pressure gradient may be separated from the transverse component, and we may write

$$p = p_0(s) + \delta p_1(r, \alpha, s) + \dots \quad (16.165)$$

Under all these restrictions, the governing equations become:

$$\frac{\partial u}{\partial r} + \frac{u}{r} + \frac{1}{r} \frac{\partial v}{\partial \alpha} = 0, \quad (16.166)$$

$$u \frac{\partial u}{\partial r} + \frac{v}{r} \frac{\partial u}{\partial \alpha} - \frac{v^2}{r} - w^2 \cos \alpha = -\frac{\partial p_1}{\partial r} - \frac{2}{\kappa} \frac{1}{r} \frac{\partial}{\partial \alpha} \left( \frac{\partial v}{\partial r} + \frac{v}{r} - \frac{1}{r} \frac{\partial u}{\partial \alpha} \right), \quad (16.167)$$

$$u \frac{\partial v}{\partial r} + \frac{v}{r} \frac{\partial v}{\partial \alpha} + \frac{uv}{r} + w^2 \sin \alpha = -\frac{1}{r} \frac{\partial p_1}{\partial \alpha} + \frac{2}{\kappa} \frac{\partial}{\partial r} \left( \frac{\partial v}{\partial r} + \frac{v}{r} - \frac{1}{r} \frac{\partial u}{\partial \alpha} \right), \quad (16.168)$$

$$u \frac{\partial w}{\partial r} + \frac{v}{r} \frac{\partial w}{\partial \alpha} = -\frac{\partial p_0}{\partial s} + \frac{2}{\kappa} \left( \frac{\partial^2 w}{\partial r^2} + \frac{1}{r} \frac{\partial w}{\partial r} + \frac{1}{r^2} \frac{\partial^2 w}{\partial \alpha^2} \right). \quad (16.169)$$

The boundary conditions are:

$$u = v = w = 0 \quad \text{at } r = 1, \quad \text{no singularity at } r = 0. \quad (16.170)$$

The flow is governed by just one parameter  $\kappa$  in the equations, and it is called the *Dean number*. It is given by

$$\kappa = \sqrt{\delta} \frac{2a\overline{W}_0}{\nu} = \sqrt{\delta} \, 2Re, \quad (16.171)$$

where  $\overline{W}_0$  is the mean axial velocity in the pipe. The Dean number is the Reynolds number modified by the pipe curvature. The appearance of the 2 in the definition of the Dean number is by convention. At higher Dean numbers, the flow can separate along the inner boundary curve.

There are many different definitions of Dean number in the literature and the reader must be careful to see which particular form is being used in any given discussion.

From (16.169),  $\partial p_0/\partial s$  is independent of  $s$ , and  $P_0$  can be written as  $P_0(s) = -G s$ , where  $G$  is a constant. Equation (16.166) admits the existence of a stream function for the secondary flow,  $\psi$ , defined by

$$u = \frac{1}{r} \frac{\partial \psi}{\partial \alpha'}, \quad v = -\frac{\partial \psi}{\partial r}. \quad (16.172)$$

Substitution of (16.172) into (16.169) yields

$$\nabla_1^2 w - \frac{\kappa}{2} \frac{\partial p_0}{\partial s} = \frac{\kappa}{2r} \left( \frac{\partial \psi}{\partial \alpha} \frac{\partial w}{\partial r} - \frac{\partial \psi}{\partial r} \frac{\partial w}{\partial \alpha} \right), \quad (16.173)$$

while elimination of pressure from (16.167) and (16.168) yields

$$\frac{2}{\kappa} \nabla_1^4 \psi - \frac{1}{r} \left( \frac{\partial \psi}{\partial r} \frac{\partial}{\partial \alpha} - \frac{\partial \psi}{\partial \alpha} \frac{\partial}{\partial r} \right) \nabla_1^2 \psi = -2w \left( \sin \alpha \frac{\partial w}{\partial r} + \frac{\cos \alpha}{r} \frac{\partial w}{\partial \alpha} \right), \quad (16.174)$$

where

$$\nabla_1^2 \psi = \frac{\partial^2}{\partial r^2} + \frac{1}{r} \frac{\partial}{\partial r} + \frac{1}{r^2} \frac{\partial^2}{\partial \alpha^2}. \quad (16.175)$$

The boundary conditions are:

$$\psi = \frac{\partial \psi}{\partial r} = w = 0, \quad \text{at } r = 1. \quad (16.176)$$

Equations (16.173) and (16.174) subject to conditions (16.176) have to be solved.

For small Dean number, following Dean (1928), we expand  $w$  and  $\psi$  in terms of a series in powers of the Dean number as follows:

$$w = \sum_{n=0}^{\infty} \kappa^{2n} w_n(r, \alpha), \quad \text{and} \quad \psi = \kappa \sum_{n=0}^{\infty} \kappa^{2n} \psi_n(r, \alpha). \quad (16.177)$$

The  $w_0$  term corresponds to Poiseuille flow in a straight tube with rigid walls. The  $\psi_0$  term is  $O(\kappa)$ . The series expansion in  $\kappa$  is equivalent to the successive approximation of inertia terms in lubrication theory. The leading term in the secondary flow takes the form of a pair of counter-rotating helical vortices, placed symmetrically with respect to the plane of symmetry. This flow pattern arises because of a centrifugally induced pressure gradient, approximately uniform over the cross section. The dimensionless volume flux is

$$\frac{Q}{\pi a^2 \bar{W}} = 1 - 0.0306 \left( \frac{K}{576} \right)^2 + 0.0120 \left( \frac{K}{576} \right)^4 + O(K^6), \quad (16.178)$$

where  $K = (2a/R)(W_{\max} a/\nu)^2 = 2(\kappa)^2$  is another frequently used definition of Dean's number. Here,  $W_{\max} = 2\bar{W}$ ;  $W_{\max}$  and  $\bar{W}$  are the maximum and mean velocities, respectively, in a straight pipe of the same radius under the same axial pressure gradient and under fully developed flow conditions. The first term corresponds to the Poiseuille straight pipe solution. The effect of curvature is seen to reduce the flux.

Many other authors define Dean's number by

$$D = \sqrt{2\delta} \frac{\hat{G} a^2}{\mu} \frac{a}{v}, \quad (16.179)$$

where  $-\hat{G}$  is the dimensional pressure gradient,

$$\hat{G} = -\frac{8\mu\bar{W}}{a^2}. \quad (16.180)$$

In terms of  $D$ , (16.178) becomes

$$\frac{Q}{\pi a^2 \bar{W}} = 1 - 0.0306 \left(\frac{D}{96}\right)^4 + 0.0120 \left(\frac{D}{96}\right)^8 + O(D^{12}). \quad (16.181)$$

Next, consider the friction factor for flow in a curved tube. Let  $\lambda_c$  and  $\lambda_s$  denote the flow resistance in a curved and a straight pipe, respectively, while the flows are subject to pressure gradients equal in magnitude. The ratio  $\lambda$  is

$$\lambda = \frac{\lambda_c}{\lambda_s} = \left(\frac{Q_c}{Q_s}\right)^{-1} = 1 + 0.0306 \left(\frac{K}{576}\right)^2 - 0.0110 \left(\frac{K}{576}\right)^4 + \dots, \quad (16.182)$$

where  $Q_c$  and  $Q_s$  are the fluxes in straight and curved pipes, respectively. The flow resistance in a curved tube is not affected by the first-order terms and is increased only by higher order terms. With regard to shear stress, the curvature increases axial wall shear on the outside wall and decreases it on the inside, and it also generates a positive secondary shear in the  $\alpha$  direction.

The size of the coefficients suggests that the small  $D$  expansion is valid for values of  $D$  up to about 100 or  $K \approx 600$ , and the results here are useful only for smaller blood vessels. Pedley points out that in the canine aorta, where  $\delta \approx 0.2$ , the mean  $D$  is greater than 2000. As mentioned earlier, flow in a curved tube is much more stable than that in a straight tube and the critical Reynolds number could be as high as 5000 which corresponds to  $K \approx 1.6 \times 10^6$ .

For intermediate values of  $D$ , only numerical solutions are possible due to the importance of nonlinear terms. Numerical results of [Collins and Dennis \(1975\)](#) for developed flow up to a Dean number of 5000 are stated to compare very well with experimental results. At intermediate values of  $D$ , a boundary layer develops on the outside wall of the bend where the axial shear is high. The secondary flow in the core is approximately uniform and continues to manifest a two-vortex structure. At higher values of  $D$ , there is greater distortion of the secondary streamlines. The wall shear at  $r = 1$ ,  $\alpha = 0$ , is proportional to  $D$  ( $\approx 0.85D$ ); see [Pedley \(2000\)](#).

At large Dean numbers, the centers of the two vortices move toward the outer bend,  $\alpha = 0$ , and the flow is very much reduced compared with a straight pipe for equal magnitude pressure gradients. Detailed studies using advanced computational methods are required to resolve the flow structure at large  $D$ . They are as yet unavailable in the published literature.

[Pedley \(2000\)](#) discusses nonuniqueness of curved-tube flow results. When  $D$  is sufficiently small, the steady-flow equations have just one solution and there is a single secondary flow vortex in each half of the tube. However, there is a critical value of  $D$ , above which more than

one steady solution exists and these may correspond to four vortices, two in each half. Again, detailed computational studies are necessary to resolve these features.

We will next study the flow of blood in collapsible tubes. The role of pressure difference,  $(P_e - P(x))$ , on the vessel wall will be significant in such flows.

## Flow in Collapsible Tubes

At large negative values of the transmural pressure difference (the difference between the pressure inside and the pressure outside), the cross-sectional area of a blood vessel is either very small—the lumen being reduced to two narrow channels separated by a flat region of contact between the opposite walls—or it may even fall to zero. There is an intermediate range of values of transmural pressure difference in which the cross section is very compliant and even the small viscous or inertial pressure drop of the flow may be enough to cause a large reduction in area, that is, collapse. Collapse occurs in a number of situations; a listing is given by [Kamm and Pedley \(1989\)](#). Collapse occurs, for example, in systemic veins above the heart (and outside the skull) as a result of the gravitational decrease in internal pressure with height; intramyocardial coronary blood vessels during systole; systemic arteries compressed by a sphygmomanometer cuff, or within the chest during cardiopulmonary resuscitation; pulmonary blood vessels in the upper levels of the lung; large intrathoracic airways during forced expiration or coughing; and the urethra during micturition and in the ureter during peristaltic pumping. Collapse, therefore occurs both in small and large blood vessels, and as a result both at low and high Reynolds numbers. In certain cases, at high Reynolds number, collapse is accompanied by self-excited, flow-induced oscillations. There is audible sound. For example, Korotkoff sounds heard during sphygmomanometry are associated with this.

### **A Note on Korotkoff Sounds**

Korotkoff sounds, named after Dr. Nikolai Korotkoff, a physician who described them in 1905, are sounds that physicians listen for when they are taking blood pressure. When the cuff of a sphygmomanometer is placed around the upper arm and inflated to a pressure above the systolic pressure, there will be no sound audible because the pressure in the cuff would be high enough to completely occlude the blood flow. If the pressure is now dropped, the first Korotkoff sound will be heard. As the pressure in the cuff is the same as the pressure produced by the heart, some blood will be able to pass through the upper arm when the pressure in the artery rises during systole. This blood flows in spurts as the pressure in the artery rises above the pressure in the cuff and then drops back down, resulting in turbulence that results in audible sound. As the pressure in the cuff is allowed to fall further, thumping sounds continue to be heard as long as the pressure in the cuff is between the systolic and diastolic pressures, as the arterial pressure keeps on rising above and dropping back below the pressure in the cuff. Eventually, as the pressure in the cuff drops further, the sounds change in quality, then become muted, then disappear altogether when the pressure in the cuff drops below the diastolic pressure. Korotkoff described five types of Korotkoff sounds. The first Korotkoff sound is the snapping sound first heard at the systolic pressure. The second sounds are the murmurs heard for most of the area between the systolic and diastolic pressures. The third and the fourth sounds appear at

pressures within 10 mm Hg above the diastolic blood pressure, and are described as “thumping” and “muting.” The fifth Korotkoff sound is silence as the cuff pressure drops below the diastolic pressure. Traditionally, the systolic blood pressure is taken to be the pressure at which the first Korotkoff sound is first heard and the diastolic blood pressure is the pressure at which the fourth Korotkoff sound is just barely audible. There has recently been a move toward the use of the fifth Korotkoff sound (i.e., silence) as the diastolic pressure, as this has been felt to be more reproducible.

### ***Starling Resistor: A Motivating Experiment for Flow in Collapsible Tubes***

The study of flows in collapsible tubes is facilitated by a well-known experiment carried out under varying conditions by different researchers. In the experiment, a length of uniform collapsible tube is mounted at each end to a shorter length of rigid tube and is enclosed in a chamber whose pressure  $p_e$  can be adjusted. Fluid, say water, flows through the tube. The inlet and outlet pressures at the ends of the collapsible tube are  $p_1$  and  $p_2$ . The volume rate of flow is  $Q$ . The pressures and the flow rate are next varied in a systematic way and the results are noted. The setup described is called a *Starling resistor* after physiologist Starling (see [Fung, 1997](#)). This experiment will enable us understand some aspects of actual flows in physiological systems. There are many different versions of the description of the Starling resistor experiment in the literature. The experiments have been carried out under both steady flow and unsteady flow conditions. We will describe the experiments as reported by [Kamm and Pedley \(1989\)](#).

#### **CASE (1): $(P_1 - P_2)$ IS INCREASED WHILE $(P_1 - P_E)$ IS HELD CONSTANT**

This is accomplished either by reducing  $p_2$  with  $p_1$  and  $p_e$  fixed, or by simultaneously increasing  $p_1$  and  $p_e$  while  $p_2$  is held constant. With either procedure,  $Q$  at first increases, but above a critical value it levels off and the condition of *flow limitation* is reached. In this condition, however much the driving pressure is increased the flow rate remains constant, or it may even fall as a result of increasingly severe tube collapse. This experiment is relevant to forced expiration from the lung, to venous return, and to micturition.

#### **CASE (2): $(P_1 - P_2)$ OR $Q$ IS INCREASED WHILE $(P_2 - P_E)$ IS HELD CONSTANT AT SOME NEGATIVE VALUE**

In this case, the tube is collapsed at low flow rates, but starts to open up from the upstream end as  $Q$  increases above a critical value, so that the resistance falls and  $(p_1 - p_2)$  ceases to rise. This is termed *pressure-drop limitation*. This experiment does not seem to apply to any particular physiological condition.

#### **CASE (3): $(P_1 - P_2)$ IS HELD CONSTANT WHILE $(P_2 - P_E)$ IS DECREASED FROM A LARGE POSITIVE VALUE**

In this case, the tube first behaves as though it were rigid and the flow rate is nearly constant. Then as  $(p_2 - p_e)$  becomes sufficiently negative to produce partial collapse, the resistance rises and  $Q$  begins to fall. This experiment is relevant to pulmonary capillary flows.

**CASE (4):  $P_E$  FIXED**

The outlet end is connected to a flow resistor. The pressure downstream of the flow resistor is fixed (flow is exposed to atmosphere). Thus  $p_2$  is equal to atmospheric pressure plus  $Q$  times the fixed resistance;  $p_1$  is varied.

In this case,  $p_2$  varies with  $Q$  due to the presence of a fixed downstream resistance. The degree of tube collapse (progressive collapse) also varies with  $Q$  for the same reason. At high flow rates, the tube is distended and its resistance is low. As the flow rate is reduced below a critical value the tube starts to collapse. Its resistance and  $(p_1 - p_2)$  both increase as  $Q$  is decreased. Only when the tube is severely collapsed along most of its length does  $(p_1 - p_2)$  start to decrease again as  $Q$  approaches zero. When  $p_1$  is approximately equal to  $p_e$ , virtually the entire tube is collapsed (Fung, 1997). The tube often flutters in Case 4 (see discussions in Fung).

**CASE (5): UNSTEADY FLOW EXPERIMENTS**

Excepting at small Reynolds numbers, there is always some parameter range where flow oscillations occur. The oscillations have a wide variety of modes.

The experiments reveal the importance of a tube law relating transmural pressure difference with the area of cross section of the collapsible tube and the flow and pressure drop limitations when analyzing collapsible tubes. Shapiro (1977a, 1977b) has developed a comprehensive one-dimensional theory for steady flow based on a suitable tube law. Kamm and Shapiro (1979) have extended it to unsteady flow in a collapsible tube. In the following, we shall discuss the steady-flow theory.

**One-Dimensional Flow Treatment**

The equations describing one-dimensional flow in a collapsible tube are similar to those in gas dynamics or channel flow of a liquid with a free surface (see Shapiro, 1977a). Here, we will study the one-dimensional, steady-flow formulation for the collapsible tube. However, first let us recapitulate the traditional basic equations for one-dimensional flow in a smoothly varying elastic tube (see "Pulse Wave Propagation in an Elastic Tube: Inviscid Theory" in Section 16.3).

We studied flow in an elastic tube with cross section  $A(x, t)$  and longitudinal velocity  $u(x, t)$ . The constant external pressure on the tube was set at  $p_e$ . The primary mechanism of unsteady flow in the tube was wave propagation. The transmural pressure difference  $(p - p_e)$  was related to the local cross-sectional area by a "tube law" which involved hoop tension, which may be expressed as

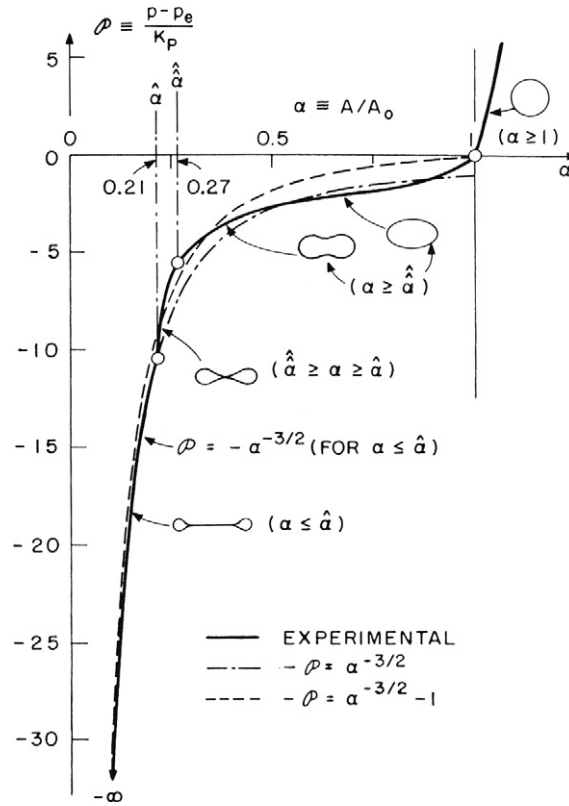
$$(p - p_e) = \hat{P}(A), \quad (16.183)$$

where the functional form  $\hat{P}$  depends on data. For disturbances of small amplitude and long wavelength compared to the tube diameter:

$$A = A_0 + A', \quad p - p_e = \hat{P}(A_0) + p', \quad |A'| \ll A_0, \quad |p'| \ll \hat{P}(A_0), \quad (16.184)$$

and the wave speed is given by

$$c^2 = \frac{A}{\rho} \frac{d\hat{P}}{dA} = \frac{A}{\rho} \frac{d(p - p_e)}{dA}. \quad (16.185)$$



**FIGURE 16.19** Behavior of a collapsible tube. Here  $\alpha$  is the tube area ratio and is 1 when the pressure inside the tube is greater than the pressure outside the tube. The vertical axis is proportional to the interior minus exterior pressure difference. As the pressure in the tube decreases, the available cross-sectional area is reduced, and this reduction takes place rapidly when the tube collapses. *Reproduced with permission from the American Society of Mechanical Engineers, NY.*

Tube collapse is associated with negative transmural pressure difference, and the pressure difference is supported by bending stiffness of the tube wall (see [Figure 16.19](#)). Contrast this with positive transmural pressure difference discussed earlier, which was supported by hoop tension. Following [Shapiro \(1977a\)](#), introduce

$$P = \frac{(p - p_e)}{K_p}, \quad \text{and} \quad \alpha = \frac{A}{A_0}, \quad (16.186)$$

where  $K_p$  is a parameter proportional to the bending stiffness of the wall material, and  $A_0$  is the reference area of the tube for zero transmural pressure difference. The pressure difference is supported primarily by the bending stiffness of the tube wall. For a linear elastic tube wall material,  $K_p$  is proportional to the modulus of elasticity  $E$ , and the bending moment of inertia  $I$ , as in



$$K_p \propto EI, \quad I = (h/a_0)^3 / (1 - \hat{\nu}^2), \quad (16.187)$$

where  $h$  is wall thickness and  $\hat{\nu}$  is Poisson's ratio.

From a fit of experimental data (see [Shapiro, 1977a](#)), the tube law for flow in a collapsible tube is taken to be

$$-P \approx \alpha^{-n} - 1, \quad \text{and} \quad n = \frac{3}{2}. \quad (16.188)$$

For  $P < 0$ , the tube is partially collapsed. If the tube is in longitudinal tension, say,  $T_L$ , then there will be a local curvature  $R_L$  in the longitudinal plane. The effect of  $T_L$  is to change  $P_e$  by  $T_L/R_L$ , and the tube law (16.188) will not hold (see [Cancelli & Pedley, 1985](#)). We will here assume that  $T_L/R \ll (p - p_e)$ . Now, if the tube law (16.188) and transmural pressure difference are assumed to be uniform along the length of the tube, then with (16.185), at any location  $x$ , the phase velocity of long area waves is given by

$$c^2 = \frac{A}{\rho} \frac{\partial(p - p_e)}{\partial A} = \left[ \frac{nK_p \alpha^{-n}}{\rho} \right], \quad (16.189)$$

for the square of the wave speed.

The assumptions of uniformity of tube law and transmural pressure difference are not valid under most physiological circumstances and these have to be relaxed. The physical causes that negate uniformity include: friction, gravity, variations of external pressure or of muscular tone, longitudinal variations in  $A_0$ , and longitudinal changes in the mechanical properties of the tube. To address some of these issues, we consider a more general formulation given by Shapiro.

The flow will still be considered steady, one dimensional, and incompressible.

The governing equations now are:

$$\frac{dA}{A} + \frac{du}{u} = 0, \quad (16.190)$$

and

$$-Adp - \tau_w s dx - \rho g A dz = \rho A u du = \rho A u^2 \frac{du}{u}, \quad (16.191)$$

where  $\tau_w$  is the wall shear stress,  $s$  is the perimeter of the tube, and  $z$  is the elevation in the gravity field  $g$ . For the shear stress, [Shapiro \(1977a\)](#) considers the cases of fully developed turbulent flow and fully developed laminar Poiseuille flow in the tube. For turbulent flow,

$$\frac{\tau_w s dx}{A} = \frac{1}{2} \rho u^2 \frac{4f_T dx}{d_e}, \quad (16.192)$$

where  $d_e = 4A/s$  is the equivalent hydraulic diameter and  $f_T$  is skin friction coefficient for turbulent flow, while for laminar flow:

$$\frac{\tau_w s dx}{A} = \frac{\mu u}{d_0} \frac{1}{\alpha} \frac{4f'_L dx}{d_0}, \quad \text{where} \quad f'_L(\alpha) = \left( \frac{A}{A_e} \right) f_L, \quad (16.193)$$

and  $d_0$  is the diameter for  $A_0$ , and  $f_L$  is laminar skin friction coefficient.

With (16.190), (16.191) may be written

$$d(p + \rho gz) + \frac{\tau_w s dx}{A} - \rho u^2 \frac{dA}{A} = 0, \quad (16.194)$$

where the appropriate expression for the shear stress must be introduced depending on the nature of the flow.

Shapiro (1977a) introduces a dimensionless speed index,  $S$ :

$$S = \frac{u}{c}, \quad \text{so that} \quad \left( \frac{dS^2}{S^2} \right) = 2 \frac{du}{u} - 2 \frac{dc}{c}. \quad (16.195)$$

This index facilitates in the development of the theory and in the interpretation of results. Its role is comparable in significance to that of Mach number and Froude number in gas dynamics and in free-surface channel flow, respectively (Shapiro, 1977a). By analogy with gas dynamics, in steady flow, when  $S < 1$  (subcritical), friction causes the area and pressure to decrease in the downstream direction, and the velocity to increase. When  $S > 1$  (supercritical), the area and pressure increase along the tube, while the velocity decreases. In general, whatever the effect of changes of  $A_0$ ,  $P_e$ ,  $z$ , etc., in a subcritical flow, the effect is of opposite sign in supercritical flow. For example, let  $P_e$  be increased while all other independent variables such as  $A_0$ , elasticity, etc., are held constant. Then  $A$  and  $p$  will decrease for  $S < 1$ , but they will increase for  $S > 1$ . When  $S = 1$ , choking of flow and flow limitation as at the throat of a Laval nozzle will occur. Again, as in gas dynamics, there is the possibility of continuous transitions from supercritical to subcritical flow, and also rapid transitions from supercritical to subcritical as in shock waves.

In the steady-flow problem, the known quantities are  $dA_0$ ,  $dP_e$ ,  $gdz$ ,  $fdx$ ,  $dK_p$ ,  $\partial P/\partial x$ , and  $\partial P/\partial a$ , while the unknowns are  $du$ ,  $dA$ ,  $dp$ ,  $da$ ,  $dS$ , and so on.

In order to develop the final set of equations relating the dependent and independent variables, a number of useful relationships may be established between the differential quantities.

The external pressure is  $p_e(x)$ ,  $dp_e = (dp_e/dx) dx$ , the area  $A_0 = A_0(x)$ , and  $dA_e = (dA_0/dx) dx$ . Since  $\alpha = A/A_0$ ,

$$\frac{d\alpha}{\alpha} = \left( \frac{dA}{A} - \frac{dA_0}{A_0} \right). \quad (16.196)$$

The bending stiffness parameter is  $K_p = K_p(x)$ ,  $dK_p = (dK_p/dx) dx$ , and the tube law is

$$P = \frac{p - p_e}{K_p(x)} = P(\alpha, x), \quad \rightarrow dp = dp_e + K_p dP + P dK_p. \quad (16.197)$$

The appropriate form of (16.185) is

$$c^2(A, x) = \frac{A}{\rho} \left[ \frac{\partial(p - p_e)}{\partial A} \right]_x \rightarrow c^2(\alpha, x) = \frac{\alpha}{\rho} K_p \frac{\partial P}{\partial \alpha} \Big|_{x=\text{constant}}. \quad (16.198)$$

In (16.197),

$$dP = \frac{\partial P}{\partial \alpha} d\alpha + \frac{\partial P}{\partial x} dx. \quad (16.199)$$

With (16.198) and (16.199), (16.197) becomes

$$dp = dp_e + \rho c^2 \frac{d\alpha}{\alpha} + K_p \frac{\partial P}{\partial x} dx + Pd K_p. \quad (16.200)$$

With (16.198) and (16.197), we obtain

$$2 \frac{dc}{c} = \left( 1 + \frac{\alpha \partial^2 P / \partial \alpha^2}{\partial P / \partial \alpha} \right) \frac{d\alpha}{\alpha} + \frac{dK_p}{K_p} + \frac{\alpha K_p}{\rho c^2} \frac{\partial}{\partial x} \left( \frac{\partial P}{\partial x} \right) dx, \quad (16.201)$$

and, with (16.195), (16.196) becomes

$$\left( \frac{dS^2}{S^2} \right) = -2 \frac{d\alpha}{\alpha} - 2 \frac{dA_0}{A_0} - 2 \frac{dc}{c}. \quad (16.202)$$

We now have (16.194), (16.196), (16.200), (16.201), and (16.202). With these, [Shapiro \(1977a\)](#) developed a series of equations that relate each dependent variable as a linear sum of terms, each containing an independent variable multiplied by appropriate coefficients (influence coefficients by analogy with one-dimensional gas dynamics). A comprehensive listing of equations is provided in the paper by Shapiro. From the listing, the most important dependent variables turn out to be  $d\alpha/dx$  and  $dS^2/dx$ . Once these are known, other dependent quantities such as  $P$ ,  $u$ , and  $c$  may be calculated easily. We now list these equations.

Let us consider cases where  $P$  is just a function of  $\alpha$  alone, that is,  $P(\alpha)$ . For the tube law,

$$p - p_e(x) = K_p(x)P(\alpha), \quad (16.203)$$

the equation governing the variation in  $\alpha$  is

$$(1 - S^2) \frac{1}{\alpha} \frac{d\alpha}{dx} = \frac{S^2}{A_0} \frac{dA_0}{dx} - \frac{1}{\rho c^2} \left[ \frac{dp_e}{dx} + \rho g \frac{dz}{dx} + RQ + P \frac{dK_p}{dx} \right], \quad (16.204)$$

where  $R$  is viscous resistance per unit length (laminar or turbulent) and  $Q$  is flow rate, and the equation governing the speed index is

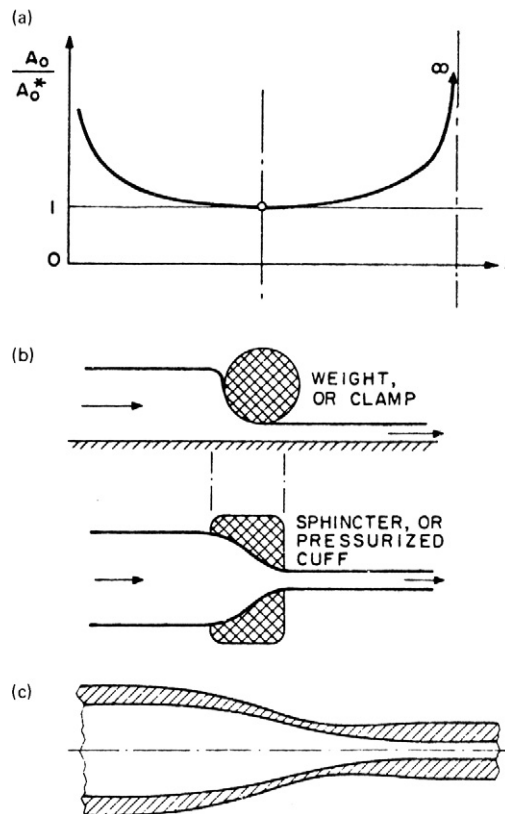
$$\begin{aligned} (1 - S^2) \frac{1}{S^2} \frac{dS^2}{dx} &= \frac{1}{A_0} \frac{dA_0}{dx} [-2 + (2 - M)S^2] \\ &+ \frac{M}{\rho c^2} \left[ \frac{dp_e}{dx} + \rho g \frac{dz}{dx} + RQ \right], \\ &+ \frac{1}{\rho c^2} \frac{dK_p}{dx} \left[ MP - (1 - S^2) \alpha \frac{dP}{d\alpha} \right], \end{aligned} \quad (16.205)$$

where

$$M = 3 + \frac{\alpha \partial^2 P / \partial \alpha^2}{\partial P / \partial \alpha}. \quad (16.206)$$

The equations for  $da/dx$  and  $dS^2/dx$  are coupled and must be solved simultaneously by using numerical procedures. Shapiro (1977a) has included results for several limit cases. These include several examples in which a smooth transition through the critical condition  $S = 1$  is possible, that is, continuous passage of flow from regime  $S < 1$  through  $S = 1$  into  $S > 1$  might occur. Figure 16.20 shows the transition from subcritical to supercritical flow by means of a minimum in the neutral area  $A_0$ . The pressure decreases continuously in the axial direction, and the area  $A$  of the deformed cross section would also decrease continuously in the axial direction. Figure 16.20 shows the transition through  $S = 1$  caused by a weight or clamp, a sphincter or pressurized cuff, due to changing  $p_e$ . The fluid pressure and the area both decrease continuously in the axial direction.  $S = 1$  occurs in the region where a sharp constriction exists.

Pedley (2000) points out that when  $S = 1$ , the right-hand side of (16.205) is  $-M$  times that of (16.204). Therefore, at  $S = 1$ , it is possible for  $da/dx$  or  $dS^2/dx$  to be nonzero as long as the right-hand sides are zero. Of the terms on the right-hand side,  $RQ$  is associated with friction and is always positive. This means that at least one of  $d(p_e + \rho gz)/dx$ ,  $dK_p/dx$ , or  $-dA_0/dx$



**FIGURE: 16.20** Smooth transition through the critical condition. In each case the fluid speed increases and the pressure drops continuously as the area decreases. *Reproduced with permission from the American Society of Mechanical Engineers, NY.*

should be negative, that is, the external pressure, the height, or the stiffness should decrease with  $x$  or the undisturbed cross-sectional area should increase. An example where  $dz/dx$  in a vertical collapsible tube is negative ( $= -1$ ) is the jugular vein of an upright giraffe and this problem has been discussed in detail by Pedley. Apparently, the giraffe jugular vein is normally partially collapsed!

In the next section, we learn about the modeling of a Casson fluid flow in a tube. We recall that blood behaves as a non-Newtonian fluid at low shear rates below about 200/s, and the apparent viscosity increases to relatively large magnitudes at low rates of shear. The modeling of such a fluid flow is important and will enable us to understand blood flow at various shear rates.

### Laminar Flow of a Casson Fluid in a Rigid-Walled Tube

As shear rates decrease below about 200/s, the apparent viscosity of blood rapidly increases (see Figure 16.7). As mentioned earlier, the variation of shear stress in blood flow with shear rate is accurately expressed by (16.6):

$$\tau^{1/2} = \tau_y^{1/2} + K_c \dot{\gamma}^{1/2}, \quad \text{for } \tau \geq \tau_y, \quad \text{and} \quad \dot{\gamma} = 0, \quad \text{for } \tau < \tau_y, \quad (16.207)$$

where  $\tau_y$  and  $K_c$  are determined from viscometer data. The yield stress  $\tau_y$  for normal blood at 37°C is about 0.04 dynes/cm<sup>2</sup>. In modeling the flow, this behavior must be included.

Consider the steady laminar axisymmetric flow of a Casson fluid in a rigid-walled, horizontal, cylindrical tube under the action of an imposed pressure gradient,  $(p_1 - p_2)/L$ . We shall employ cylindrical coordinates  $(r, \theta, x)$  with velocity components  $(u_y, u_\theta, \text{ and } u_x)$ , respectively. With the assumption of axisymmetry, ( $u_\theta = 0$ , and  $\partial/\partial\theta = 0$ ) For convenience, we write the  $u_y$  component as  $v$ , and we omit the subscript  $x$  in  $u_x$ .

The maximum shear stress in the flow,  $\tau_w$ , would be at the vessel wall. If the magnitude of  $\tau_w$  is equal to or greater than the yield stress,  $\tau_y$ , then there will be flow. We may estimate the minimum pressure gradient required to cause flow of a yield stress fluid in a cylindrical tube by a straightforward force balance on a cylindrical volume of fluid of radius  $r$  and length  $\Delta x$ . For steady flow, the viscous force opposing motion must be balanced by the force due to the applied pressure gradient. Thus,

$$\tau_{rx} \, 2\pi r \, \Delta x = -\pi r^2 (p|_{x+\Delta x} - p|_x), \quad (16.208)$$

and, as  $\Delta x \rightarrow 0$ ,

$$\tau_{rx}(r) = \frac{r}{2} \frac{dp}{dx} = \frac{(p_1 - p_2)r}{2L}. \quad (16.209)$$

The shear stress at the wall,  $\tau_w = -(a/2) (dp/dx) = (p_1 - p_2)a/2L$ . When  $\tau_y$  is equal to or less than  $\tau_w$  there will be fluid motion. The minimum pressure differential to cause flow is given by  $(p_1 - p_2)|_{\min} = 2L\tau_y/a$ . With  $\tau_y = 0.04$  dynes/cm<sup>2</sup>, for a blood vessel of  $L/a = 500$ , the minimum pressure drop required for flow is 0.04 dynes/cm<sup>2</sup> or 0.03 mm Hg. Recall that during systole, the typical pressures in the aorta and the pulmonary artery rise to 120 mm Hg and 24 mm Hg, respectively.

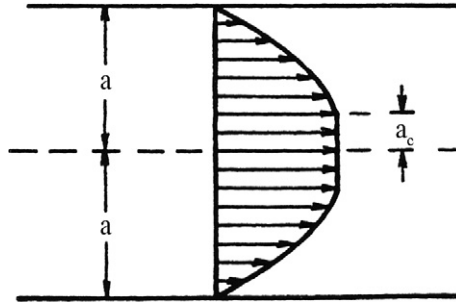


FIGURE 16.21 Velocity profile for axisymmetric blood flow in a circular tube. Here the profile is flattened in the center of the tube because of the non-Newtonian character of blood.

For axisymmetric blood flow in a cylindrical tube, at low shear rates, the fully developed flow is noted to consist of a central core region where the shear rate is zero and the velocity profile is flat, surrounded by a region where the flow has a varying velocity profile (see Figure 16.21). In the core, the fluid moves as if it were a solid body (also called *plug flow*).

Let the radius of this core region be  $a_c$ . Then,

$$\tau = \tau_y \quad \text{at } r = a_c, \quad \text{and} \quad \dot{\gamma} = 0 \quad \text{for } 0 \leq r < a_c,$$

$$a_c = 2L\tau_y/(p_1 - p_2) = a \left( \frac{\tau_y}{\tau_w} \right),$$

$$\tau^{1/2} = \tau_y^{1/2} + K_c \dot{\gamma}^{1/2} \quad \text{for } a_c < r \leq a. \quad (16.210)$$

In the core region,  $\dot{\gamma} = 0 \Rightarrow (du/dr) = 0 \Rightarrow u = \text{constant} = u_c$  (say).

Outside the core region, the velocity is a function of  $r$  only, and

$$\dot{\gamma} = -\frac{du}{dr} = \frac{[\tau + \tau_y - 2\sqrt{\tau\tau_y}]}{K_c^2}. \quad (16.211)$$

Let  $(p_1 - p_2) = \Delta p$ ,  $\tau = \Delta p r / 2L$ , and  $\tau_y = \Delta p a_c / 2L$ . From (16.211),

$$-\frac{du}{dr} = \frac{1}{2K_c^2} \frac{\Delta p}{L} (r + a_c - 2\sqrt{ra_c}). \quad (16.212)$$

By integration,

$$u = \frac{1}{2K_c^2} \frac{\Delta p}{L} \left( \frac{4}{3} \sqrt{a_c r^3} - \frac{r^2}{2} - a_c r + C \right), \quad (16.213)$$

where  $C$  is the integration constant. With the no-slip boundary condition at the wall of the vessel,  $u = 0$  at  $r = a$ :

$$C = -\left( \frac{4}{3} \sqrt{a_c a^3} - \frac{a^2}{2} - a_c a \right). \quad (16.214)$$

Therefore,

$$u = \frac{1}{4K_c^2} \frac{\Delta p}{L} \left[ (a^2 - r^2) - \frac{8}{3} \sqrt{a_c} (\sqrt{a^3} - \sqrt{r^3}) + 2a_c(a - r) \right], \quad (16.215)$$

in  $(a_c \leq r \leq a)$ . With  $u = u_c$  at  $r = r_c$ , in terms of  $\tau_w$  and  $\tau_y$  (16.215) becomes

$$u = \frac{a\tau_w}{2K_c^2} \left\{ \left[ 1 - \left( \frac{r}{a} \right)^2 \right] - \frac{8}{3} \sqrt{\frac{\tau_y}{\tau_w}} \left[ 1 - \left( \frac{r}{a} \right)^{3/2} \right] + 2 \left( \frac{\tau_y}{\tau_w} \right) \left( 1 - \frac{r}{a} \right) \right\}, \quad (16.216)$$

in  $(a_c \leq r \leq a)$ . We get the velocity in the core,  $u_c$ , by setting:

$$\left( \frac{r}{a} \right) = \left( \frac{a_c}{a} \right) = \left( \frac{\tau_y}{\tau_w} \right), \quad (16.217)$$

in (16.216). In terms of pressure gradient,  $a$  and  $a_c$ ,  $u_c$  becomes

$$u_c = \frac{1}{4K_c^2} \frac{\Delta p}{L} (\sqrt{a} - \sqrt{a_c})^3 \left( \sqrt{a} + \frac{1}{3} \sqrt{a_c} \right). \quad (16.218)$$

The volume rate of flow is given by

$$Q = \pi a_c^2 u_c + \int_{a_c}^a 2\pi r u dr. \quad (16.219)$$

After considerable algebra,

$$Q = \frac{\pi}{8} \frac{1}{K_c^2} \frac{\Delta p}{L} a^4 \left[ 1 - \frac{16}{7} \left( \frac{a_c}{a} \right)^{1/2} + \frac{4}{3} \left( \frac{a_c}{a} \right) - \frac{1}{21} \left( \frac{a_c}{a} \right)^4 \right]. \quad (16.220)$$

The Casson model predicts results that are in very good agreement with experimental results for blood flow over a large range of shear rates (see Charm & Kurland, 1974).

## Pulmonary Circulation

Pulmonary circulation is the movement of blood from the heart, to the lungs, and back to the heart again. The veins bring oxygen-depleted blood back to the right atrium. The contraction of the right ventricle ejects blood into the pulmonary artery. In the human heart, the main pulmonary artery begins at the base of the right ventricle. It is short and wide—approximately 5 cm in length and 3 cm in diameter, and extends about 4 cm before it branches into the right and left pulmonary arteries that feed the two lungs. The pulmonary arteries are larger in size and more distensible than the systemic arteries and the resistance in pulmonary circulation is lower. In the lungs, red blood cells release carbon dioxide and pick up oxygen during respiration. The oxygenated blood then leaves the lungs through the pulmonary veins, which return it to the left heart, completing the pulmonary cycle. The pulmonary veins, like the pulmonary arteries, are also short, but their distensibility characteristics are similar to those of the systemic circulation (Guyton, 1968). The blood is then distributed to the body through the systemic circulation before returning again to the pulmonary circulation. The pulmonary circulation loop is virtually

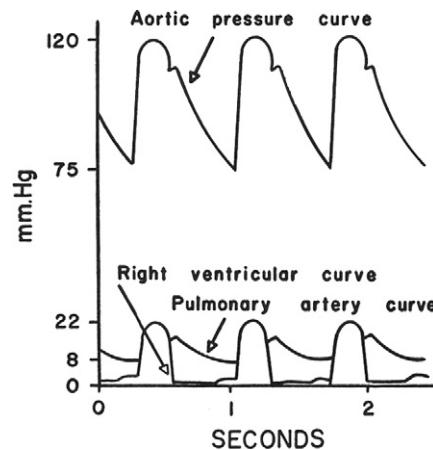
bypassed in fetal circulation. The fetal lungs are collapsed, and blood passes from the right atrium directly into the left atrium through the foramen ovale, an open passage between the two atria. When the lungs expand at birth, the pulmonary pressure drops and blood is drawn from the right atrium into the right ventricle and through the pulmonary circuit.

The rate of blood flow through the lungs is equal to the cardiac output except for the one to two percent that goes through the bronchial circulation (Guyton, 1968). Since almost the entire cardiac output flows through the lungs, the flow rate is very high. However, the low pulmonic pressures generated by the right ventricle are still sufficient to maintain this flow rate because pulmonary circulation involves a much shorter flow path than systemic circulation, and the pulmonary arteries are, as noted earlier, larger and more distensible.

The nutrition to lungs themselves are supplied by bronchial arteries which are a part of systemic circulation. The bronchial circulation empties into pulmonary veins and returns to the left atrium by passing alveoli.

### The Pressure Pulse Curve in the Right Ventricle

The pressure pulse curves of the right ventricle and pulmonary artery are illustrated in Figure 16.22. As described by Guyton (1968), approximately 0.16 second prior to ventricular systole, the atrium contracts, pumping a small quantity of blood into the right ventricle, and thereby causing about 4 mm Hg initial rise in the right ventricular diastolic pressure even before the ventricle contracts. Following this, the right ventricle contracts, and the right ventricular pressure rises rapidly until it equals the pressure in the pulmonary artery. The pulmonary valve opens, and for approximately 0.3 second blood flows from the right ventricle into the pulmonary artery. When the right ventricle relaxes, the pulmonary valve closes, and the right ventricular pressure falls to its diastolic level of about zero. The systolic



**FIGURE 16.22** Pressure pulse contours in the right ventricle, and pulmonary artery. *Reproduced with permission from Guyton, A. C. and Hall, J. E. (2000), Textbook of Medical Physiology, W. B. Saunders Company, Philadelphia.*



pressure in the right ventricle of the normal human being averages approximately 22 mm Hg, and the diastolic pressure averages about 0 to 1 mm Hg.

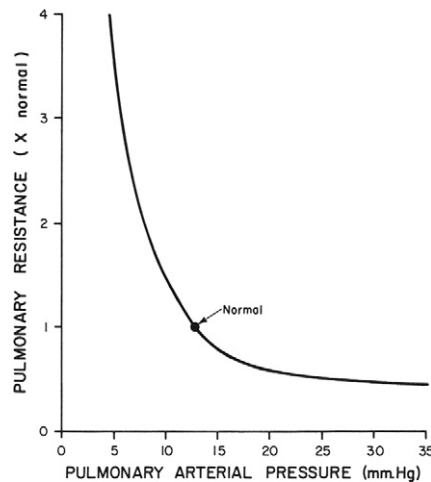
### Effect of Pulmonary Arterial Pressure on Pulmonary Resistance

At the end of systole, the ventricular pressure falls while the pulmonary arterial pressure remains elevated, then falls gradually as blood flows through the capillaries of the lungs. The pulse pressure in the pulmonary arteries averages 14 mm Hg which is almost two-thirds as much as the systolic pressure. Figure 16.23 shows the variation in pulmonary resistance with pulmonary arterial pressure. At low arterial pressures, pulmonary resistance is very high and at high pressures the resistance falls to low values. The rapid fall is due to the high distensibility of the pulmonary vessels.

The ability of lungs to accommodate greatly increased blood flow with little increase in pulmonary arterial pressure helps to conserve the energy of the heart. As described by Guyton, the only reason for flow of blood through the lungs is to pick up oxygen and to release carbon dioxide. The ability of pulmonary vessels to accommodate greatly increased blood flow without an increase in pulmonary arterial pressure accomplishes the required gaseous exchange without overworking the right ventricle.

In the earlier sections, we discussed several modeling procedures in relation to systemic blood circulation. The modeling of the blood flow in pulmonary vessels is similar to what we studied in those sections.

A discussion of gas and material exchange in the capillary beds is beyond the scope of this introductory chapter. Additional information on this topic can be found in Grotberg (1994).



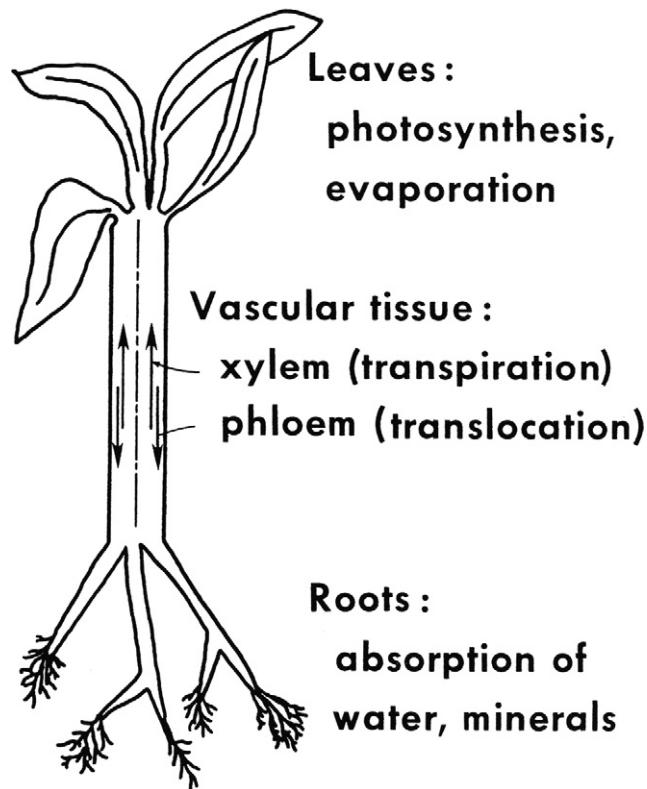
**FIGURE 16.23** Effect of pulmonary arterial pressure on pulmonary resistance. At low pressures, the lungs' resistance drops dramatically, and this allows increased blood flow rates for moderate increases in pulmonary arterial pressure. *Reproduced with permission from Guyton, A. C. and Hall, J. E. (2000), Textbook of Medical Physiology, W. B. Saunders Company, Philadelphia.*

## 16.4. INTRODUCTION TO THE FLUID MECHANICS OF PLANTS

Plant life comprises 99% of the earth's biomass (Bidwell, 1974; Rand, 1983).

The basic unit of a plant is a plant cell. Plant cells are formed at meristems, and then develop into cell types which are grouped into tissues. Plants have three tissue types: 1) dermal; 2) ground; and 3) vascular. Dermal tissue covers the outer surface and is composed of closely packed epidermal cells that secrete a waxy material that aids in the prevention of water loss. The ground tissue comprises the bulk of the primary plant body. Parenchyma, collenchyma, and sclerenchyma cells are common in the ground tissue. Vascular tissue transports food, water, hormones, and minerals within the plant.

Basically, a plant has two organ systems: 1) the shoot system, and 2) the root system. The shoot system is above ground and includes the organs such as leaves, buds, stems, flowers, and fruits. The root system includes those parts of the plant below ground, such as the roots, tubers, and rhizomes. There is transport between the roots and the shoots (see Figure 16.24).



**FIGURE 16.24** Overview of plant fluid mechanics. Transport of water and solutes between the leaves and the roots through the vascular tissues is essential. Transpiration of water at the leaves actually helps to lift sap from the roots. *Reproduced with permission from Annual Review of Fluid Mechanics, Vol. 15 © 1983. Annual Reviews: [www.AnnualReviews.org](http://www.AnnualReviews.org).*

Transport in plants occurs on three levels: 1) the uptake and loss of water and solutes by individual cells, 2) short-distance transport of substances from cell to cell at the level of tissues or organs, and 3) long-distance transport of sap within xylem and phloem at the level of the whole plant.

The transport occurs as a result of gradients in chemical concentration (Fickian diffusion), hydrostatic pressure, and gravitational potential. These three driving potentials are grouped under one single quantity, the water potential. The water potential is designated  $\psi$ , and

$$\psi = p - RTc + \rho gz, \quad (16.221)$$

where  $p$  is hydrostatic pressure (bar),  $R$  is gas constant ( $= 83.141 \text{ cm}^3 \text{ bar/mole K}$ ),  $T$  is temperature (K),  $c$  is the concentration of all solutes in assumed dilute solution ( $\text{mole/cm}^3$ ),  $\rho$  is density of water ( $\text{g/cm}^3$ ),  $g$  is acceleration due to gravity ( $= 980 \text{ cm/sec}^2$ ), and  $z$  is height (cm);  $\psi$  is in bars (Conversion:  $1 \text{ bar} = 10^6 \text{ dyne/cm}^2$ ).

Transport at the cellular level in a plant depends on the selective permeability of plasma membranes which controls the movement of solutes between the cell and the extracellular solution. Molecules move down their concentration gradient across a membrane without the direct expenditure of metabolic energy (Fickian diffusion). Transport proteins embedded in the membrane speed up the movement across the membrane. Differences in water potential,  $\psi$ , drive water transport in plant cells. Uptake or loss of water by a cell occurs by osmosis across a membrane. Water moves across a membrane from a higher water potential to a lower water potential. If a plant cell is introduced into a solution with a higher water potential than that of the cell, osmotic uptake of water will cause the cell to swell. As the cell swells, it will push against the elastic wall, creating a “turgor” pressure inside the cell. Loss of water causes loss of turgor pressure and may result in wilting.

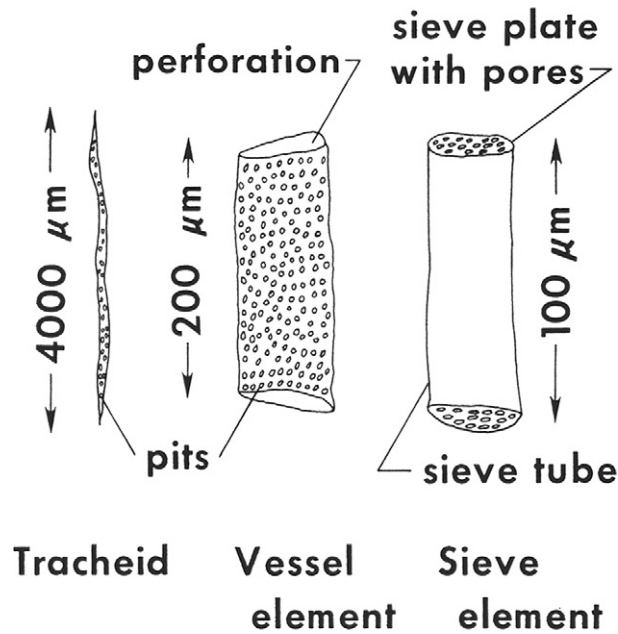
In contrast to the human circulatory system, the vascular system of plants is open. Unlike the blood vessels of human physiology, the vessels (conduits) of plants are formed of individual plant cells placed adjacent to one another. During cell differentiation the common walls of two adjacent cells develop pores which permit fluid to pass between them. Vascular tissue includes xylem, phloem, parenchyma, and cambium cells. Xylem and phloem make up the big transportation system of vascular plants. Long-distance transport of materials (such as nutrients) in plants is driven by the prevailing pressure gradient.

In this section we restrict attention to the vascular system that includes xylem and phloem cells.

### ***Xylem***

The term *xylem* applies to woody walls of certain cells of plants. Xylem cells tend to conduct water and minerals from roots to leaves. Generally speaking, the xylem of a plant is the system of tubes and transport cells that circulates water and dissolved minerals. Xylem is made of vessels that are connected end to end to enable efficient transport. The xylem contains tracheids and vessel elements (see Figure 16.25, from Rand, 1983). Xylem tissue dies after one year and then develops anew (e.g., rings in the tree trunk).

Water and mineral salts from soil enter the plant through the epidermis of roots, cross the root cortex, pass into the stele, and then flow up xylem vessels to the shoot system. The xylem



**FIGURE 16.25** Fluid-conducting cells in the vascular tissue of plants. *Reproduced with permission from Annual Review of Fluid Mechanics, Vol. 15 © 1983. Annual Reviews: [www.annualreviews.org](http://www.annualreviews.org).*

flow is also called *transpirational flow*. Perforated end walls of xylem vessel elements enhance the bulk flow.

The movement of water and solutes through xylem vessels occurs due to a pressure gradient. In xylem, it is actually tension (negative pressure) that drives long-distance transport. Transpiration (evaporation of water from a leaf) reduces pressure in the leaf xylem and creates a tension that pulls xylem sap upward from the roots. While transpiration enables the pull, the cohesion of water due to hydrogen bonding transmits the upward pull along the entire length of the xylem from the leaves to the root tips. The pull extends down only through an unbroken chain of water molecules. Cavitation, formation of water vapor pockets in the xylem vessel, may break the chain. Cavitation will occur when xylem sap freezes in water and as a result the vessel function will be compromised. Absorption of solar energy drives transpiration by causing water to evaporate from the moist walls of mesophyll cells of a leaf and by maintaining a high humidity in the air spaces within the leaf. To facilitate gas exchange between the inner parts of leaves, stems, and fruits, plants have a series of openings known as *stomata*. These enable exchange of water vapor, oxygen, and carbon dioxide.

The pressure gradient for transpiration flow is essentially created by solar power, and in principle, a plant expends no energy in transporting xylem sap up to the leaves by bulk flow. The detailed mechanism of transpiration from a leaf is very complicated and depends on the interplay of adhesive and cohesive forces of water molecules at mesophyll cell–air space interfaces, resulting in surface tension gradients and capillary forces. This will not be discussed in this section.

Xylem sap flows upward to veins that branch throughout each leaf, providing each with water. Plants lose a huge amount of water by transpiration—an average-sized maple tree loses more than about 200 liters of water per hour during the summer. Flow of water up the xylem replaces water lost by transpiration and carries minerals to the shoots. At night, when transpiration is very low, root cells are still expending energy to pump mineral ions into the xylem, accumulation of minerals in the stele lowers water potential, generating a positive pressure, called *root pressure*, that forces fluid up the xylem. It is the root pressure that is responsible for guttation, the exudation of water droplets that can be seen in the morning on tips of grass blades or leaf margins of some plants. Root pressure is not the main mechanism driving the ascent of xylem sap. It can force water upward by only a few meters, and many plants generate no root pressure at all. Small plants may use root pressure to refill xylem vessels in spring. Thus, for the most part, xylem sap is not pushed from below but pulled upward by the leaves.

### **Xylem Flow**

Water and minerals absorbed in the roots are brought up to the leaves through the xylem. The upward flow in the xylem (also called the *transpiration flow*) is driven by evaporation at the leaves. In the xylem, the flow may be treated as quasi-steady. The rigid tube model for flow description is appropriate because plant cells have stiff walls. The xylem is about 0.02 mm in radius and the typical values for flow are velocity 0.1 cm/s, the kinematic viscosity of the fluid 0.1 cm<sup>2</sup>/s, and the Reynolds number,  $Re = ud/v$  is 0.04. In view of the low Reynolds number, the Stokes flow in a rigid tube approximation is appropriate.

### **Phloem**

Phloem cells are usually located outside the xylem and conduct food from the leaves to the rest of the plant. The two most common cells in the phloem are the companion cells and sieve cells. Phloem cells are laid out end-to-end throughout the plant to form long tubes with porous cross walls between cells. These tubes enable translocation of the sugars and other molecules created by the plant during photosynthesis. Phloem flow is also called *translocation flow*. Phloem sap is an aqueous solution with sucrose as the most prevalent solute. It also contains minerals, amino acids, and hormones. Dissolved food, such as sucrose, flows through the sieve cells. In general, sieve tubes carry food from a sugar source (for example, mature leaves) to a sugar sink (roots, shoots, or fruits). A tuber or a bulb may be either a source or a sink, depending on the season. Sugar must be loaded into sieve-tube members before it can be exported to sugar sinks. Companion cells pass sugar they accumulate into the sieve-tube members via plasmodesmata. Translocation through the phloem is dependent on metabolic activity of the phloem cells (in contrast to transport in the xylem).

Unlike the xylem, phloem is always alive. In contrast to xylem sap, the direction that phloem sap travels is variable depending on locations of source and sink.

The pressure-flow hypothesis is employed to explain the movement of nutrients through the phloem. It proposes that water-containing nutrient molecules flow under pressure through the phloem. The pressure is created by the difference in water concentration of the solution in the phloem and the relatively pure water in the nearby xylem ducts.

At their “source”—the leaves—sugars are pumped by active transport into the companion cells and sieve elements of the phloem. The exact mechanism of sugar transport in the phloem is not known, but it cannot be simple diffusion. As sugars and other products of photosynthesis accumulate in the phloem, the water potential in the leaf phloem is decreased and water diffuses from the neighboring xylem vessels by osmosis. This increases the hydrostatic pressure in the phloem. Turgor pressure builds up in the sieve tubes (similar to the creation of root pressure). Water and dissolved solutes are forced downward to relieve the pressure. As the fluid is pushed down (and up) the phloem, sugars are removed by the cortex cells of both stem and root (the “sinks”) and consumed or converted into starch. Starch is insoluble and exerts no osmotic effect. Therefore, the osmotic pressure of the contents of the phloem decreases. Finally, relatively pure water is left in the phloem. At the same time, ions are being pumped into the xylem from the soil by active transport, reducing the water potential in the xylem. The xylem now has a lower water potential than the phloem, so water diffuses by osmosis from the phloem to the xylem. Water and its dissolved ions are pulled up the xylem by tension from the leaves. Thus it is the pressure gradient between “source” (leaves) and “sink” (shoot and roots) that drives the contents of the phloem up and down through the sieve tubes.

### Phloem Flow

Phloem flow occurs mainly through cells called *sieve tubes* which are arranged end to end and are joined by perforated cell walls called *sieve plates* (see Figure 16.26, from Rand & Cooke, 1978). As a model of Phloem flow, Rand et al. (1980) have derived an approximate formula for the pressure drop for flow through a series of sieve tubes with periodically placed sieve plates with pores (see Figure 16.27, from Rand et al., 1980). The approximation arises from treating the transport through the pore as creeping conical flow (see Happel & Brenner, 1983).

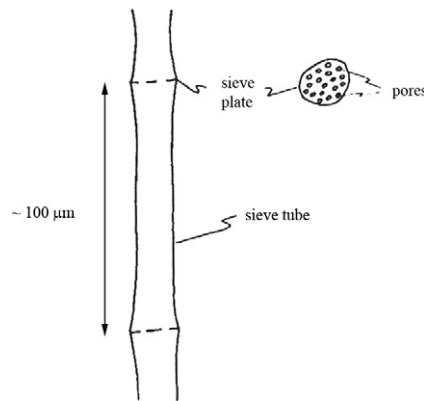
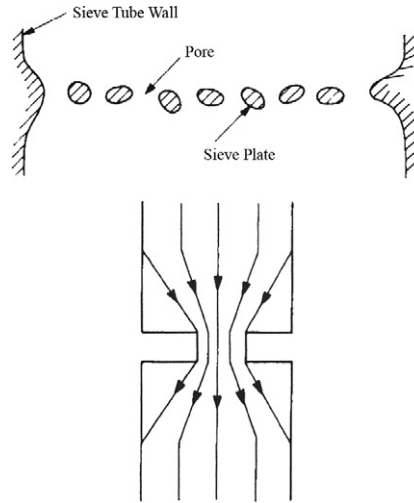


FIGURE 16.26 Sieve tube with sieve plate. These cells and cell structure convey phloem through the plant. Reproduced with permission from the American Society of Agricultural Engineers, MI.



**FIGURE 16.27** Sieve tube with pores and stream lines for conical flow through one pore. This geometry was used to derive the pressure drop formula (16.222) which is based on creeping conical flow. *Reproduced with permission from the American Society of Agricultural Engineers, MI.*

The approximate formula given by [Rand et al. \(1980\)](#) is:

$$\Delta p = \frac{8\mu Q}{\pi a^4} \left[ L + \frac{\ell}{N} \left( \frac{a}{r} \right)^4 \right] + 2 \Delta p', \quad \text{where} \quad (16.222)$$

$$\Delta p' = \frac{8\mu Q}{\pi a^3} \left( \frac{a_e}{r} \right) \left\{ 0.57N \left[ \left( \frac{a_e}{r} \right)^3 - 1 \right] - 1.5 \left( 1 - \frac{r}{a_e} \right) \right\}.$$

In (16.222),  $\Delta p$  is the pressure drop due to one sieve tube and one sieve plate,  $\mu$  is the viscosity of fluid in (g/cms),  $Q$  is the flow rate in (cm<sup>3</sup>/s),  $N$  is the number of pores in the sieve plate,  $a$  is sieve tube radius in cm,  $r$  is average radius of sieve pore in cm,  $L$  is the sieve tube length in cm,  $\ell$  is sieve plate thickness in cm, and the effective tube radius  $a_e = a/\sqrt{N}$ .

[Rand et al. \(1980\)](#) note that the approximate formula has not been tested for  $N \neq 1$ .

## EXERCISES

**16.1.** Consider steady laminar flow of a Newtonian fluid in a long, cylindrical, elastic tube of length  $L$ . The radius of the tube at any cross section is  $a = a(x)$ . Poiseuille's formula for the flow rate is a good approximation in this case.

- Develop an expression for the outlet pressure  $p(L)$  in terms of the higher inlet pressure, the flow rate  $\dot{Q}$ , fluid viscosity  $\mu$ , and  $a(x)$ .
- For a pulmonary blood vessel, we may assume that the pressure-radius relationship is linear:  $a(x) = a_0 + \alpha p/2$ , where  $a_0$  is the tube radius when the

transmural pressure is zero and  $\alpha$  is the compliance of the tube. For a tube of length  $L$ , show that

$$\dot{Q} = \frac{\pi}{20\mu\alpha L} \{ [a(0)]^5 - [a(L)]^5 \},$$

where  $a(0)$  and  $a(L)$  are the values of  $a(x)$  at  $x = 0$  and  $x = L$ , respectively.

- 16.2. For pulsatile flow in a rigid cylindrical tube of length  $L$ , the pressure drop  $\Delta p$  may be expressed as:  $\Delta p = f(L, a, \rho, \mu, \omega, U)$ , where  $a$  is tube radius,  $\rho$  is density,  $\mu$  is viscosity,  $\omega$  is frequency, and  $U$  is the average velocity of flow. Using dimensional analysis, show that

$$\frac{\Delta p}{\rho U^2} = C_1 \left( \frac{L}{a} \right)^{C_2} (Re)^{C_3} (St)^{C_4},$$

where  $C_1, C_2, C_3$ , and  $C_4$  are constants,  $Re$  is Reynolds number, and  $St$  is Strouhal number defined as  $a\omega/U$ .

- 16.3. Localized narrowing of an artery may be caused by the formation of arteriosclerotic plaque in that region. Such localized narrowing is called *stenosis*. It is important to understand the flow characteristics in the vicinity of a stenosis. Flow in a tube with mild stenosis may be approximated by axisymmetric flow through a converging-diverging tube. In this context, follow the details described in [Morgan & Young \(1974\)](#) and obtain expressions for the velocity profile and wall shear stress.
- 16.4. Shapiro (1997a) in his analysis of the steady flow in collapsible tubes has developed a series of equations that relate the dependent variables  $du, dA, dp, d\alpha, dS$ , etc., with the independent variables such as  $dA_0, dp_e, g dz, f_T dx$ , etc. In [Section IV](#) of that study, explicit calculations of certain simple flows are presented. In particular, consider pure pressure-gravity flows. Discuss the flow behavior patterns in this case.
- 16.5. Consider the Power-law model to describe the non-Newtonian behavior of blood. In this model,  $\tau = \mu \dot{\gamma}^n$ , where  $\tau$  is the shear stress and the  $\dot{\gamma}$  is the rate of shearing strain. Determine the flux for the flow of such a fluid in a rigid cylindrical tube of radius  $R$ . Show that when  $n = 1$ , the results correspond to the Poiseuille flow.
- 16.6. Consider the Herschel-Bulkley model to describe the non-Newtonian behavior of blood. In this model,

$$\tau = \mu \dot{\gamma}^n + \tau_0, \quad \tau \geq \tau_0$$

$$\dot{\gamma} = 0, \quad \tau < \tau_0$$

Determine the flux for the flow of such a fluid in a rigid cylindrical tube of radius  $R$ . Show that in the limit  $\tau_0 = 0$ , the results for the Herschel-Bulkley model coincide with those for the Power-law model.

## Acknowledgment

The help received from Dr. K. Mukundakrishnan and Mrs. Olivia Brubaker during the development of this chapter is gratefully acknowledged.



## Literature Cited

- Baish, J. W., Ayyaswamy, P. S., & Foster, K. R. (1986a). Small scale temperature fluctuations in perfused tissue during local hyperthermia. *J. BioMech. Eng.*, 108, 246–250.
- Baish, J. W., Ayyaswamy, P. S., & Foster, K. R. (1986b). Heat transport mechanisms in vascular tissues: A model comparison. *J. BioMech. Eng.*, 108, 324–331.
- Berger, S. A., Talbot, L., & Yao, L.-S. (1983). Flow in curved pipes. *Annual Review of Fluid Mechanics*, 15, 461–512.
- Bidwell, R. G. S. (1974). *Plant Physiology*. New York: MacMillan.
- Brown, B. H., Smallwood, R. H., Barber, D. C., Lawford, P. V., & Hose, D. R. (1999). *Medical Physics and Biomedical Engineering*. London: Institute of Physics Publishing.
- Cancelli, C., & Pedley, T. J. (1985). A separated flow model for collapsible tube oscillations. *Journal of Fluid Mechanics*, 157, 375–404.
- Chandran, K. B., Yoganathan, A. P., & Rittgers, S. E. (2007). *Biofluid Mechanics—The Human Circulation*. Boca Raton, FL: Taylor & Francis.
- Charm, S. E., & Kurland, G. S. (1974). *Blood Flow and Microcirculation*. New York: John Wiley & Sons.
- Collins, W. M., & Dennis, S. C. R. (1975). The steady motion of a viscous fluid in a curved tube. *Q.J. Mech. Appl. Math.*, 28, 133–156.
- Dean, W. R. (1928). The streamline motion of fluid in a curved pipe. *Philosophical Magazine, Series*, 7(30), 673–693.
- Fournier, R. L. (2007). *Basic Transport Phenomena in Biomedical Engineering*. New York: Taylor & Francis.
- Fung, Y. C. (1993). *Biomechanics: Mechanical Properties of Living Tissues, Second Edition*. Boca Raton, FL: Springer.
- Fung, Y. C. (1997). *Biomechanics: Circulation, Second Edition*. Boca Raton, FL: Springer.
- Goldsmith, H. L., Cokelet, G. R., & Gaetgens, P. (1989). Robin Fahraeus: Evolution of his concepts in cardiovascular physiology. *Am. J of Physiology—Heart and Circulatory Physiology*, 257(3), H1005–H1015.
- Grothberg, J. B. (1994). Pulmonary flow and transport phenomena. *Annual Review of Fluid Mechanics*, 26, 529–571.
- Guyton, A. C. (1968). *Textbook of Medical Physiology*. Philadelphia: W.B. Saunders Company.
- Happel, J., & Brenner, H. (1983). *Low Reynolds Number Hydrodynamics*. New York: McGraw-Hill.
- He, X., & Ku, D. N. (1994). Unsteady entrance flow development in a straight tube. *Journal of Biomechanical Engineering*, 116, 355–360.
- Kamm, R. D., & Pedley, T. J. (1989). Flow in collapsible tubes: A brief review. *Journal of Biomechanical Engineering*, 111, 177–179.
- Kamm, R. D., & Shapiro, A. H. (1979). Unsteady flow in a collapsible tube subjected to external pressure or body forces. *Journal of Fluid Mechanics*, 95, 1–78.
- Kleinstreuer, C. (2006). *Biofluid Dynamics: Principles and Selected Applications*. Boca Raton, FL: Taylor & Francis.
- Ku, D. N. (1997). Blood flow in arteries. *Annual Review of Fluid Mechanics*, 29, 399–434.
- Lighthill, M. J. (1978). *Waves in Fluids*. Cambridge: Cambridge University Press.
- Liu, Y., & Liu, W. K. (2006). Rheology of red blood cell aggregation by computer simulation. *J. Comput. Phys.*, 220(1), 139–154.
- Mazumdar, J. N. (1999). *An Introduction to Mathematical Physiology and Biology* (second ed.). Cambridge: Cambridge University Press.
- Mazumdar, J. N. (2004). *Biofluid Mechanics* (third ed.). Singapore: World Scientific.
- McConalogue, D. J., & Srivastava, R. S. (1968). Motion of a fluid in a curved tube. *Proc. Roy. Soc. A.*, 307, 37–53.
- McDonald, D. A. (1974). *Blood Flow in Arteries, Second Edition*. Baltimore: The Williams & Wilkins Company.
- Mohanty, A. K., & Asthana, S. B. L. (1979). Laminar flow in the entrance region of a smooth pipe. *Journal of Fluid Mechanics*, 90, 433–447.
- Morgan, B. E., & Young, D. F. (1974). *Bull. Math. Biol.*, 36, 39–53.
- Morgan, G. W., & Ferrante, W. R. (1955). Wave propagation in elastic tubes filled with streaming liquid. *The Journal of the Acoustical Society of America*, 27(4), 715–725.
- Morgan, G. W., & Kiely, J. P. (1954). Wave propagation in a viscous liquid contained in a flexible tube. *The Journal of the Acoustical Society of America*, 26(3), 323–328.
- Nichols, W. W., & O'Rourke, M. F. (1998). *McDonald's Blood Flow in Arteries: Theoretical, Experimental and Clinical Principles*. London: Arnold.
- Pedley, T. J. (1980). *The Fluid Mechanics of Large Blood Vessels*. Cambridge: Cambridge University Press.

- Pedley, T. J. (2000). Blood flow in arteries and veins. In G. K. Batchelor, H. K. Moffat, & M. G. Worster (Eds.), *Perspectives in Fluid Dynamics*. Cambridge: Cambridge University Press.
- Rand, R. H. (1983). Fluid mechanics of green plants. *Annual Review of Fluid Mechanics*, 15, 29–45.
- Rand, R. H., & Cooke, J. R. (1978). Fluid dynamics of phloem flow: An axi-symmetric model. *Trans. ASAE*, 21, 898–900, 906.
- Rand, R. H., Upadhyaya, S. K., & Cooke, J. R. (1980). Fluid dynamics of phloem flow. II. An approximate formula. *Trans. ASAE*, 23, 581–584.
- Shapiro, A. H. (1977a). Steady flow in collapsible tubes. *Journal of Biomechanical Engineering*, 99, 126–147.
- Shapiro, A. H. (1977b). Physiologic and medical aspects of flow in collapsible tubes. *Proc. 6th Can. Congr. Appl. Mech.* 883–906.
- Singh, M. P. (1974). Entry flow in a curved pipe. *Journal of Fluid Mechanics*, 65, 517–539.
- Whitmore, R. L. (1968). *Rheology of the Circulation*. Oxford: Pergamon Press.
- Womersley, J. R. (1955a). Method for the calculation of velocity, rate of flow and viscous drag in arteries when the pressure gradient is known. *Journal of Physiology*, 127, 553–563.
- Womersley, J. R. (1955b). Oscillatory motion of a viscous liquid in a thin-walled elastic tube. I. The linear approximation for long waves. *Philosophical Magazine*, 46, 199–221.
- Womersley, J. R. (1957a). The mathematical analysis of arterial circulation in a state of oscillatory motion. Technical Report WADC-TR-56-614. Dayton, OH: Wright Air Development Center.
- Womersley, J. R. (1957b). Oscillatory flow in arteries: The constrained elastic tube as a model of arterial flow and pulse transmission. *Physics in Medicine and Biology*, 2, 178–187.
- Zhou, J., & Fung, Y. C. (1997). The degree of nonlinearity and anisotropy of blood vessel elasticity. *Proc. Natl. Acad. Sci. USA*, 94, 14255–14260.

## Supplemental Reading

- Lighthill, M. J. (1975). *Mathematical Biofluidynamics*. Philadelphia: Soc. Ind. Appl. Math.